UNIVERSITÉ DE NEUCHÂTEL

Center for Hydrogeology and Geothermics (CHYN)
University of Neuchâtel
www.unine.ch/chyn

Isotope fractionation of volatile organic compounds in porous media under variably saturated conditions

PhD thesis presented to the faculty of Sciences of the University of Neuchâtel to satisfy the requirement for the degree of Doctor of Philosophy in Science

by

Simon Jeannottat

Thesis defence date: December 14th 2012
Public presentation date: February 21th 2013

PhD thesis evaluation committee:

Daniel Hunkeler, Professor (thesis director), University of Neuchâtel, Switzerland
Mette Martina Broholm, Associate professor, Technical University of Denmark
Olivier Atteia, Professor, University of Bordeaux, France
Philip Brunner, Professor, University of Neuchâtel, Switzerland

UNIVERSITÉ DE NEUCHÂTEL

Faculté des sciences
Secrétariat-décanat de Faculté
Rue Emile-Argand 11
2000 Neuchâtel - Suisse
Tél: + 41 (0)32 718 2100
E-mail: secretariat.sciences@unine.ch

IMPRIMATUR POUR THESE DE DOCTORAT

La Faculté des sciences de l'Université de Neuchâtel autorise l'impression de la présente thèse soutenue par

Monsieur Simon JEANNOTTAT

Titre:

"Isotope fractionation of volatile organic compounds in porous media under variably saturated conditions"

sur le rapport des membres du jury:

- Prof. Daniel Hunkeler, Université de Neuchâtel, *directeur de thèse*
- Prof. Philip Brunner, Université de Neuchâtel
- Prof. Olivier Atteia, Université Michel de Montagne, Bordeaux, France
- Prof. Mette Broholm, Danish Technical University, Lynby, Denmark

Neuchâtel, le 15 février 2013

Le Doyen, Prof. P. Kropf

Acknowledgments

I would like to thank all the persons who, with their help, their patience, time and friendship made it possible to realize this PhD thesis:

- My thesis director Daniel Hunkeler. He gave me the opportunity to discover the world of scientific research and laboratory work. I thank him for his patience, his enthusiasm and to have guided me throughout this work. A PhD is always full of unexpected events, but he always managed to find solutions to my problems, as well as innovative ideas to go ahead in this work. I learned a lot from him during these 4 years of work in the CHYN.

- Florian Breider. It was a real pleasure to spend 4 years together in the same office. We had thousand of discussions about theoretical problems, laboratory troubleshooting, science and life. He helped me a lot during laboratory experiments, as well as during the writing of this PhD.

- All the staff of the hydrochemistry and contaminants group of the CHYN, and especially Jordi Palau, Daniel Bouchard, Bibiane Schlunegger, Xanthippe Boutsiadou, Pascale Ducommun, Alice Badin and Philipp Wanner. We have always worked together in a good atmosphere to enable our laboratory to run. We had great moments in the laboratory and in the field, and they have always helped me when I needed.

- Roberto Costa. He helped me with a lot of the technical issues encountered in the laboratory during these 4 years and has always found inventive solutions for every problem.

- Christian Hêche and all the technical staff of the University of Neuchâtel. They built all my experimental setups with a great professionalism. My laboratory experiments could not have been conducted without them.

- All my colleagues of the CHYN. It was always pleasant to work and spend time in this institute.

- My mother, my girlfriend, and all my family who have always supported me throughout this PhD thesis.

- The Swiss National Science Foundation (SNSF) for their financial support.

Extended abstract

Compound-specific isotope analysis (CSIA) has proven to be an effective tool to assess in-situ biodegradation of volatile organic compounds (VOCs) in groundwater and to distinguish between different contaminant sources. There is an increasing interest to apply the CSIA method also in unsaturated zone studies. However, under variably saturated conditions, physical processes such as phase partitioning and diffusion might influence isotope ratios as well. The main aim of this study was to quantify isotope fractionation associated with physical processes relevant for the unsaturated zone and to explore how isotope ratios evolve if different processes interact. The study focussed on chlorinated hydrocarbons, which are among the most common contaminants detected in the subsurface. In addition to carbon, the behaviour of chlorine isotopes was also investigated. Since the mass difference between the stable chlorine isotopes is two, larger isotope effects are expected to occur than for carbon, especially for diffusion. In order to make chlorine isotope analysis feasible, some analytical method development was required as well.

A new analytical method for chlorine isotope ratio analyses based on gas chromatography quadrupole mass-spectrometry (GC-qMS) measurements was evaluated by comparing it with established IRMS based methods. The study highlighted the need to perform a two-point calibration and to bracket samples with standards of the same concentrations. Using this approach, a precision of $1\sigma \approx 0.2\text{-}0.5\%$ (n=10) was reached for TCE measurements with an Agilent GC-qMS. Additionally, the relationship between isotope and isotopologue fractionation during vaporization and diffusion was explored theoretically. While fractionation takes place among isotopologues it is usually more convenient to express results as isotope ratios. It was demonstrate that during vaporization and diffusion chlorine isotope and isotopologue fractionation is proportional in good approximation even when several isotopologues with multiple heavy isotopes are present. As a consequence, isotope ratios can be determined even if only some isotopologues are quantified and isotope fractionation factors can be derived from either isotope or isotopologue ratios.

In a next step, isotope fractionation during processes relevant for the release of compounds from NAPL (vaporization) or groundwater (air-water partitioning) was quantified in isolation for the trichloroethylene (TCE) using various laboratory experiments. During NAPL-vapor equilibration, carbon and chlorine isotope ratios evolved in opposite directions although both elements are present in the same bond, with a normal isotope effect for chlorine (ε_{Cl} = -

0.39±0.03‰) and an inverse effect for carbon (ε_C = +0.75±0.04‰). During air-water partitioning, no significant chlorine isotope fractionation occurred, while an inverse carbon isotope effect (ε_C = +0.38±0.04‰) was observed, that was however weaker than for vaporization.

Then, the combined effect of release of compounds from NAPL or groundwater and transport by diffusion through unsaturated porous media was investigated. Contaminant release to the unsaturated zone from an NAPL source was simulated using a 1D column. A TCE NAPL source was emplaced at one end of the column and the other end was open to the atmosphere to maintain a concentration close to zero. In the initial phase of the experiment, gaseous TCE became depleted in heavy isotopes with increasing distance from the source due to the more rapid diffusion of light isotopologues. Once steady state concentration profiles were established, isotope ratios of gaseous TCE were constant along the column. At the NAPL source, carbon isotope ratios remained constant (ε_C = +0.10±0.05‰) while chlorine isotope ratios became enriched (ε_{Cl} = -1.39±0.06‰) as vaporization proceeded. Based on theoretically consideration, it is expected that the observed isotope effect is a combination of isotope fractionation associated with vaporization and diffusion. For carbon, the inverse isotope fractionation associated with NAPL-vapor equilibration cancelled out with the normal diffusion isotope fractionation while for chlorine, both processes followed normal isotope fractionation and hence they cumulated.

Contaminant release from a groundwater plume to the unsaturated zone was simulated in a 2D laboratory system. A 2D system with horizontal groundwater flow in the lower part was chosen because the rate of contaminant release is strongly influenced by transverse vertical dispersion. PCE was selected as a model compound since it does not degrade under aerobic conditions, which were maintained in the experiment. Unlike in the NAPL experiment, no significant depletion of the heavy isotopes with distance from the groundwater plume was observed. This can be explained by the slower release of contaminants from groundwater compared to the NAPL source. Hence, constant quasi-steady state isotope profiles are maintained throughout the experiment. However, numerical modeling suggested that, depending on the thickness of the unsaturated zone and the lithology, depletion in heavy isotopes could occur with distance during the transient migration of contaminant through the unsaturated zone. Additionally, a small offset of about 0.5 ‰ was observed in the isotope ratios between and aqueous and gaseous values across the capillary fringe for both carbon and chlorine isotopes. Numerical modeling indicated that this offset is due to isotope fractionation during air-water partitioning, as well as to the

preferential loss of light isotopologues from the unsaturated zone by diffusion. Variations of chlorine isotope ratios of 1.5‰ were also observed in the unsaturated zone during water table fluctuations.

Finally, the combined effect of biodegradation and transport by diffusion on the isotope ratios of VOCs migrating through the unsaturated zone was studied. Vinyl chloride (VC) was selected as model compound. Carbon isotope fractionation associated with biodegradation only was investigated in microcosm experiments using material from a contaminated site. An average carbon isotope enrichment factor of -7.2‰ was obtained. The coupling of degradation and diffusive transport in the unsaturated zone was also evaluated with numerical modeling. It was shown that the effective enrichment factor of biodegradation coupled to diffusion in the unsaturated conditions is reduced compare to saturated conditions (ε_C = -2.1‰). Numerical modeling suggested that biodegradation could be identified in a diffusion-controlled system using CSIA if degradation rate is fast enough. Shifts in isotope ratios due to biodegradation were amplified if layers of fine sediments were present or if the unsaturated zone was thick.

In conclusion, this work confirms that significant isotope fractionation can occur during physical processes affecting VOCs in the unsaturated zone even for molecules with a relatively large mass such as TCE and PCE. Moreover, during the combination of several processes, isotope effects associated with different processes can reinforce or cancel each other. In the case of diffusion-controlled vaporization from an unsaturated zone NAPL source, diffusion will always be associated with a normal isotope effect, while during vaporization either a normal (chlorine isotopes) or inverse (carbon isotopes) effects can occur. Hence, for diffusion-controlled vaporization, a fairly strong isotope effect can generally be expected for chlorine because the two processes reinforce each other. During the transfer of compounds though the capillary fringe from a groundwater plume to the unsaturated zone, air-water partitioning (normal and inverse isotope effect for chlorine and carbon, respectively) and the preferential lost of light isotopologues from the unsaturated zone due to diffusion cancel for carbon isotopes, but reinforce each other for chlorine. In unsaturated conditions where diffusion is the major transport process, the net isotope fractionation for biodegradation is reduced compare to saturated conditions, as the preferential removal of light molecules due to biodegradation is partly counterbalanced by the larger mass flux of light molecules brought along by diffusion from the source. Finally, the extent of the observed isotope shifts strongly depends whether a system is under steady state or in a transient state conditions. A significant isotope fraction is expected at transient

state in the case of NAPL source, as well as if the unsaturated zone is thick and/or layer of fine sediments are present in the case of a groundwater source. In contrary, if the unsaturated zone is thin and/or if coarser sediments are present above groundwater level, isotope profiles generally do not vary with distance from the water table at a given time, even at transient state. Constant isotopic ratios are however always observed at steady state across the unsaturated zone.

This study has several implications for the application of CSIA methods to characterize sources of contamination and/or to assess biodegradation of chlorinated ethenes in unsaturated zone contamination studies. It can be expected that the isotope signature of the vapor around an unsaturated zone NAPL source does not vary with distance as long as steady state conditions are reached. A small offset equivalent to the vaporization enrichment factor is expected between the vapor contamination and the NAPL source. This offset will nevertheless not affect the source identification methods as it will be the same for each NAPL source. For groundwater source, a small isotopic shift is expected between the groundwater and the gas phase (in the unsaturated zone) depending on subsurface lithology. Constant isotopic values are then expected through the unsaturated zone. Since constant isotopic values were expected across the unsaturated zone at steady state in absence of biodegradation, an enrichment of heavy isotopes indicates the presence of significant biodegradation. It seems thus possible to access biodegradation with CSIA in unsaturated zone studies, as long as the net isotope fractionation factor is sufficiently high.

Keywords:
Carbon and chlorine isotope analysis, chlorinated ethenes, unsaturated zone, vaporization, diffusion, air-water partitioning, biodegradation

Table of contents

Chapter 1

General Introduction

1.1 Behaviour of volatile organic compounds in the environment, and specifically in the unsaturated zone

Chlorinated compounds such as the tetrachloroethylene (PCE) and trichloroethylene (TCE) found in the environment are often released at or near the land surface as a dense non-aqueous phase liquid (DNAPL). DNAPLs can then migrate vertically (depending on gravity and capillary forces) through the unsaturated zone to reach the underlying aquifer (Cotel & al., 2011). After penetrating the aquifer they tend to form pools over low permeability geological layers (Figure 1) and, as their solubility in water is generally low, create long-term groundwater contaminations (Johnson & Pankow, 1992). Chlorinated ethenes can volatilize from groundwater and then migrate by diffusion, which is the most significant transport process in the gas phase (Jury & al., 1983; Christophersen & al., 2005), through the unsaturated zone to the soil surface. Moreover, due to interfacial tension, a certain amount of NAPLs can be retained in the unsaturated zone (Figure 1) and create a persistent source of contamination. This fraction may represent between 2 to 20% of the available pore space (Mercer & Cohen 1990). Due to their high vapour pressure, chlorinated compounds vaporize, creating a vapor-phase contaminant plume (Jury et al., 1984; Conant & al., 1996; Pasteris et al., 2002; Werner & Höhener, 2002; Christophersen & al., 2005; Bohy & al., 2006; Bouchard & al., 2008a). Chlorinated ethenes are transported away from the NAPL source by gaseous diffusion and may induce groundwater contamination even if the NAPL has not reached the water table (Baehr, 1987; Baehr et al., 1999; Falta et al., 1989). The vapor phase diffusion is strongly influenced by the partitioning of VOCs between the gas, water and solid phase, as well as by the geometry of the soil pores. Moreover, density-driven forces and gas-pressure gradient may occasionally significantly contribute to the expansion of the vapor plume (Conant et al., 1996; Smith et al., 1996). Mass transport between unsaturated and saturated zones and inside the unsaturated zone plays thus an important role in controlling the fate of contaminations (McCarthy & Johnson, 1993).

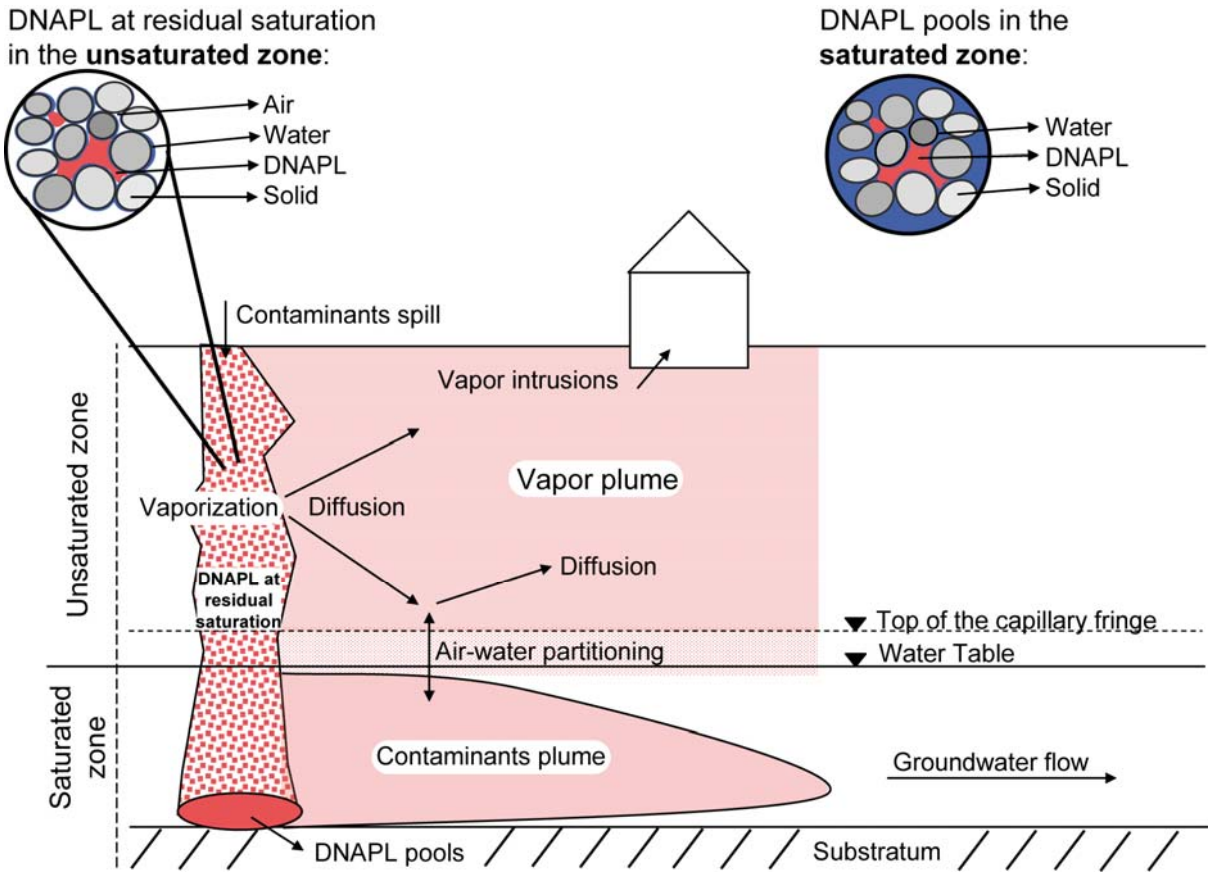

Figure 1: Conceptual sketch of a DNAPL spill in the unsaturated and saturated zone, and various processes influencing expansion of contaminants plume.

1.2 Use of compound specific isotope analysis (CSIA) in the environment

Groundwater pollution by organic contaminants such as petroleum hydrocarbons and chlorinated solvents is common in many industrialized countries. Stable isotope analysis is increasingly used to investigate the behaviour of organic or inorganic contaminants in the subsurface. Compound-specific isotope analysis (CSIA) has proven to be an effective tool to confirm and quantify in-situ biodegradation of contaminants in groundwater (Hunkeler & al., 1999; Sherwood Lollar & al., 2001; Meckenstock & al., 2004; Hunkeler & al., 2005; Elsner & al., 2005; Hunkeler & al., 2010). Heavy isotopes progressively become enriched during biodegradation, as microorganisms degrade light isotopes preferentially. Because isotope fractionation occurs in groundwater only due to chemical or biological degradation and not because of other physical processes as sorption and dispersion, the isotope approach makes it possible to distinguish concentration changes due to degradation from changes due to physical processes (Harrington *et al.* 1999; Slater *et al.* 2000; Abe & Hunkeler, 2006).

This isotope enrichment caused by biodegradation is usually described by the Rayleigh equation, which links the variation of isotope ratios to the changes in concentrations over time (Abe & Hunkeler, 2006) and may be defined as (Clark & Fritz, 1997):

$$1000 \cdot \ln\left(\frac{R}{R_0}\right) = \varepsilon \cdot \ln\left(\frac{C}{C_0}\right) \qquad \textit{(equation 1)}$$

where R is the observed isotope ratio, R_0 the initial isotope ratio, ε the enrichment factor [‰], C the observed concentration, and C_0 the initial concentration.

CSIA is also increasingly used to differentiate different contaminant sources and relate contaminant plumes to their source in groundwater (Jendrzejewski & al., 2001; Shouakar-Stash & al., 2003; Hunkeler & al., 2004; Blessing & al., 2009). Moreover, dual isotope analysis has recently been demonstrated to be useful to distinguish between different contaminant sources (Schmidt & al., 2004; Shouakar-Stash & al., 2003), as well as to evaluate contaminant degradation pathways (Van Warmerdam & al., 1995; Hofstetter & al., 2007). New analytical techniques recently developed for chlorine isotope analysis measurements make it possible to applying dual isotope analysis more widely for chlorinated ethenes (Sakaguchi-Söder & al., 2007; Aeppli & al., 2010).

There is also an increasing interest to apply CSIA in unsaturated zone studies to relate vapor phase contamination in the unsaturated zone to NAPL source or groundwater plumes, or to demonstrate contaminant degradation. However, previous laboratory studies have suggested that in the unsaturated zone, isotope ratios may also be influenced by transport and partitioning processes. In fact, isotope fractionation has been observed for diffusion of volatile organic compounds (VOCs) across a porous media, vaporization from a NAPL phase, and air-water partitioning (Baertschi & al., 1953; Harrington & al., 1999; Huang & al., 1999; Poulson & Drever, 1999; Bouchard &al., 2008a&b; Kuder & al., 2009). Bouchard & al. (2008a&b) investigated carbon isotope fractionation during vaporization and diffusion of petroleum hydrocarbons in laboratory and field studies. They observed a depletion of heavy isotopes with distance from a NAPL source during the initial expansion of a vapor plume and an enrichment of heavy isotopes in the NAPL source during its progressive depletion. Kuder & al. (2009) investigated the combined effect of phase partitioning and vapor diffusion on carbon and hydrogen isotope ratios of MTBE using sand-filled column studies that simulated soil vapor extraction of non-aqueous phase liquids (NAPL), air sparging of dissolved compounds and passive vaporization of dissolved compound or NAPL. They reported carbon isotope enrichment factor ranging from -1.0 to 0.7‰ and hydrogen enrichment factors from -12 to + 7‰. Although the isotope changes are generally lower than those

associated with biodegradation, the studies with petroleum hydrocarbons and MTBE showed that especially for smaller molecules, detectable isotope fractionation occurs that could complicate interpretation of isotope data. In contrast to petroleum hydrocarbons, less information is available on isotope fractionation during vaporization and air-water partitioning of chlorinated hydrocarbons, especially for chlorine isotopes. Although the atomic weight of chlorine and the weight of molecules containing chlorine are relatively high, significant isotope fractionation might occur due to the mass difference of 2 between isotopes. Poulson & al. (1999) and Huang & al. (1999) investigated chlorine and carbon isotope fractionation during vaporization of trichloroethene (TCE) from open vessels. They observed inverse isotope fractionation for carbon isotopes while for chlorine normal isotope fractionation occurred. However, because of the design of the experimental setups used in these studies, a contribution of diffusion to isotope fractionation cannot be excluded.

1.3 Isotope fractionation during various physical processes

As a basis for using isotopes methods in unsaturated zone studies for tracing processes and distinguishing between different vapor sources, the isotope fractionation associated with physical processes relevant in the unsaturated zone needs to be known. In the following the current knowledge about processes that induce isotope fractionation during vaporization, air-water partitioning, diffusion, biodegradation and coupling of these processes is summarized. A review of theoretical aspect behind isotope fractionation of these various physico-chemical processes and coupling is presented in the present chapter according to previous studies.

1.3.1 Vaporization

It is well established since the 1930' that different isotopologues (chemically identical molecule with a different isotopic composition) of a compound frequently have slightly different vapor pressures, a phenomena usually denoted as vapor pressure isotope effect (VPIE) (Van Hook, 2006). The presence of a supplementary neutron in the nucleus of an atom (heavy isotope) leads to slightly different physical properties to the molecule containing this atom compare to the more abundant light isotope molecule. It was for example shown by Narten & Kuhn (1961) that ^{13}C-benzene had a higher vapour pressure than ^{12}C-benzene. However, although vaporization is one of the common processes affecting chlorinated solvents in natural systems due to their large volatility, carbon and chlorine stable isotope fractionations accompanying this process have been little investigated (Huang & al., 1999). One of the earliest studies was reported by Baertschi & al. (1953), who found that distillation of tetrachloromethane, chloroform, methanol and benzene leads for all four cases to an

enrichment of ^{13}C in the vapor phase, while ^{37}Cl and ^{18}O become depleted. A similar phenomenon was observed for carbon and oxygen isotope fractionation during the vaporization of liquid CO_2 by Grootes & al (1969). In these earlier studies VPIE were investigated by measuring vapor pressures of pure isotopologues with very precise manometers or by distilling mixtures of different isotopologues. The isotopologue ratios between the organic phase and the condensate were then compared (Höpfner, 1969; Jancso & Van Hook, 1974). In the pure compounds studies, the VPIE is usually quantified from the vapor pressure of light and heavy isotopologues according to (Van Hook, 2006):

$$VPIE^{*} = \ln \frac{{}^{l}P}{{}^{h}P} \qquad \textit{(equation 2)}$$

or using the ratios between the vapor pressures (Van Hook, 2006):

$$VPIE = R = \frac{{}^{l}P}{{}^{h}P} \qquad \textit{(equation 3)}$$

where ${}^{l}P$ and ${}^{h}P$ are the vapor pressure for the light and heavy isotopologue, respectively.

More recently, isotope effects during vaporization were investigated using organic compounds labelled at natural abundance. Values of isotope fractionation factors (expressed in terms of enrichment factors to facilitate comparison) of common organic groundwater contaminants determined during these previous studies are summarized in Table 1. Enrichment factors (ε) were calculated using the Rayleigh equation based on isotope data (and not based on isotopologue as above) and defined by:

$$\alpha_{vap} = \frac{V_L / V_H}{L_H / L_L} \quad \textit{and} \quad \varepsilon = (\alpha - 1) \cdot 1000 \qquad \textit{(equation 4)}$$

where α is the fractionation factor, V_L and V_H are the mole fractions of light and heavy isotopes, respectively in the gas phase and L_L and L_H are the mole fraction of light and heavy isotopes, respectively in the liquid phase. At natural abundance, molecules with more than one heavy isotope are rare for carbon and hydrogen. The obtained isotope fractionation factors can be thus considered to be approximately equivalent to the isotopologue fractionation. However, depending on the molecule considered and especially in the case of chlorine isotope where several heavy isotopes may be present in molecules of chlorinated ethenes, it has to be taken in account that fractionation during vaporization takes place among isotopologues and not directly isotopes. The systematic comparison between isotope and isotopologue fractionation during vaporization of trichloroethylene will thus be addressed in this thesis. Frequently, for carbon and hydrogen isotopes an inverse isotope effect is

observed, while a normal isotope effect is observed for chlorine isotopes. Isotope fractionation during vaporization reflects interactions between molecules in the condensed phase (Van Hook, 2006). The direction of isotope fractionation is the result of an interplay between the effect of the restricted rotation and translation in the condensed phase (external mode) and the shift of internal vibrational frequencies upon condensation (internal mode). The former always leads to a normal isotope effect because the molecular motion becomes hindered in the condensed phase, whereas the latter is usually associated with an inverse isotope effect because frequencies of internal vibration are lower due to the interaction between molecules in the condensed phase (Jansco & Van Hook, 1974; Van Hook, 2006). In case of carbon and hydrogen changes in the internal mode dominate, whereas for chlorine changes in the external mode control isotope fractionation. These concepts are complex and are further developed in section 3.4.1.

Table 1: Enrichment factors during vaporization expressed as isotopes enrichment factor for selected organic compounds. Positive values correspond to an inverse isotope effect, negative values to a normal isotope effect.

Substance	**Carbon** ε^{ITL}_{vap}	**Temp. °C**	**Hydrogen** ε^{ITL}_{vap}	**Temp. °C**	**Chlorine** ε^{ITL}_{vap}	**Temp. °C**
Benzene	0.25 (2) (Baertschi et al., 1953)	34.6				
Benzene	0.23 (Narten and Kuhn, 1961)					
Benzene	0.17 (1) (Harrington et al., 1999)	20-35	3.1 (1) (Wang and Huang, 2003)	24		
Chloroform	0.8 (2) (Baertschi et al., 1953)	34.6				
Carbon-tetrachloride	1.3 (2) (Baertschi et al., 1953)	34.6				
Trichloroethene	0.35 (1) (Poulson and Drever, 1999)	22	8.9 (1) (Poulson and Drever, 1999)	22	-1.74 (1) (Poulson and Drever, 1999)	22
MTBE			5.2 (1) (Wang and Huang, 2003)	24		

Measurement method
1) Progressive vaporization at natural abundance
2) Mono-labeled substance
3) Extrapolated from poly-labeled substance using the rule of the geometric mean.

1.3.2 Air-water partitioning

As chlorinated ethenes NAPLs dissolved in groundwater can volatilize from a plume toward the unsaturated zone, isotope fractionation associated with air-water partitioning needs to be known. Only few studies are related to the isotope effect of air-water partitioning of VOCs. Isotope fractionation during air-water partitioning was most of the time evaluated during headspace equilibration experiments. According to Hunkeler & Aravena (2000), molecules of chlorinated methanes, ethanes, and ethenes in the gas phase were enriched in ^{13}C compared to molecules in aqueous samplesby up to 1.46‰ in the case of chlorinated methanes.

More information is however available for gaseous compounds such as methane. Based on experiments and calculations, Bacsik & al. (2002) and Costa-Gomez & Grolier (2001) have highlighted opposite enrichment factors for carbon and hydrogen isotopes of methane during phase partitioning between air and water. In fact, deuterated methane was shown to be less soluble in water than methane (about 1.6% at room temperature) (Costa-Gomez & Grolier, 2001), while the solubility is higher for $^{13}CH_4$ than that for $^{12}CH_4$ (about 0.06% at 20°C) (Bacsik & al, 2002). Isotope effect during air-water partitioning of methane can be evaluated using IR spectroscopy and simulation methods (Bacsik & al., 2002). Jansco & al. (1974 & 2002) has shown that hindered translations and rotations will always work in the direction of a normal isotope effect. In contrary, the frequencies of the internal vibrations will in most cases shift toward lower frequencies (red shift) upon dissolution of molecules in aqueous phase, leading to an inverse isotope effect. The opposite isotope fractionation observed for carbon and hydrogen isotopes by Bacsik & al. (2002) and Costa-Gomez & Grolier (2001) can be explained with spectroscopic data. While the $^{12}C/^{13}C$ solubility isotope effect is mainly influenced by the hindered translational motions and the frequency shifts of the asymmetric vibrations of the methane molecules in the aqueous solution, the H/D isotope effect results from the hindered rotations and symmetric vibrations (Costa-Gomez & Grolier, 2001; Jansco, 2002).

1.3.3 Diffusion

Since the diffusion coefficient in air is dependent on the molecule mass (Fuller et al., 1966), the isotopologues of a compound diffuse at different velocities and hence a diffusion isotope effect can occur. The molecular diffusion coefficients available from the literature often refer to measurements of the overall diffusion and can be considered to be equal to that of the light isotopologue which usually dominates. However, this is not the case for polychlorinated hydrocarbons, as light and heavy chlorine isotopes both occur at relatively high natural abundances in the environment. Due to the supplementary weight, a heavy isotopologue is

expected to diffuse slower than a light one. The mass dependence of the diffusion coefficient for diffusion in air is usually described by (Craig, 1953; Cerling & al., 1991):

$$\alpha_{DIFF}^{ITL} = \frac{D_h}{D_l} = \sqrt{\frac{(M_h + M_{air}) \cdot M_l}{(M_l + M_{air}) \cdot M_h}} \qquad \textit{(equation 5)}$$

where D_h and D_l are the diffusion coefficient for heavy and light isotopologues respectively, M_l is the molecular weight of the light molecule, M_h the molecular weight of the heavy molecule, and M_{air} the molecular weight of air (28.8 in this case). Differences in diffusion coefficients can be expressed on a per mille scale in analogy to the isotope enrichment factor (ε):

$$\varepsilon_{DIFF}^{ITL} = (\frac{D_h}{D_l} - 1) \cdot 1000 \quad (‰) \qquad \textit{(equation 6)}$$

A number of studies have demonstrated isotope fractionation during diffusion of CO_2 (Craig, 1953; Jost, 1960; Cerling & al., 1991), CH_4 (Prinzhofer & Pernaton, 1997; De Visscher & al., 2004; Urmann & al., 2007; Mahieu & al., 2008) and N_2O (Well & Flessa, 2008) in porous medium at the field and laboratory scale. De Visscher & al. (2004) have highlighted that neglecting the isotope fractionation by diffusion results in underestimation of the methane oxidation based on isotope data in landfill cover soils. The vertical profile of the $\delta^{13}C$ value of methane in a column experiment confirmed that isotope fractionation associated with gas transport occurred. Similar effects were observed in the field, but at a less pronounced extend (De Visscher & al., 2004). In the same study, the isotope-dependence of the diffusion coefficient was also determined experimentally and compared to the theoretical value determined with equation 5. For methane, the column experiment gave a value of -17.8‰ that correspond well to the theoretical value of -19.5‰ calculated using equation 5 for carbon isotopes. In another study, a carbon isotope enrichment factor of -4.2‰ was measured for CO_2 in soils, which is close to the value (-4.4‰) obtained with equation 5 (Cerling & al., 1991). While most studies considered only two isotopologues (e.g. $^{12}CH_4$ vs $^{13}CH_4$), a study on N_2O diffusion evaluated expected isotope trends for different diffusion scenario taking into account the four dominant isotopologues of N_2O (Well & Flessa, 2008).

1.3.4 Biodegradation

Numerous studies have demonstrated that isotope fractionation occurs during aerobic and anaerobic biodegradation of common organic contaminants such as chlorinated ethenes and ethanes, aromatic hydrocarbons and short chain alkanes as summarized in several reviews (Meckenstock & al., 2004; Schmidt & al., 2004; Elsner & al., 2005; Hunkeler & Morasch,

2010). In addition to carbon isotope fractionation, hydrogen isotope fractionation was demonstrated by several authors (Elsner & al., 2005; Meckenstock & al., 2004; Schmidt & al., 2004). These studies have shown that the magnitude of isotope fractionation depends on the degradation mechanism and also on the size of the molecules (Elsner, 2010). Most of the laboratory studies were carried out under saturated conditions but it can be expected that similar isotope fractionation factors are obtained for similar processes under unsaturated conditions.

As already mentioned, heavy isotopes progressively become enriched during biodegradation. Microorganisms degrade molecules containing light isotopes preferentially, as cleavage of chemical bonds between two light isotopes is faster compared to bonds between a light and a heavy isotope (Bouchard & al., 2008c). Since different biodegradation pathways of organic compounds may involve different bonds and reaction mechanisms, the magnitude of isotope fractionation depends on the degradation pathway (Morasch & al., 2001; Morasch & al., 2002; Hunkeler & al., 2005). Chlorine isotope fractionation is for example significantly larger during reductive dechlorination of cis-dichlorothylene (cDCE) and vinylchloride (VC) than during aerobic oxidation of the same molecule (Abe & al., 2009). Moreover, this result highlights the advantage of using carbon and chlorine dual isotope analysis to differentiate degradation pathways. The magnitude of fractionation is also dependent on the position of heavy isotopes in the molecule. For larger molecules, the heavy isotope is more frequently located at a non reactive position, which ‘’dilute” isotope effect (Bouchard & al., 2008c). The ratio in reaction rate between molecules containing light and heavy isotopes located at the reactive position is denoted as kinetic isotope effect:

$$KIE = {}^{l}k/{}^{h}k \qquad \textit{(equation 7)}$$

where ${}^{l}k$ and ${}^{h}k$ are the degradation rate coefficients (first order) of light and heavy isotope, respectively. For enzymatic processes, the observed isotope effect is often lower than the KIE because binding steps that precede bond cleavage can be rate limiting and hence is denoted as apparent kinetic isotope effect (AKIE) (Elsner & al., 2005). The observed isotope effect may also be reduced if isotopes of the same ion are located at non-reactive positions. The effect of non-reactive positions is thus taken into account using the following equation (Elsner & al., 2005):

$$AKIE \approx \frac{1}{1+n\varepsilon/1000} \qquad \textit{(equation 8)}$$

where n is the number of atoms of interest composing the molecule.

1.3.5 Coupling of processes

In the unsaturated zone, vaporization, diffusion and biodegradation of chlorinated solvent often occur at the same time. Hence, the isotope ratios are potentially influenced by all these processes simultaneously. As demonstrated in details by Bouchard & al. (2008b), the isotope evolution of a source of NAPL subject to vaporization and diffusion across a porous media is expected to follow a Rayleigh trend. The isotope fractionation factor of the source of contamination (α_{source}) is then expected to follow the following relation (for carbon isotopes):

$$\alpha_{source} = \frac{{}^{h}D_{m}}{{}^{l}D_{m}} \cdot \frac{{}^{h}P}{{}^{l}P} = \alpha_{vap} \cdot \alpha_{diff} \qquad \textit{(equation 9)}$$

where ${}^{l}P$ and ${}^{h}P$ are the vapor pressures of molecules with light isotopes only and molecules with one heavy isotope, respectively; ${}^{l}D_{m}$ and ${}^{h}D_{m}$ the gas-phase diffusion coefficients of molecules with light isotopes only and molecules with one heavy isotope, respectively; and α_{vap} and α_{diff} the isotope fractionation factors of vaporization and diffusion, respectively. Moreover, as all these processes take place between isotopologues and not isotopes, it will be necessary to show if isotope and isotopologue evolve in the same way during vaporization and diffusion, as already described for reactive processes by Elsner & Hunkeler (2008).

So far, the combined effect of transport and biodegradation in the unsaturated zone has mainly been investigated for methane, but not organic contaminants (Reeburgh & al., 1997; De Visscher & al., 2004; Urmann & al., 2007; Mahieu & al., 2008). The isotope evolution of methane due to the combined effect of degradation and diffusion is frequently described using the following equation (De Visscher & al., 2004):

$$\delta E = \delta A + 1000 \cdot f_{ox} \cdot (\alpha_{ox} - \alpha_{trans}) \qquad \text{(equation 10)}$$

where δE is the isotope ratio of methane leaving the system in which transformation takes place, δA the initial isotope ratio of the methane, α_{ox} and α_{trans} the isotope fractionation factors associated with oxidation and transport, respectively, and f_{ox} the fraction of methane oxidized. This equation is mainly used for methane transport and degradation in landfill covers and the transport of methane is assumed to be dominated by advection (Liptay et al., 1998; Chanton and Liptay, 2000; De Visscher & al., 2004). In previous studies, the fractionation factor for methane transport (α_{trans}) was thus often assumed to 1 (i.e. no fractionation). However, diffusion is often an important transport mechanism for gases in the unsaturated zone, and contrary to advection, lead to an isotope fractionation (Mahieu & al.,

2007). De Visscher & al. (2004) have found a value of α_{trans} as high as 1.014 during field investigation. Neglecting isotope fractionation by diffusion will thus lead to underestimate methane oxidation. Furthermore, there are also some fundamental questions regarding the validity of the equation. If the equation was valid, it should converge to the Rayleigh equation in an advection dominated system, as α_{trans} approaches 1. However, this is clearly not the case and the following equation is obtained:

$$\delta E = \delta A + f_{ox} \cdot (a_{ox} - 1) \cdot 1000 \qquad \textit{(equation 11)}$$

which shows a very different trend as function of f_{ox} compared to the Rayleigh equation:

$$\delta E = \delta A + \ln(1 - f_{ox}) \cdot (a_{ox} - 1) \cdot 1000 \qquad \textit{(equation 12)}$$

In several studies, the isotope evolution due to biodegradation and diffusion was simulated using analytical or numerical models and diffusion was described by either Fickian or Stefan-Maxwell equations (Reeburgh & al., 1997; De Visscher & al., 2004; Urmann & al., 2007; Mahieu & al., 2008). The different parameters such as the amount of methane degradation were then estimated by fitting the modeled data to the measured data.

In summary, except for methane, little is known about the combined effect of vaporization, diffusion and biodegradation on the isotope ratio of organic compounds in porous media under variable saturated conditions and such information for chlorinated solvents will be on great interest.

1.4 Aims and approach of the thesis

In order to apply CSIA to differentiate sources of contamination and assess biodegradation under variably saturated conditions, the effect of relevant processes on isotope ratios of VOCs need to be known. For chlorinated ethenes, which are the focus of the project, the major processes include vaporization, air-water partitioning, diffusion and biodegradation. In contrast to petroleum hydrocarbons, less information is available on isotope fractionation during these processes for chlorinated hydrocarbons, especially for chlorine isotopes. Additionally, little is known on how isotope ratios evolve when these processes interact. The main aim of this study is thus to quantify the magnitude of isotope fractionation during different physical processes occurring in the unsaturated zone, as well as to investigate how isotope ratios evolve if several processes interact. The present work focuses on chlorinated hydrocarbons since less it known about isotope fractionation for this group of compounds

and since they are among the most common contaminants found in the environment. The experimental part of the PhD considered two different scenarios, a NAPL source from which compounds vaporize and diffuse through the unsaturated zone, and a groundwater plume from which contaminants are released and diffuse through the unsaturated zone. In a first step, isotope fractionation during processes relevant for the release of compounds from NAPL (vaporization) or groundwater (air-water partitioning) was investigated. High precision equilibrium isotope fractionation factors for air-water partitioning and vaporization were determined using a new experimental approach that excluded kinetic contributions. In a second step, the combined effect of release of compounds from NAPL or groundwater and transport by diffusion through unsaturated porous media was investigated. In case of a NAPL source, a 1D column setup was used. In case of a groundwater source, a 2D system was used in order to reproduce groundwater flow that influences the transfer of compounds from the saturated to the unsaturated zone. In addition to these experimental studies, numerical simulations were carried out for the interpretation of the results of the 2D experiment and to evaluate the magnitude of isotope fractionation of biodegradation in unsaturated zone studies. As the study focuses on chlorinated hydrocarbons, some methodological developments were also necessary regarding the analysis of chlorine isotopes and data interpretation. For polychlorinated hydrocarbons, several isotopologues occur at relevant concentrations and might show a different behavior during partitioning, transport and reactive processes. A new analytical method, based on GC-qMS measurements, was evaluated. As the GC-qMS method makes it possible to track chlorine isotopologue ratios directly, it was possible, for the first time, to compare isotope and isotopologue evolution during vaporization, diffusion and combination of them at a theoretical and experimental level. Specific objectives and study methods of individual chapters are summarized below.

Chapter 2: Carbon and chlorine isotopes were investigated together as in practical applications a dual isotope approach is more promising to relate isotope variations to different processes. However, in order to investigate chlorine isotope behaviour, it was first necessary to develop analytical methods and methods for data interpretation. In the first part of this chapter, the precision, linearity and accuracy of a new analytical method for chlorine isotope ratio analyses based on GC-qMS measurements were evaluated. In a second part, it was evaluated theoretically how isotope and isotopologue ratios are expected to evolve during physical processes and are related to each other. As both light and heavy chlorine isotopes are present naturally at high abundances, several isotopologues occur at relevant concentrations. Hence, physical processes occurring in the unsaturated zone take place

among isotopologues and not directly isotopes. However, during analysis not all isotopologues might be quantified. For the data interpretation, it needs to be known how isotope ratios and isotope enrichment factors can be derived from isotopologue data.

Chapter 3: In order to apply CSIA for the evaluation of the origin and fate of organic contaminants in unsaturated conditions, the effect of physical processes on isotope ratios needs to be known. In this chapter, the scenario of a NAPL source located in the unsaturated zone from which compounds vaporize and diffuse was specially evaluated. Chlorine and carbon isotope fractionation during vaporization and air-water partitioning were first evaluated in isolation using a multistep equilibration approach. The isotope fractionation during the combination of vaporization from a NAPL source and diffusion in porous media (diffusion-controlled vaporization) was then quantified using a 1D column filled with sand.

Chapter 4: The scenario of a groundwater plume from which contaminants are released and diffuse through the unsaturated zone was then evaluated in order to evaluate if CSIA can be used to link a contaminant plume to contaminant vapors in the unsaturated zone. The effect of air-water partitioning on isotope ratios was first evaluated in isolation. Isotope fractionation during the transfer of VOCs across the capillary fringe and diffusion through the unsaturated zone was then investigated with a 2D system laboratory experiments and numerical modeling. As PCE is stable under oxic conditions which are typically encountered in sandy unsaturated zones (Bradley, 2000), it was used as a model compound to avoid any influence of biodegradation.

Chapter 5: In this chapter, the magnitude of isotope fractionation during biodegradation of VOCs in unsaturated conditions where diffusion is the main transport process was investigated. Vinyl chloride (VC) was chosen as model compound as it degrades under oxic conditions that commonly occur in the unsaturated zone. Isotope fractionation during biodegradation was first studied in isolation during microcosm experiments. Numerical modelling was then used to explore the coupled effect of air-water partitioning, diffusion and biodegradation on isotope ratios. Effective isotope enrichment factors for biodegradation in such conditions were evaluated.

Chapter 6: Finally, the last chapter provides a conclusion about the different studies of the thesis, draws general conclusions and includes an outlooks about the applications of CSIA in unsaturated zone studies.

1.5 References

- **Abe**, Y.; Hunkeler, D. Does the Rayleigh equation apply to evaluate field isotope data in contaminant hydrogeology? *Environ. Sci. Technol.* **2006**, 40 (5), 1588-1596.
- **Abe**, Y.; Aravena, R.; Zopfi, J.; Shouakar-Stash, O.; Cox, E.; Roberts, J.D.; Hunkeler, D. Carbon and chlorine isotope fractionation during aerobic oxidation and reductive dechlorination of vinyl chloride and cis-1,2-dichloroethene. *Environ. Sci. Technol.* **2009**, 43 (1), 101-107.
- **Aeppli**, C.; Holmstrand, H.; Andersson, P.; Gustafsson, O. Direct compound-specific stable chlorine isotope analysis of organic compounds with quadrupole GC/MS using standard isotope bracketing. *Anal. Chem.* **2010**, 82 (1), 420-426.
- **Baehr**, A.L. Selective transport of hydrocarbons in the unsaturated zone due to aqueous and vapor phase partitioning. *Water Resour. Res.* **1987**, 23 (10), 1926-1938.
- **Baehr**, A.L.; Stackelberg, P.E.; Baker, R.J. Evaluation of the atmosphere as a source of volatile organic compounds in shallow groundwater. *Water Resour. Res.* **1999**, 35 (1), 127-136.
- **Baertschi**, P.; Kuhn, W.; Kuhn, H. Fractionation of isotopes by distillation of some organic substances. *Nature* **1953**, 171 (4362), 1018-1020.
- **Bacsik**, Z.; Lopes, J.N.C.; Costa Gomes, M.F; Jancso, G.; Mink, J.; Padua, A.A.H. Solubility isotope effects in aqueous solutions of methane. *J. Chem. Phys.* **2002**, 116 (24), 10816-10824.
- **Bigeleisen**, J.; Mayer, M.G. Calculation of equilibrium constants for isotopic exchange reactions. *J. Chem. Phys.* **1947**, 15 (5), 261-267.
- **Bigeleisen**, J. Statistical mechanics of isotope effects on thermodynamic properties of condensed systems. *J. Chem. Phys.* **1961**, 34 (5), 1485-&.
- **Blessing**, M.; Schmidt, T.C.; Dinkel, R.; Haderlein, S. B. Delineation of multiple chlorinated ethene sources in an industrialized area-a forensic field study using. *Environ. Sci. Technol.* **2009**, 43 (8), 2701-2707.
- **Bohy**, M.; Dridi, L.; Schafer, G.; Razakarisoa, O. Transport of a mixture of chlorinated solvent vapors in the vadose zone of a sandy aquifer: Experimental study and numerical modeling. *Vadose Zone J.* **2006**, 5 (2), 539-553.
- **Bouchard**, D.; Hunkeler, D.; Gaganis, P.; Aravena, R.; Hohener, P.; Broholm, M.M.; Kjeldsen, P. Carbon isotope fractionation during diffusion and biodegradation of petroleum hydrocarbons in the unsaturated zone: Field experiment at Vaerlose airbase, Denmark, and modeling. *Environ. Sci. Technol.* **2008**, 42 (2), 596-601.
- **Bouchard**, D.; Hohener, P.; Hunkeler, D. Carbon isotope fractionation during volatilization of petroleum hydrocarbons and diffusion across a porous medium: A column experiment. *Environ. Sci. Technol.* **2008**, 42 (21), 7801-780.
- **Bouchard**, D.; Hunkeler, D.; Hohener, P. Carbon isotope fractionation during aerobic biodegradation of n-alkanes and aromatic compounds in unsaturated sand. *Organic Geochemistry* **2008**, 39 (1), 23-33.
- **Bradley**, P.M. Microbial degradation of chloroethenes in groundwater systems. *Hydrogeol. J.* **2000**, 8 (1), 104-111.
- **Cerling**, T.E.; Solomon, D.K.; Quade, J.; Bowman, J.R. On the isotopic composition of carbon in soil carbon-dioxide. *Geochim. Cosmochim. Acta* **1991**, 55 (11), 3403-3405.
- **Chanton**, J.; Liptay, K. Seasonal variation in methane oxidation in a landfill cover soil as determined by an in situ stable isotope technique. *Glob. Biogeochem. Cycle* **2000**, 14 (1), 51-60.
- **Christophersen**, M.; Broholm, M.M.; Mosbaek, H.; Karapanagioti, H.K.; Burganos, V.N.; Kjeldsen, P. Transport of hydrocarbons from an emplaced fuel source experiment in the vadose zone at airbase Vaerlose, Denmark. *J. Contam. Hydrol.* **2005**, 81 (1-4), 1-33.
- **Clark**, I.D.; Fritz, P. Environmental isotopes in hydrogeology. Lewis Publishers, Boca Raton, Florida, USA, **1997**, 328 pp.

- **Conant**, B.H.; Gillham, R.W.; Mendoza, C.A. Vapor transport of trichloroethylene in the unsaturated zone: Field and numerical modeling investigations. *Water Resour. Res.* **1996**, 32 (1), 9-22.
- **Costa Gomes**, M.F., Grolier, J-P. Determination of Henry's law constants for aqueous solutions of tetradeuteriomethane between 285 and 325 K and calculation of the H/D isotope effect. *Phys Chem Chem Phys* **2001**, 3, 1047–1052.
- **Cotel**, S.; Schafer, G.; Barthes, V.; Baussand, P. Effect of density-driven advection on trichloroethylene vapor diffusion in a porous medium. *Vadose Zone J.* **2011**, 10 (2), 565-581.
- **Craig**, H. The geochemistry of the stable carbon isotopes. *Geochim. Cosmochim. Acta* **1953**, 3 (2-3), 53-92.
- **De Visscher**, A.; De Pourcq, I.; Chanton, J. Isotope fractionation effects by diffusion and methane oxidation in landfill cover soils. *J. Geophys. Res.-Atmos.* **2004**, 109 (D18), 8.
- **Elsner**, M.; Zwank, L.; Hunkeler, D.; Schwarzenbach, R.P. A new concept to link observed stable isotope fractionation to degradation pathways of organic groundwater contaminants. *Environ. Sci. Technol.* **2005**, 39 (18), 6896-6916.
- **Elsner**, M.; Hunkeler, D. Evaluating chlorine isotope effects from isotope ratios and mass spectra of polychlorinated molecules. *Anal. Chem.* **2008**, 80 (12), 4731-4740.
- **Elsner**, M. Stable isotope fractionation to investigate natural transformation mechanisms of organic contaminants: Principles, prospects and limitations. *J. Environ. Monit.* **2010**, 12 (11), 2005-2031.
- **Falta**, R.W.; Javandel, I.; Pruess, K.; Witherspoon, P.A. Density-driven flow of gas in the unsaturated zone due to the evaporation of volatile organic-compounds. *Water Resour. Res.* **1989**, 25 (10), 2159-2169.
- **Fuller**, E.N.; Schettle, Pd; Giddings, J.C.A. new method for prediction of binary gas-phase diffusion coeffecients. *Industrial and Engineering Chemistry* **1966**, 58 (5), 19-&.
- **Grootes**, P.M.; Mook, W.G.; Vogel, J.C. Isotopic fractionation between gaseous and condensed carbon dioxide. *Zeitschrift fur Physik* **1969**, 221 (3), 257-&.
- **Harrington**, R.R., Poulson, S.R., Drever, J.I., Colberg, P.J.S. and Kelly, E.F., 1999. Carbon isotope systematics of monoaromatic hydrocarbons: vaporization and adsorption experiments. *Organic Geochemistry* **1999**, 30 (8A), 765-775.
- **Hofstetter**, T.B.; Reddy, C.M.; Heraty, L.J.; Berg, M.; Sturchio, N.C. Carbon and chlorine isotope effects during abiotic reductive dechlorination of polychlorinated ethanes. *Environ. Sci. Technol.* **2007**, 41 (13), 4662–4668.
- **Höpfner**, A. Vapor pressure isotope effects. *Angew. Chem.-Int. Edit.* **1969**, 8 (10), 689-&.
- **Huang**, L.; Sturchio, N.C.; Abrajano, T.; Heraty, L.J.; Holt, B.D. Carbon and chlorine isotope fractionation of chlorinated aliphatic hydrocarbons by evaporation. *Organic Geochemistry* **1999**, 30 (8A), 777-785.
- **Hunkeler**, D.; Aravena, R.; Butler, B.J. Monitoring microbial dechlorination of tetrachloroethene (PCE) in groundwater using compound-specific stable carbon isotope ratios: Microcosm and field studies. *Environ. Sci. Technol.* **1999**, 33 (16), 2733-2738.
- **Hunkeler**, D.; Aravena, R. Determination of compound-specific carbon isotope ratios of chlorinated methanes, ethanes, and ethenes in aqueous samples. *Environ. Sci. Technol.* **2000**, 34 (13), 2839-2844.
- **Hunkeler**, D.; Chollet, N.; Pittet, X.; Aravena, R.; Cherry, J.A.; Parker, B.L. Effect of source variability and transport processes on carbon isotope ratios of TCE and PCE in two sandy aquifers. *J. Contam. Hydrol.* **2004**, 74 (1-4), 265-282.
- **Hunkeler**, D.; Aravena, R.; Berry-Spark, K.; Cox, E. Assessment of degradation pathways in an aquifer with mixed chlorinated hydrocarbon contamination using stable isotope analysis. *Environ. Sci. Technol.* **2005**, 39 (16), 5975-5981.
- **Hunkeler**, D.; Abe, Y.; Broholm, M.M.; Jeannottat, S.; Westergaard, C.; Jacobsen, C.S.; Aravena, R.; Bjerg, P.L. Assessing chlorinated ethene degradation in a large scale contaminant plume by dual carbon-chlorine isotope analysis and quantitative PCR. *J. Contam. Hydrol.* **2010**, 119 (1-4), 69-79.

- **Hunkeler**, D. and Morasch, B. Isotope fractionation during transformation processes. In: C. Press (Editor), Environmental isotopes in biodegradation and bioremediation. CRC Press, Boca Raton, **2010**, pp. 79-125.
- **Jancso**, G.; Vanhook, W.A. Condensed phase isotope-effects (especially vapor-pressure isotope-effects). *Chem. Rev.* **1974**, 74 (6), 689-750.
- **Jancso**, G. Interpretation of isotope effects on the solubility of gases. *Nukleonika* **2002**, 47 (1), 53–57.
- **Jendrzejewski**, N.; Eggenkamp, H.G.M.; Coleman, M.L. Characterisation of chlorinated hydrocarbons from chlorine and carbon isotopic compositions: Scope of application to environmental problems. *Appl. Geochem.* **2001**, 16 (9-10), 1021-1031.
- **Johnson**, R.L.; Pankow, J.F. Dissolution of dense chlorinated solvents into groundwater. 2. Source functions for pools of solvent. *Environ. Sci. Technol.* **1992**, 26 (5), 896-901.
- **Jost**, W. Diffusion in Solids, Liquids and Gases, 3d ed. Academic Press, New-York, **1960**.
- **Jury**, W. A.; Spencer, W. F.; Farmer, W. J. Behavior assessment model for trace organics in soil .1. Model description. *J. Environ. Qual.* **1983**, 12 (4), 558-564.
- **Jury**, W.A.; Spencer, W.F.; Farmer, W.J. Behavior assessment model for trace organics in soil: IV. Review of experimental evidence. *J. of Environ. Qual.* **1984**, 13 (4), 580-586.
- **Kuder**, T.; Philp, P.; Allen, J. Effects of volatilization on carbon and hydrogen isotope ratios of MTBE. *Environ. Sci. Technol.* **2009**, 43 (6), 1763-1768.
- **Liptay**, K.; Chanton, J.; Czepiel, P.; Mosher, B. Use of stable isotopes to determine methane oxidation in landfill cover soils. *J. Geophys. Res.-Atmos.* **1998**, 103 (D7), 8243-8250.
- **McCarthy**, K.A.; Johnson, R.L. Transport of volatile organic-compounds across the capillary-fringe. *Water Resour. Res.* **1993**, 29 (6), 1675-1683.
- **Mahieu**, K.; De Visscher, A.; Vanrolleghem, P.A.; Van Cleemput, O. Carbon and hydrogen isotope fractionation by microbial methane oxidation: Improved determination. *Waste Manage.* **2006**, 26 (4), 389-398.
- **Mahieu**, K.; De Visscher, A.; Vanrolleghem, P.A.; Van Cleemput, O. Modeling of stable isotope fractionation by methane oxidation and diffusion in landfill cover soils. *Waste Manage.* **2008**, 28 (9), 1535-1542.
- **Meckenstock**, R.U.; Morasch, B.; Griebler, C.; Richnow, H.H. Stable isotope fractionation analysis as a tool to monitor biodegradation in contaminated aquifers. *J. Contam. Hydrol.* **2004**, 75 (3-4), 215-255.
- **Mercer**, J.W.; Cohen, R.M. A review of immiscible fluids in the subsurface: Properties, models, characterization and remediation. *J. Contam. Hydrol.* **1990**, 6 (2), 107-163.
- **Morasch**, B.; Richnow, H.H.; Schink, B.; Meckenstock, R.U. Stable hydrogen and carbon isotope fractionation during microbial toluene degradation: Mechanistic and environmental aspects. *Appl. Environ. Microbiol.* **2001**, 67 (10), 4842-4849.
- **Morasch**, B.; Richnow, H.H.; Schink, B.; Vieth, A.; Meckenstock, R.U. Carbon and hydrogen stable isotope fractionation during aerobic bacterial degradation of aromatic hydrocarbons. *Appl. Environ. Microbiol.* **2002**, 68 (10), 5191-5194.
- **Narten**, A.; Kuhn, W. Genaue Bestimmung kleiner Dampfdruckunterschiede isotoper Verbindungen. II) Der $^{13}C/^{12}C$-Isotopieeffekt in Tetrakohlenstoff und in Benzol. *Helv. Chim. Acta* **1961**, 44, 1474-1479.
- **Pasteris**, G.; Werner, D.; Kaufmann, K.; Höhener, P. Vapor phase transport and biodegradation of volatile fuel compounds in the unsaturated zone: a large scale lysimeter experiment. *Environ. Sci. Technol.* **2002**, 36, 30–39.
- **Poulson**, S.R.; Drever, J.I. Stable isotope (C, Cl, and H) fractionation during vaporization of trichloroethylene. *Environ. Sci. Technol.* **1999**, 33 (20), 3689-3694.
- **Prinzhofer**, A.; Pernaton, E. Isotopically light methane in natural gas: Bacterial imprint or diffusive fractionation? *Chem. Geol.* **1997**, 142 (3-4), 193-200.

- **Reeburgh**, W.S.; Hirsch, A.I.; Sansone, F.J.; Popp, B.N.; Rust, T.M. Carbon kinetic isotope effect accompanying microbial oxidation of methane in boreal forest soils. *Geochim. Cosmochim. Acta* **1997**, 61 (22), 4761-4767.
- **Sakaguchi-Soder**, K.; Jager, J.; Grund, H.; Matthaus, F.; Schuth, C. Monitoring and evaluation of dechlorination processes using compound-specific chlorine isotope analysis. *Rapid Commun. Mass Spectrom.* **2007**, 21 (18), 3077-3084.
- **Schmidt**, T.C.; Zwank, L.; Elsner, M.; Berg, M.; Meckenstock, R.U.; Haderlein, S.B. Compound-specific stable isotope analysis of organic contaminants in natural environments: A critical review of the state of the art, prospects, and future challenges. *Anal. Bioanal. Chem.* **2004**, 378 (2), 283-300.
- **Sherwood Lollar**, B.; Slater, G.F.; Sleep, B.; Witt, M.; Klecka, G.M.; Harkness, M.; Spivack, J. Stable carbon isotope evidence for intrinsic bioremediation of tetrachloroethene and trichloroethene at area 6, Dover air force base. *Environ. Sci. Technol.* **2001**, 35 (2), 261-269.
- **Shouakar-Stash**, O.; Frape, S.K.; Drimmie, R.J. Stable hydrogen, carbon and chlorine isotope measurements of selected chlorinated organic solvents. *J. Contam. Hydrol.* **2003**, 60 (3-4), 211-228.
- **Slater**, G.F.; Dempster, H.S.; Lollar, B.S.; Ahad, J. Headspace analysis: A new application for isotopic characterization of dissolved organic contaminants. *Environ. Sci. Technol.* **1999**, 33 (1), 190-194.
- **Slater**, G.F. Stable Isotope Forensics - When Isotopes Work. *Environ. Forensics* **2003**, 4 (1), 13-23.
- **Smith**, J.A., Tisdale, A.K.; Cho, H.J. Quantification of natural vapor fluxes of trichloroethene in the unsaturated zone at Picatinny Arsenal, New Jersey. *Environ. Sci. Technol.* **1996**, 30 (7), 2243-2250.
- **Urmann**, K.; Norina, E.S.; Schroth, M.H.; Zeyer, J. Methanotrophic activity in a diffusive methane/oxygen counter-gradient in an unsaturated porous medium. *J. Contam. Hydrol.* **2007**, 94 (1-2), 126-138.
- **Van Hook**, A.W. Condensed matter isotope effects. In Isotope Effects in Chemistry and Biology; Kohen, A.; Limbach, H. H. Eds.; CRC Press - Taylor & Francis Group, LLC: Boca Raton, **2006**, 1096 pp.
- **Van Warmerdam**, E.M.; Frape, S.K.; Aravena, R.; Drimmie, R.J.; Flatt, H.; Cherry, J.A. Stable chlorine and carbon isotope measurements of selected chlorinated organic solvents. *Appl. Geochem.* **1995**, 10 (5), 547–552.
- **Wang**, Y.; Huang, Y.S. Hydrogen isotope fractionation of low molecular weight n-alkanes during progressive vaporization. *Organic Geochemistry* **2001**, 32 (8), 991-998.
- **Wang**, Y.; Huang, Y.S. Hydrogen isotopic fractionation of petroleum hydrocarbons during vaporization: Implications for assessing artificial and natural remediation of petroleum contamination. *Appl. Geochem.* **2003**, 18 (10), 1641-1651.
- **Well**, R.; Flessa, H. Isotope fractionation factors of N_2O diffusion. *Rapid Commun. Mass Spectrom*. **2008**, 22 (17), 2621-2628.
- **Werner**, D.; Hohener, P. Diffusive partitioning tracer test for nonaqueous phase liquid (NAPL) detection in the vadose zone. *Environ. Sci. Technol.* **2002**, 36 (7), 1592-1599.

Chapter 2

Analytical and conceptual developments for the application of chlorine isotopes in unsaturated zone studies

Abstract

In order to investigate chlorine isotope behaviour, it was necessary to develop analytical methods and methods for data interpretation. The accuracy, precision and amount dependency of chlorine isotope ratio analyses performed with gas chromatography quadrupol mass-spectrometry (GC-qMS) were evaluated for two Agilent and Thermo instruments. The calibration of raw data to SMOC scale (Standard Mean Ocean Chloride) with external standards has been shown to deviate between instruments and over time. For that reason, at least two calibration standards are required to obtain reproducible isotopic values and true isotopic variations between samples. Precision of measurements varies from an instrument to another ($1\sigma \approx 0.2$-0.5% for Agilent and 0.2-0.9% for Thermo GC-qMS). Additionally, different amount dependencies of $\delta^{37}Cl$ values were observed for each instrument, but could be eliminated by adjusting amplitudes of standards and samples. Nevertheless, $\delta^{37}Cl$ measurements showed good agreement between various instruments when the same external standards were used. In the second part of this chapter, a theoretical comparison between isotope and isotopologue fractionation during vaporization and diffusion was performed, as physical processes occurring in the unsaturated zone take place among isotopologues and not directly isotopes. It was demonstrated that, during vaporization, diffusion and combination of them, the isotope ratio evolves parallel to the isotopologue ratio.

Partially published in Analytical Chemistry and Environmental Science and Technology:

- Bernstein, A.; Shouakar-Stash, O.; Ebert, K.; Laskov, C.; Hunkeler, D.; Jeannottat, S.; Sakaguchi-Söder, K.; Laaks, J.; Jochmann, M. A.; Cretnik, S.; Jager, J.; Haderlein, S. B.; Schmidt, T. C.; Aravena, R.; Elsner, M. Compound-specific chlorine isotope analysis: A comparison of gas chromatography/isotope ratio mass spectrometry and gas chromatography/quadrupole mass spectrometry methods in an interlaboratory study. Anal. Chem. 2011, 83 (20), 7624-7634.
- Jeannottat, S.; Hunkeler, D. Chlorine and carbon isotopes fractionation during volatilization and diffusive transport of trichloroethene in the unsaturated zone. Environ. Sci. Technol. 2012, 46 (6), 3169-3176.

2.1 Introduction and aim of the chapter

Compound specific isotope analysis (CSIA) essentially relies on isotope ratio mass spectrometry (IRMS) coupled to either gas or liquid chromatography (GC or LC) for the measurement of $^{13}C/^{12}C$ ratios (with both GC and LC), as well as $^{15}N/^{14}N$ and $^{2}H/H$ ratios (with GC). These online techniques generally require combustion or pyrolyse to simple analyte gases, extensive preconcentration of samples and a dedicated instrumentation to reach high precision. As chlorinated compounds such as tetrachloroethylene (PCE) and trichloroethylene (TCE) are among the most abundant groundwater contaminants, chlorine is another element of high relevance for CSIA analysis (Sakaguchi-Söder & al., 2007). Moreover, dual isotope analysis has recently demonstrated to be very insightful to evaluate contaminant degradation pathways (Van Warmerdam & al., 1995; Hofstetter & al., 2007) and to distinguish between different contaminant sources (Schmidt & al., 2004; Shouakar-Stash & al., 2003). While the dual isotope approach can be used for hydrocarbon, for which $\delta^{13}C$ and δD methods are available, it is rarely used for chlorinated ethenes despite an increased interest, because of the complexity of $\delta^{37}Cl$ analyses. Traditional offline chlorine isotope analysis require the conversion of chlorinated compounds into molecules containing only one chlorine atom, such as methyl chloride (CH_3Cl) or cesium chloride (CsCl) (Holt & al., 1997; Holmstrand & al., 2004). Analyses are then performed using dual-inlet isotope ratio mass spectrometry (DI-IRMS) for CH_3Cl and using thermal ionization mass spectrometry (TIMS) for CsCl.

Recently, Shouakar-Stash et al. (2006) have established the first online method for chlorine CSIA using direct injections into a GC coupled to a continuous flow (CF)-IRMS. As only two GC/IRMS instruments worldwide (Munich and Waterloo) are configured for direct $\delta^{37}Cl$ measurements (Bernstein et al., 2011), a more universal method was established by Sakaguchi-Söder et al. (2007) using widely available gas chromatography-quadrupole mass spectrometry (GC-qMS) in selected ion monitoring (SIM) mode. In this study, both fragments and molecular ions were taken into account during isotope ratios measurements and calculations. This method was then modified by Aeppli et al. (2010) that considered only molecular ions for their calculations, and performed a calibration with external standards to obtain δ values on the SMOC scale. In contrast to carbon or hydrogen isotopes, light and heavy chlorine isotopes both occur at relatively high natural abundances in the environment (75.78% for ^{35}Cl and 24.22% for ^{37}Cl) and are two mass apart (Aelion & al., 2010). These characteristics make it possible to record mass spectral data with a scanning quadrupole MS sufficiently precise to calculate isotope ratios (Elsner & Hunkeler, 2008). Stable chlorine

isotope ratios of measured compounds are calculated based on peak areas of selected target ions using a set of mathematical equations (Sakaguchi-Söder & al., 2007).

In order to investigate chlorine isotope behaviour, it was necessary to develop analytical methods and methods for chlorine isotope data interpretation. In the first part of this chapter, a new analytical method for δ^{37}Cl analyses based on GC-qMS measurements was evaluated in order to apply it in the experiments presented in this thesis. In a second part, a conceptual development was performed in order to evaluate if isotopes and isotopologue (chemically identical molecule with a different isotopic composition) ratios evolve in parallel during the various physical processes occurring in the unsaturated zone.

In the first part of this chapter, tests to determine the precision, amount dependency and accuracy of the GC-qMS method were thus carried out as part of an interlaboratory comparison study including 6 laboratories (Bernstein & al., 2011). This study makes it possible to compare GC-qMS measurements with GC-IRMS results. It also allows for the first time to determine if measurements performed with various GC-qMS and in different laboratory are reliable and comparable. In chapter 2.2, the results obtained in the laboratory of Neuchâtel with GC-qMS systems from two different manufacturers (Thermo and Agilent) and conclusions on the use of GC-qMS for δ^{37}Cl analyses are provided. These results were also compared to GC-IRMS measurements carried out in the University of Waterloo. This study also validates this new measurement method in the laboratory of Neuchâtel.

In the second part of this chapter, isotope and isotopologue fractionation during vaporization and diffusion of polychlorinated hydrocarbons are compared using TCE as an example. As both light and heavy isotopes are present naturally at high abundances, several isotopologues occur at relevant concentrations in the environment. These isotopologues might thus show a different degree of fractionation during transport and partitioning processes occurring in the unsaturated zone. Moreover, analytical methods based on GC-qMS and GC-IRMS usually only measure the abundance of selected fragment and molecular ions. Elsner & Hunkeler (2008) already show that, for reactive processes such as biodegradation, chlorine isotope and isotopologue fractionation is proportional in good approximation. However, it is necessary to determine if, in a diffusion controlled system, the isotope ratio evolves parallel to the isotopologue ratio as well, and if it is admissible to derive isotope ratios from isotopologue ratios even if not all isotopologues are measured. The chapter 2.3 thus provides a theoretical basis to compare isotope and isotopologue fractionation during vaporization and diffusion. It also provides the basis on how to quantify isotope and isotopologue fractionation from the raw data and how to model chlorine isotope trends.

2.2 Compound-specific chlorine isotope analysis using a GC-qMS (interlaboratory comparaison study)

Recently, new approaches were developed for the analysis in continuous flow of chlorine isotope ratios of chlorinated compounds. These analytical methods are based on either GC-IRMS or GC-qMS measurements. However, a benchmark for standard routine applications was missing. The interlaboratory comparison study systematically compared the performance of GC-MS versus GC-IRMS in six laboratories involving eight different instruments (GC/IRMS, Isoprime and Thermo MAT-253; GC/qMS, Agilent 5973N, two Agilent 5975C, two Thermo DSQII, and one Thermo DSQI) (Bernstein & al, 2011). In the following sections, the results of the laboratory of Neuchâtel are highlighted in order to validate the measurement approach for the laboratory and define the methodology chosen for δ^{37}Cl measurements in the various experiments of the present thesis. The results of GC-qMS measurements were compared to the values measured with the IRMS of Waterloo, as the results of this instrument were in fact used as the consensus values during the interlaboratory comparison study (Bernstein & al., 2011).

2.2.1 Materials and methods

In Neuchâtel, two different GC-qMS were evaluated. A Thermo Trace GC-DSQII MS (Thermo Fisher Scientific, Waltham, MA) and an Agilent 7890A GC coupled to an Agilent 5975C quadrupole mass selective detector (Agilent Technologies, Santa Clara, CA).

The Thermo GC-qMS was used with an Agilent DB-VRX column (60 m, 0.32 mm ID, 1.8 µm). Flow velocity was set to 1.5 ml/min, with a split ratio of 1:10. The temperature program was 150ºC for 4 min, followed by a ramp of 15 ºC/min to 200ºC for 1 min. Ions defined by the single ion mode were m/z 60, 62, 95, 97, 130 and 132. A dwell time of 30 msec with a SIM width of 0.2 were defined for all measurements. Electron energy was set to 70 eV and auto-tuning was performed before each sequence. Headspace injections were performed using a Combi Pal autosampler. Samples were prepared in 20 ml headspace vials, filled with 10 mL of the sample. 500µl of gas from the headspace were injected in the GC-qMS

The Agilent GC-qMS was used with an Agilent DB-5 column (30 m, 0.25 mm ID, 0.25 µm). Flow velocity was set to 1.2 ml/min, with a split ratio of 1:10. The temperature program was 40ºC for 2 min, followed by a ramp of 10 ºC/min to 50ºC, 35 ºC/min to 100ºC, and 100ºC for 1 min. For all measurements, the first two molecular ions of the TCE (m/z 130 and 132) were measured in SIM mode, with a dwell time of 50 msec and a SIM width of 0.3. Electron energy was set to 70 eV. Sample injection was performed with a Combi Pal Autosampler as described for the Thermo GC-qMS.

Various TCE, purchased from 5 different manufacturers, were used in the study. The pure TCE products were divided into 1.8 ml glass vials using a 50 ml glass syringe, to ensure homogeneity. To avoid volatilization, vials were filled without headspace and sealed immediately with Teflon lined caps before shipment to all participating laboratories. Two of these TCE were analyzed as calibration standards (Eil-1 (3.05‰) and Eil-2 (-2.7‰)) and 5 were analyzed as samples. The standards were calibrated to the SMOC scale (n=15) against defined standards using a GC-IRMS in Waterloo (Shouakar-Stash & al., 2006). A concentrated TCE stock solution (940 mg/l) was prepared in the laboratory of Neuchâtel for each pure TCE by adding 162 µl of TCE to 250 ml of pure water and was stirred for about 12 hours with a magnetic stirrer. The stock solution was distributed into 24 ml vials and a new vial was used for each new standards preparation. Different amounts of stock solution were transferred into headspace vials prefilled with water using a high precision pipette with plastic tips (which were shown to no interfere) and immediately closed by a second person. The low relative standard deviation of the peak area for samples with the same concentration (about 4%) indicated that the sample preparation was reliable.

Amount dependency and accuracy tests were carried out for the two GC-MS instruments. During amount dependency tests, two vials were prepared for each TCE samples at each concentration, and 5 replicates were analyzed per vial. During accuracy tests, two headspace vials were prepared for each TCE sample and 5 replicates were analyzed. Additionally, ten replicates of each standard (Eil-1 and 2) were analyzed at the beginning and the end of each analytical sequence (two vials per standard analyzed 5 times). During each analytical sequence, a blank was run after every 10 injections to assure the absence of carry over.

For the Thermo GC-qMS, the raw isotopic ratios were then calculated using an equation proposed by Sakaguchi-Söder & al. (2007):

$$R_{TCE} = \frac{1}{3} \cdot \frac{I_{132}}{I_{130} + I_{95} + I_{60}} + \frac{1}{2} \cdot \frac{I_{97}}{I_{130} + I_{95} + I_{60}} + \frac{I_{62}}{I_{130} + I_{95} + I_{60}} \qquad \textit{(equation 1)}$$

where I is the corresponding molecular ion abundance at different m/z values.

For the Agilent GC-qMS, the raw isotopic ratios were then calculated using an equation proposed by Aeppli & al. (2010), which relies on molecular ions of two isotopologues:

$$R_{TCE} = \frac{I_{132}}{3 \cdot I_{130}} \qquad \textit{(equation 2)}$$

2.2.2 Results for Neuchâtel laboratory

In order to test the amount dependency of the system (often referred as linearity) and to evaluate how the precision varies as a function of the signal height, different amounts of TCE were injected several times. For the Agilent-qMS, standard deviations of 0.16 – 0.49 (n=10) are observed and Thermo qMS values have a lower precision (σ = 0.37 – 0.92, n=5). Additionally, standard deviations obtained for replicate injections of the same amount of TCE were higher on GC-qMS instruments than on GC/IRMS of Waterloo (used as consensus value for the Interlaboratory study). For the Thermo-qMS, the amount dependency experiments demonstrate clearly that the amount dependency effects are pronounced if the standards have a constant concentration, whereas the concentrations of the samples vary (Figure 1a). In contrast, these effects become negligible if the amount of the standard is adapted to sample concentrations (Figures 1b). As adjust samples and standards to the same concentration is an interesting strategy when samples with known concentrations are analyzed, it will be necessary to analyze standards with various concentrations along the sequence if sample concentrations are not known. On the other hand, the Agilent-qMS provide a good amount dependency for the TCE even if standard concentrations are not adjusted to the amount of samples (figure 1c).

Different instruments thus do not show the same amount dependency and similar analytical concepts do not necessarily involve an identical pattern of amount dependency (Bernstein & al., 2011). Moreover, the interlaboratory study highlights that even instruments of similar construction (same manufacturer) gave different amount dependency trends (data not shown). An important finding of the section is that a proper standardization scheme may eliminate the need of amount dependency correction. Standard bracketing and appropriate corrections are necessary when nonlinearity effects occur, as already brought forward by Shouakar-Stash & al (2006). Additionally, each GC-qMS must be calibrated individually and calibration standards analyzed during each sequence in order to obtain reproducible results.

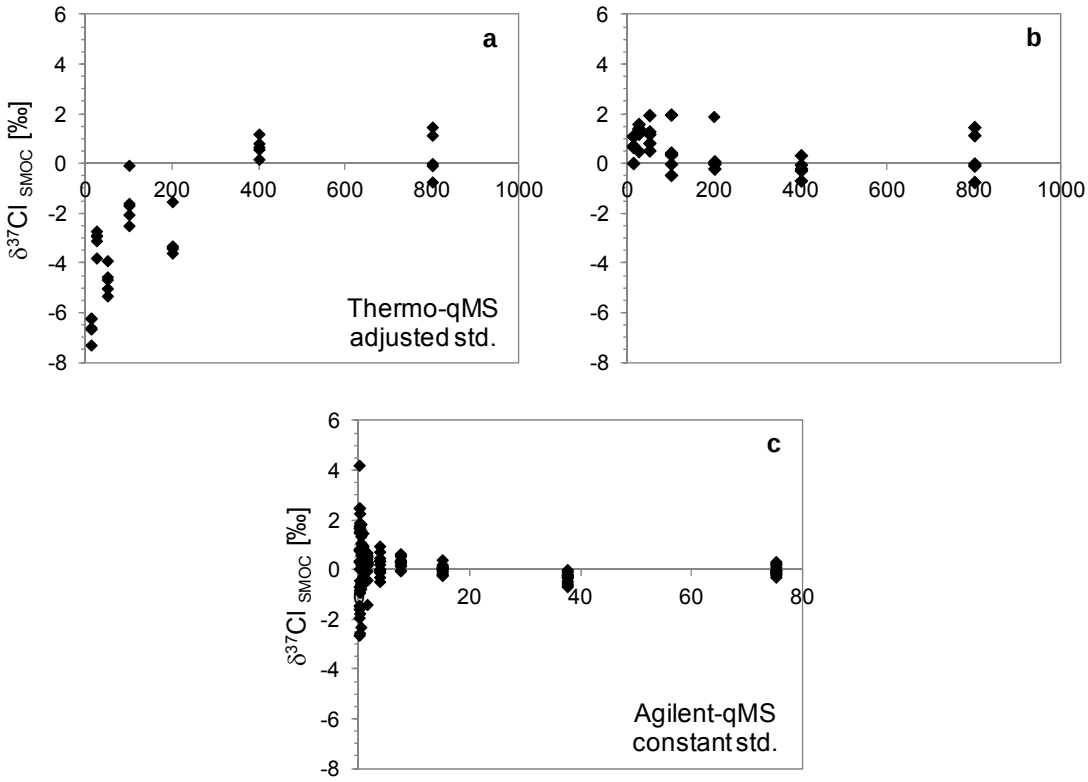

Figure 1: Measured δ^{37}Cl depending on the on-column amount of TCE. Values are presented as the difference from the average of the replicates in the highest on-column amount. (a) Thermo-qMS (amplitude of standards along the sequence was held constant). (b) Thermo-qMS (standards were adapted to the amplitude of target peaks). (c) Agilent-qMS (amplitude of standards along the sequence was held constant). Modified after Bernstein & al. (2011).

In order to evaluate the precision and accuracy of GC-qMS measurements to determine chlorine isotope ratios of chlorinated ethenes, a comparison of the performances of the two GC-qMS of Neuchâtel was carried out by analyzing 7 distinct pure TCE products (Figure 2). Two of these TCE were analyzed as calibration standards (Eil-1 (3.05‰) and Eil-2 (-2.7‰)) in order to obtain a two-point calibration. The measurements reveal that the slopes of calibration curves were different between instruments, with a slope of 1.09±0.06 for the Agilent-qMS and 1.24±0.22 for the Thermo-qMS (The given uncertainty corresponds to 95% confidence intervals that were calculated from the slope's standard error multiplied by the appropriate student t factor for α = 0.05.). Calibration slopes did not only differ between instruments, but also change over time. Calibration slopes ranged between 1.10 and 1.21 for the Agilent-qMS over 6 months during the various experiments carried out with the TCE in chapter 3. Therefore, even differences of isotope values measured between two samples analyzed at different times would be inaccurate without a proper calibration.

The need for a two-point calibration is also supported by the results of the accuracy test, as shown in Figure 2. Five TCE products of different producers were analyzed with the two GC-qMS, using either one or two TCE standards for calibration to the SMOC scale. The results were compared to the values measured with the IRMS of Waterloo, as the results of this instrument were used as the consensus values during the interlaboratory comparison study (Bernstein & al., 2011). When results are projected on the SMOC scale using one standard only (Eil-2), large differences of chlorine isotopic values are obtained (Figure 2b). In contrast, when using two standards for the calibration, a better agreement is obtained between instruments (Figure 2a), with differences between the two GC-qMS and the GC-IRMS generally in a range of 1σ (n = 10). Therefore, differences of isotope values measured between two samples would be inaccurate without a proper calibration.

Finally, this interlaboratory comparison makes it possible to roughly estimate the accuracy of the different methods compared to the consensus value. If the averages values measured for the five TCE samples by the Agilent and Thermo GC-qMS are compared to these consensus values, the most extreme difference between each instrument and the consensus value may provide an estimation of the error of the instrument (Bernstein & al., 2011). An interval of 0.21‰ was obtained for the Agilent-qMS. In the case of the Thermo-qMS, this interval is larger, with a value of 0.92‰. Taking into account that this instrument is also more influenced by amount dependency, it seems thus less suitable for chlorine isotope analysis. Moreover, the Thermo-qMS values shown in the figure 2 represent the best run completed on this instrument, and the precision of measurements strongly varied with time. These results suggest that different types of GC-qMS instruments do not show the same performance for isotope analysis due to differences in the construction of the instrument or data processing. The accuracy test of the interlaboratory comparison study has also highlighted the need of a two point calibration to convert raw data to SMOC scale.

According to the results of this comparison, the Agilent-qMS have only a small amount dependency, a better precision and accuracy that the Thermo-qMS. The Agilent-qMS was thus selected to carry out δ^{37}Cl measurements of the present thesis.

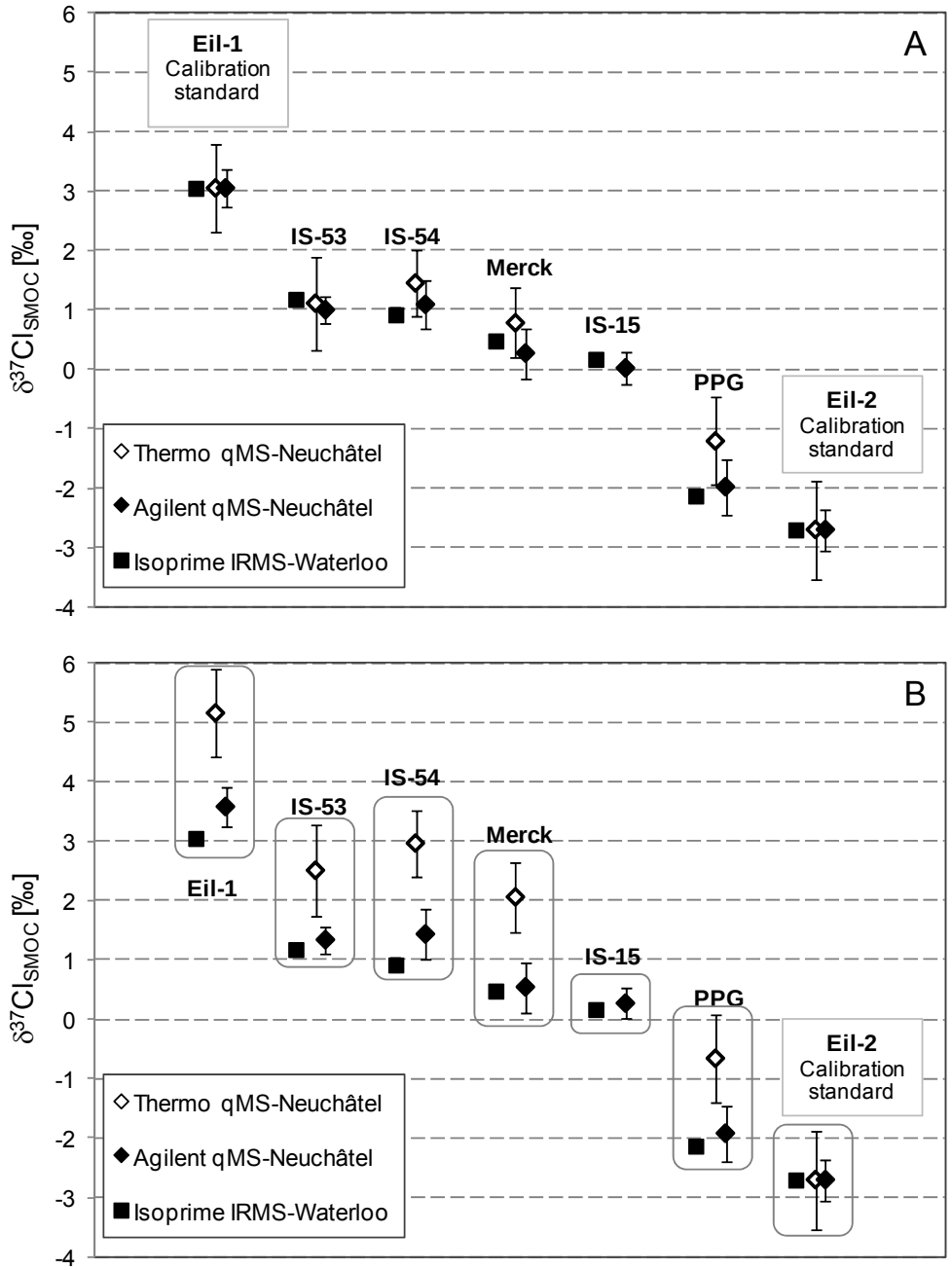

Figure 2: Measured $\delta^{37}Cl$ of 5 different TCE products with different instruments. A) Calibration to the SMOC scale was carried out using two standards. B) Calibration to the SMOC scale was carried out using a single standard. Error bars represent standard deviations. Measurements on the IRMS-Isoprime in Waterloo represent the consensus value. Modified after Bernstein & al. (2011). (IRMS values of TCE products: Eil-1 3.05‰, IS-53 1.18‰, IS-54 0.92‰, Merck 0.48‰, IS-15 0.17‰, PPG -2.13‰, Eil-2 -2.7‰)

2.3 Isotope and isotopologue fractionation during vaporization and diffusion

Since heavy isotopes of chlorine are present at a high abundance, several isotopologues of polychlorinated hydrocarbons occur at relevant concentrations. These isotopologues will show different concentration trends during fractionating physico-chemical and reactive processes. However, analytical methods based on GC-qMS and GC-IRMS will usually only measure the abundance of selected fragment and molecular ions. This raises the questions whether isotope ratios and isotope fractionation factors can be quantified from such partial information. For reactive processes, it has been demonstrated that isotope fractionation is proportional to isotopologue fractionation and hence isotope ratios can confidently be derived from fragment and/or molecular ion ratios (Elsner & Hunkeler, 2008). However, for physico-chemical processes occurring in the unsaturated zone, such a derivation is lacking so far.

The main goal of this section is to determine how isotopes and isotopologue fractionation is related during major physical processes controlling the fate of chlorinated hydrocarbons in the unsaturated zone. Chlorinated hydrocarbons might frequently be presented as NAPL, raising the question whether isotope and isotopologue fractionation occurs during transfer to the gas phase. Once vaporized, diffusion is usually the dominant transport process. Hence this chapter mainly focuses on the effect of NAPL-vapor equilibration and diffusion on isotope and isotopologue ratios. At first, the effect of NAPL-vapor equilibration only and diffusion only is evaluated. Then, it is explored how isotope and isotopologues evolve during diffusion-controlled vaporization i.e. when the two processes are coupled.

In chapter 3, the trends of four chlorine isotopologues were tracked during diffusion-controlled vaporization experiments, and chlorine isotopologue fractionation was compared to chlorine isotope fractionation on an experimental level in addition to the theoretical level of the present section. The following notation will be used:

Notation

M_{000}/ M_{001} /M_{011} /M_{111}	Amount of isotopologue with zero/one/two/three ^{37}Cl in NAPL [g]
X_{000}/ X_{001} /X_{011} /X_{111}	Mole fraction of isotopologue with zero/one/two/three ^{37}Cl [mol]
P_{000}/ P_{001} /P_{011} /P_{111}	Vapor pressure of isotopologue with zero/one/two/three ^{37}Cl [atm]
D_{000}/ D_{001} /D_{011} /D_{111}	Diffusion coefficient of isotopologue with zero/one/two/three ^{37}Cl [cm^2/s]
C_{000}/ C_{001} /C_{011} /C_{111}	Concentration of isotopologue with zero/one/two/three ^{37}Cl in source [g/l]

A	Cross-section of column [cm]	L	Length of column [cm]
τ	Tortuosity [-]	T	Temperature [°K]
R	Gas constant [l·atm/K·mol]]		

2.3.1. Isotopologue fractionation during NAPL-vapor equilibration

In order to relate isotopologue fractionation to isotope fractionation, it has to be known how ratios between different isotopologue pairs evolve. For vaporization, such relationships can be developed based on the rule of the geometric mean (RGM) for thermodynamic isotope fractionation as developed by Bigeleisen (1995). The rule basically states that the effect of adding another heavy isotope is additive and independent of how many heavy isotopes are already in the molecule. The RGM has frequently been applied for vapor pressure calculations. Assuming ideal mixing, the vapor pressure of different isotopologues can be related by:

$$P_{XY'_{n-z}Y_z}{}^{n} = P_{XY'_{n-z}}{}^{n-z} \cdot P_{XY_z}{}^{z} \qquad \textit{(equation 3)}$$

Where Y' is a light and Y a heavy isotope, n the total number of element Y in the molecule and z the number of heavy isotope of Y in the molecule.

Using TCE as an example:

$$P_{001}{}^{3} = P_{000}{}^{2} \cdot P_{111}{}^{1} \qquad \textit{(equation 4)}$$

Dividing by $P_{000}{}^{3}$ leads to:

$$\frac{P_{001}{}^{3}}{P_{000}{}^{3}} = \frac{P_{000}{}^{2} \cdot P_{111}{}^{1}}{P_{000}{}^{3}} \qquad \textit{(equation 5)}$$

Or

$$\left(\frac{P_{001}}{P_{000}}\right)^{3} = \frac{P_{111}}{P_{000}} \qquad \textit{(equation 6)}$$

Using this rule we can express the vapor pressure of mixed isotopolgues based on the vapor pressure of pure isotopologues as follows:

$$P_{001} = P_{000}{}^{2/3} \cdot P_{111}{}^{1/3} \qquad \textit{(equation 7)}$$

$$P_{011} = P_{000}{}^{1/3} \cdot P_{111}{}^{2/3} \qquad \textit{(equation 8)}$$

Based on these equations we now express vapor pressure ratios of pairs of isotopologues with one heavy isotope difference:

$$\frac{P_{001}}{P_{000}} = \frac{P_{000}{}^{2/3} \cdot P_{111}{}^{1/3}}{P_{000}} = \left[\frac{P_{111}}{P_{000}}\right]^{1/3} \qquad \textit{(equation 9)}$$

$$\frac{P_{011}}{P_{001}} = \frac{P_{000}{}^{1/3} \cdot P_{111}{}^{2/3}}{P_{000}{}^{2/3} \cdot P_{111}{}^{1/3}} = \left[\frac{P_{111}}{P_{000}}\right]^{1/3} \qquad \textit{(equation 10)}$$

$$\frac{P_{111}}{P_{011}} = \frac{P_{111}}{P_{000}^{1/3} \cdot P_{111}^{2/3}} = \left[\frac{P_{111}}{P_{000}}\right]^{1/3} \qquad \textit{(equation 11)}$$

Or $$\frac{P_{001}}{P_{000}} = \frac{P_{011}}{P_{001}} = \frac{P_{111}}{P_{011}} \qquad \textit{(equation 12)}$$

In other words, if the RGM applies, isotopologue fractionation during NAPL-vapor equilibration is identical for all isotopologue pairs.

2.3.2. Isotopologue fractionation during diffusion

For gas phase diffusion, the ratio of diffusion coefficients between two isotopologues is given by:

$$\alpha_{DIFF}^{ITL} = \frac{D_{001}}{D_{000}} = \sqrt{\frac{(MW_{001} + MW_{air}) \cdot MW_{000}}{(MW_{000} + MW_{air}) \cdot MW_{001}}} \qquad \textit{(equation 13)}$$

where $MW_{000/001/011/111}$ is molecular weight of isotopologue with zero/one/two/three heavy isotopes and MW_{air} the molecular weight of air

Since the molecular weight of TCE is high compared to the differences in weight between heavy and light chlorine isotope, the mass ratio of all isotopologue pairs differing by one heavy isotope is similar (i.e. 132/130 is similar to 134/132 to 136/134). As the result, the ratio in diffusion factor is similar in good approximation:

$$\alpha_{DIFF}^{ITL} = \frac{D_{001}}{D_{000}} \approx \frac{D_{011}}{D_{001}} \approx \frac{D_{111}}{D_{011}} \qquad \textit{(equation 14)}$$

In other words, also for diffusion isotopologue fractionation is identical in good approximation for all isotopologue pairs.

2.3.3 Isotopologue fractionation during diffusion-controlled vaporization

For this derivation, it is assumed that equilibrium conditions are established at the NAPL-vapor interface for all isotopologues and that the vaporization rate is diffusion controlled, in analogy to numerous studies on vaporization of water (Craig & Gorden, 1965; He & Smith, 1999). This assumption is consistent with field and modeling studies (Conant & al., 1996) on passive NAPL vaporization in porous media that indicate the establishment of a NAPL-vapor equilibrium in the source zone due to the relatively slow transport of gaseous compounds away from the source zone. The mathematical derivation is carried out for the limiting case where vaporization is sufficiently slow that no isotopologue fractionation occurs in the NAPL

phase. Hence kinetic isotopologue fractionation only occurs due to gas phase diffusion. As during this thesis (Chapter 3) diffusion-controlled vaporization was studied in a column, here a mathematical relation for a 1D system is derived. According to Fick's first law, the mass flux of an isotopologue across a 1D column at equilibrium is given by:

$$\frac{dM_{000}}{dt} = -A \cdot \tau \cdot D_{000} \cdot \frac{C_{000}}{L} \qquad \textit{(equation 15)}$$

$$\frac{dM_{001}}{dt} = -A \cdot \tau \cdot D_{001} \cdot \frac{C_{001}}{L} \qquad \textit{(equation 16)}$$

Assuming that a NAPL-vapor equilibrium is established at the source, the gas phase concentration at the source can be expressed using Raoult's law, which leads to:

$$\frac{dM_{000}}{dt} = -A \cdot \tau \cdot D_{000} \cdot \frac{X_{000} \cdot P_{000}}{R \cdot T \cdot L} = -A \cdot \tau \cdot D_{000} \cdot \frac{M_{000} / \sum M_i \cdot P_{000}}{R \cdot T \cdot L} \qquad \textit{(equation 17)}$$

$$\frac{dM_{001}}{dt} = -A \cdot \tau \cdot D_{001} \cdot \frac{X_{001} \cdot P_{001}}{R \cdot T \cdot L} = -A \cdot \tau \cdot D_{001} \cdot \frac{M_{001} / \sum M_i \cdot P_{001}}{R \cdot T \cdot L} \qquad \textit{(equation 18)}$$

Division of 18 by 17 leads to:

$$\frac{dM_{001}}{dM_{000}} = \frac{D_{001} \cdot M_{001} \cdot P_{001}}{D_{000} \cdot M_{000} \cdot P_{000}} \qquad \textit{(equation 19)}$$

Separation of variables leads to:

$$\frac{dM_{001}}{M_{001}} = \frac{dM_{000}}{M_{000}} \frac{D_{001} \cdot P_{001}}{D_{000} \cdot P_{000}} \qquad \textit{(equation 20)}$$

Integration of equation 20 from t=0 to t=t leads to:

$$\ln \frac{M_{001,t}}{M_{001,0}} = \frac{D_{001} \cdot P_{001}}{D_{000} \cdot P_{000}} \cdot \ln \frac{M_{000,t}}{M_{000,0}} \qquad \textit{(equation 21)}$$

Or $$\frac{M_{001,t}}{M_{001,0}} = \left(\frac{M_{000,t}}{M_{000,0}} \right)^{\alpha_{Eff}^{ITL}} \qquad \textit{(equation 22)}$$

with $$\alpha_{Eff}^{ITL} = \frac{D_{001} \cdot P_{001}}{D_{000} \cdot P_{000}} = \alpha_{Vap}^{ITL} \cdot \alpha_{Diff}^{ITL} \qquad \textit{(equation 23)}$$

Division of both sides by $M_{000,t}/M_{000,0}$ leads to:

$$\frac{M_{001,t}/M_{000,t}}{M_{001,0}/M_{000,0}} = \left(\frac{M_{000,t}}{M_{000,0}}\right)^{\alpha_{Eff}^{ITL}-1} \qquad \textit{(equation 24)}$$

Or $$\frac{R_{000/001,t}}{R_{000/001,0}} = \left(\frac{M_{000,t}}{M_{000,0}}\right)^{\alpha_{Eff}^{ITL}-1} \qquad \textit{(equation 25)}$$

Where $R_{000/001,t}$ represents the isotopologue ratio at time t and $R_{000/001,0}$ the initial isotopologue ratio.

Analogous equations hold also for other isotopologue ratios. Hence the isotopologue evolution of the NAPL source is controlled by a combination of isotopologue fractionation due to NAPL-vapor equilibration and diffusion.

In the following isotope and isotopologue fractionation during diffusion-controlled vaporization are thus compared with each other. Based on equation 12 and 14 above, the effective isotopologue fractionation factor is the same for all isotopologue pairs.

$$\alpha_{Eff}^{ITL} = \frac{D_{001}\cdot P_{001}}{D_{000}\cdot P_{000}} = \frac{D_{011}\cdot P_{011}}{D_{001}\cdot P_{001}} = \frac{D_{111}\cdot P_{111}}{D_{011}\cdot P_{011}} \qquad \textit{(equation 26)}$$

The isotopologue evolution for compounds with zero and one heavy isotopes is given by:

$$\frac{M_{001,t}/M_{000,t}}{M_{001,0}/M_{000,0}} = \left(\frac{M_{000,t}}{M_{000,0}}\right)^{\alpha_{Eff}^{ITL}-1} \qquad \textit{(equation 27)}$$

For isotopologues with one more heavy isotope each, the following equation is obtained:

$$\frac{M_{011,t}/M_{001,t}}{M_{011,0}/M_{001,0}} = \left(\frac{M_{001,t}}{M_{001,0}}\right)^{\alpha_{Eff}^{ITL}-1} \qquad \textit{(equation 28)}$$

Inserting equation 22 into equation 28 leads to:

$$\frac{M_{011,t}/M_{001,t}}{M_{011,0}/M_{001,0}} = \left(\frac{M_{000,t}}{M_{000,0}}\right)^{\alpha_{EFF}^{ITL}(\alpha_{Eff}^{ITL}-1)} \approx \left(\frac{M_{000,t}}{M_{000,0}}\right)^{\alpha_{Eff}^{ITL}-1} \qquad \textit{(equation 29)}$$

The approximation is associated with only a small error as alpha deviates from one only by a few permille in maximum. Combinining equation 28 and 29 leads to:

$$\frac{M_{001,t} / M_{000,t}}{M_{001,0} / M_{000,0}} = \frac{M_{011,t} / M_{001,t}}{M_{011,0} / M_{001,0}} \qquad \textit{(equation 30)}$$

Rearrangement of equation 30 and expressing the isotopologue concentrations at time zero in terms of relative abundances of different isotopologues (f) leads to:

$$\frac{M_{001,t} / M_{000,t}}{M_{011,t} / M_{001,t}} = \frac{M_{001,0} / M_{000,0}}{M_{011,0} / M_{001,0}} = \frac{3 \cdot {f_{35}}^2 \cdot f_{37} / {f_{35}}^3}{3 \cdot f_{35} \cdot {f_{37}}^2 / 3 \cdot {f_{35}}^2 \cdot f_{37}} = 3 \qquad \textit{(equation 31)}$$

And analoguously for isotopologues with one additional heavy isotopes:

$$\frac{M_{011,t} / M_{001,t}}{M_{111,t} / M_{011,t}} = \frac{M_{011,0} / M_{001,0}}{M_{111,0} / M_{011,0}} = \frac{3 \cdot f_{35} \cdot {f_{37}}^2 / 3 \cdot {f_{35}}^2 \cdot f_{37}}{{f_{37}}^3 / 3 \cdot f_{35} \cdot {f_{37}}^2} = 3 \qquad \textit{(equation 32)}$$

Equation 31 and 32 illustrate that also during diffusion-controlled vaporization, isotopologues fractionate proportionally. However, in contrast to a reactive processes the proportionality is only approximate.

The isotope ratio can thus be related to isopologue ratios as follows:

$$\begin{aligned}
\frac{^{37}Cl}{^{35}Cl} &= \frac{M_{001,t} + 2 \cdot M_{011,t} + 3 \cdot M_{111,t}}{M_{011,t} + 2 \cdot M_{001,t} + 3 \cdot M_{000,t}} = \frac{M_{001,t} / M_{000,t} + 2 \cdot M_{011,t} / M_{000,t} + 3 \cdot M_{111,t} / M_{000,t}}{M_{011,t} / M_{000,t} + 2 \cdot M_{001,t} / M_{000,t} + 3} \\
&= \frac{M_{001,t} / M_{000,t} + 2 \cdot (M_{011,t} / M_{001,t})(M_{001,t} / M_{000,t}) + 3 \cdot (M_{111,t} / M_{011,t})(M_{011,t} / M_{001,t})(M_{001,t} / M_{000,t})}{(M_{011,t} / M_{001,t})(M_{001,t} / M_{000,t}) + 2 \cdot M_{001,t} / M_{000,t} + 3} \\
&= \frac{M_{001,t} / M_{000,t} + 2/3 \cdot (M_{001,t} / M_{000,t})^2 + 3 \cdot (M_{001,t} / M_{000,t})^3}{1/3 \cdot (M_{001,t} / M_{000,t})^2 + 2 \cdot M_{001,t} / M_{000,t} + 3} \\
&= \frac{1/3 \cdot (M_{001,t} / M_{000,t}) \cdot [3 + 2 \cdot (M_{001,t} / M_{000,t}) + 1/3 \cdot (M_{001,t} / M_{000,t})^2]}{1/3 \cdot (M_{001,t} / M_{000,t})^2 + 2 \cdot M_{001,t} / M_{000,t} + 3} = 1/3 \cdot (M_{001,t} / M_{000,t})
\end{aligned}$$

(equation 33)

Hence also for a diffusion controlled system, the isotope ratio evolves parallel to the isotopologue ratio. It is thus admissible to derive isotope ratios from isotopologue ratios even if not all isotopologues are measured. Furthermore, fractionation factors can be quantified from either isotopologue or isotope ratios and identical values are expected.

2.4 Conclusions

The interlaboratory study compares the amount dependency, precision and accuracy of continuous flow GC-MS methods for chlorine isotope analysis of TCE. This study demonstrates that various instruments show a different amount dependency. However, the different amount dependency trends could be eliminated by bracketing samples with standards of the same concentrations. The precision and accuracy vary among instruments as well. The Agilent-qMS seems more suitable that the Thermo one. In fact, the Agilent-qMS has a better accuracy, precision, and amount dependency. Moreover, the two-point calibration gives variable slopes against SMOC scale and theses slopes show changes from a day to another. A two-point calibration is thus always necessary to measure chlorine isotopic ratios with GC-qMS instruments. It is necessary to calibrate each instrument on each measurement sequence in order to have reproducible values, too. However, despite a lower precision than GC-IRMS, GC-qMS is more universal and makes it possible to measure chlorine isotopic ratios of a wide range of chlorinated compounds. This study has also validated this new measurement method for our laboratory. Additionally, according to the results of this comparison study, the Agilent-qMS was selected to carry out all the analyses of the present thesis.

In the second part of this chapter, it was demonstrate that during vaporization and diffusion chlorine isotope and isotopologue fractionation is proportional in good approximation even when several isotopologues with multiple heavy isotopes are present, as previously also shown for reactive processes (Elsner & Hunkeler, 2008). It was also demonstrates that in a diffusion-controlled system, the isotope ratio evolves parallel to the isotopologue ratio. It seems thus possible to derive isotope ratios from isotopologue ratios even if not all isotopologues are measured and to quantify fractionation factors from either isotopologue or isotope ratios. This theoretical finding will be confirmed experimentally in chapter 3.

2.5 References

- **Aelion**, C. M; Höhener, P.; Hunkeler, D.; Aravena R. Environmental isotope in biodegradation and bioremediation. CRC Press, Taylor & Francis Group. Boca Raton, FL. **2010**, 464 pp.
- **Aeppli**, C.; Holmstrand, H.; Andersson, P.; Gustafsson, O. Direct compound-specific stable chlorine isotope analysis of organic compounds with quadrupole GC/MS using standard isotope bracketing. *Anal. Chem.* **2010**, 82 (1), 420-426.
- **Bernstein**, A.; Shouakar-Stash, O.; Ebert, K.; Laskov, C.; Hunkeler, D.; Jeannottat, S.; Sakaguchi-Söder, K.; Laaks, J.; Jochmann, M. A.; Cretnik, S.; Jager, J.; Haderlein, S. B.; Schmidt, T. C.; Aravena, R.; Elsner, M. Compound-specific chlorine isotope analysis: A comparison of gas chromatography/isotope ratio mass spectrometry and gas chromatography/quadrupole mass spectrometry methods in an interlaboratory study. *Anal. Chem.* **2011**, 83 (20), 7624-7634.
- **Bigeleisen**, J. Statistical mechanisms of isotopic systems with small quantum corrections. 1. General considerations and the rule of the geometric mean. *J. Chem. Phys.* **1955**, 23, (12), 2264-2267.
- **Conant**, B. H.; Gillham, R. W.; Mendoza, C. A. Vapor transport of trichloroethylene in the unsaturated zone: Field and numerical modeling investigations. *Water Resour. Res.* **1996**, 32, (1), 9-22.
- **Craig**, H.; Gordon, L. I. Deuterium and oxygen 18 variations in the ocean and the marine atmosphere. In Stable isotopes in oceanographic studies and paleotemperatures, Tongiorgi, E., Ed. Laboratorio di geologia nucleare: Pisa, Italy, 1965; pp 9-130.
- **Elsner**, M.; Hunkeler, D. Evaluating chlorine isotope effects from isotope ratios and mass spectra of polychlorinated molecules. *Anal. Chem.* **2008**, 80 (12), 4731-4740.
- **He**, H.; Smith, R. B. An advective-diffusive isotopic evaporation-condensation model. *J. Geophys. Res.-Atmos.* **1999**, 104, (D15), 18619-18630.
- **Hofstetter**, T. B.; Reddy, C. M.; Heraty, L. J.; Berg, M.; Sturchio, N. C. Carbon and chlorine isotope effects during abiotic reductive dechlorination of polychlorinated ethanes. *Environ. Sci. Technol.* **2007**, 41 (13), 4662–4668.
- **Hofstetter**, T. B.; Schwarzenbach, R. P.; Bernasconi, S. M. Assessing transformation processes of organic compounds using stable isotope fractionation. *Environ. Sci. Technol.* **2008**, 42 (21), 7737–7743.
- **Holmstrand**, H.; Andersson, P.; Gustafsson, O. *Anal. Chem.* **2004**, 76, 2336–2342.
- **Holt**, B. D.; Sturchio, N. C.; Abrajano, T. A.; Heraty, L. J. Conversion of chlorinated volatile organic compounds to carbon dioxide and methyl chloride for isotopic analysis of carbon and chlorine. *Anal. Chem.* **1997**, 69, 2727–2733.
- **Sakaguchi-Soder**, K.; Jager, J.; Grund, H.; Matthaus, F.; Schuth, C. Monitoring and evaluation of dechlorination processes using compound-specific chlorine isotope analysis. *Rapid Commun. Mass Spectrom.* **2007,** *21 (18)*, 3077-3084.
- **Schmidt**, T. C.; Zwank, L.; Elsner, M.; Berg, M.; Meckenstock, R. U.; Haderlein, S. B. Compound-specific stable isotope analysis of organic contaminants in natural environments: A critical review of the state of the art, prospects, and future challenges. *Anal. Bioanal. Chem.* **2004**, 378 (2), 283–300.
- **Shouakar-Stash**, O.; Frape, S. K.; Drimmie, R. J. Stable hydrogen, carbon and chlorine isotope measurements of selected chlorinated organic solvents. *J. Contam. Hydrol.* **2003,** *60 (3-4)*, 211-228.
- **Shouakar-Stash**, O.; Drimmie, R. J.; Zhang, M.; Frape, S. K. Compound-specific chlorine isotope ratios of TCE, PCE and DCE isomers by direct injection using CF-IRMS. *Appl. Geochem.* **2006**, 21, 766–781.
- **Van Warmerdam**, E. M.; Frape, S. K.; Aravena, R.; Drimmie, R. J.; Flatt, H.; Cherry, J. A. Stable chlorine and carbon isotope measurements of selected chlorinated organic solvents. *Appl. Geochem.* **1995**, 10 (5), 547–552.

Chapter 3

Chlorine and carbon isotope fractionation during volatilization and diffusive transport of trichloroethene in the unsaturated zone

Abstract

In order to apply compound-specific isotope methods to the evaluation of the origin and fate of organic contaminants in the unsaturated subsurface, the effect of physico-chemical processes on isotope ratios needs to be known. The main objective of this study is to quantify chlorine and carbon isotope fractionation during NAPL-vapor equilibration, air-water partitioning and diffusion of trichloroethene (TCE) and combinations of these effects during vaporization in porous media. Isotope fractionation is larger during NAPL-vapor equilibration than air-water partitioning. During NAPL-vapor equilibration, carbon and chlorine isotope ratios evolve in opposite directions although both elements are present in the same bond, with a normal isotope effect for chlorine (ε_{Cl}=-0.39±0.03‰) and an inverse effect for carbon (ε_{C}=+0.75±0.04‰). During diffusion-controlled vaporization in a sand column, no significant carbon isotope fractionation is observed (ε_{C} =+0.10±0.05‰) while fairly strong chlorine isotope fractionation occurs (ε_{Cl} =-1.39±0.06‰) considering the molecular weight of TCE. In case of carbon, the inverse isotope fractionation associated with NAPL-vapor equilibration and normal diffusion isotope fractionation cancel while for chlorine, both processes are accompanied by normal isotope fractionation and hence they cumulate. A source of contamination that has aged might thus show a shift toward heavier chlorine isotope ratios.

Published in Environmental Science and Technology:

- Jeannottat, S.; Hunkeler, D. Chlorine and carbon isotopes fractionation during volatilization and diffusive transport of trichloroethene in the unsaturated zone. Environ. Sci. Technol. 2012, 46 (6), 3169-3176.

3.1 Introduction and aim of the study

Stable isotope analysis is increasingly used to investigate the behaviour of organic or inorganic contaminants in the subsurface. Only few studies have investigated isotope fractionation during unsaturated zone processes such as vaporization, air-water partitioning (Baertschi & al., 1953; Harrington & al., 1999; Huang & al., 1999; Poulson & Drever, 1999; Kuder & al., 2009; Shin & Lee, 2010), or gas-phase diffusion (Bouchard & al., 2008a&b). Bouchard et al. (2008a&b) investigated carbon isotope fractionation during vaporization, diffusion and biodegradation of petroleum hydrocarbons in laboratory and field studies. They observed a depletion of heavy isotopes with distance from a NAPL source during the initial expansion of a vapor plume and an enrichment of heavy isotopes in the NAPL source during its progressive depletion. In contrast to petroleum hydrocarbons, less information is available on isotope fractionation during vaporization and air−water partitioning of chlorinated hydrocarbons, especially for chlorine isotopes. Poulson & al. (1999) and Huang & al. (1999) investigated chlorine and carbon isotope fractionation during vaporization of trichloroethene (TCE) from open vessels. They observed inverse isotope fractionation for carbon isotopes while for chlorine normal isotope fractionation occurred. Compared to carbon isotopes, chlorine isotope fractionation is more complex because several isotopologues (chemically identical molecule with a different isotopic composition) are present at high abundance in polychlorinated hydrocarbons. While for reactive processes it has recently been demonstrated that isotopologue fractionation is proportional to isotope fractionation and hence the classical Rayleigh approach can be applied (Elsner & Hunkeler, 2008), such a demonstration is lacking for partitioning processes, diffusion and the combination of them.

The mechanism of isotope fractionation during NAPL vaporization and the transfer of dissolved compounds to the gas phase has been conceptualized using a boundary layer model (Kuder & al., 2009) in analogy to the widely used Craig-Gorden model (CGM) for vaporization of water (Craig & Gordon, 1965). According to the CGM, isotope fractionation can result from different diffusion rates of isotopologues through boundary layers above and below the liquid-vapor interface and/or be associated with liquid-vapor transfer (Craig & Gordon, 1965). Isotope fractionation during liquid-vapor transfer can occur under equilibrium conditions and hence only depend on the thermodynamic properties of the compounds or under kinetic conditions whereby the configuration of the activated complex at the interface influences the magnitude of isotope fractionation as shown for water evaporation (Cappa & al., 2007). For water, liquid-vapor partitioning from open surfaces is often assumed to be rapid compared to transport through the boundary layers (Craig & Gordon, 1965; He & Smith, 1999; Horita & al., 1999). Hence, isotope fractionation during vaporization is

considered to result from equilibrium isotope fractionation at the vapor-liquid interface and an additional diffusion-controlled or kinetic contribution (Craig & Gordon, 1965; He & Smith, 1999; Horita & al., 1999). A similar concept also applies to passive vaporization of NAPL and air-water partitioning in porous media as partitioning processes are frequently at equilibrium at the local scale, usually denoted as local equilibrium assumption (LEA). Indeed the establishment of a NAPL-vapor equilibrium close to NAPL sources in porous media was observed in controlled-release field experiments and laboratory studies (Broholm & al., 2005; Conant & al., 1996). Hence, as a basis for interpretation of unsaturated zone isotope data, well-constrained isotope and isotopologue fractionation factors for equilibrium partitioning processes are required, as well as information on relative contribution of partitioning and diffusion processes on the effective isotope fractionation during vaporization.

The main goal of this study is to investigate chlorine and carbon isotope fractionation for NAPL-vapor equilibration, equilibrium air-water partitioning and diffusion-controlled vaporization of TCE as a model compound. Isotope fractionation during NAPL-vapor equilibration and air-water partitioning was investigated using a multistep equilibration approach that excluded a contribution of diffusion to isotope fractionation. The obtained fractionation factors for the NAPL-vapor system were compared to values from continuous vaporization where a diffusion contribution cannot be excluded. Diffusion-controlled vaporization in porous media was investigated in unsaturated sand-filled columns with an emplaced NAPL source. Measured fractionation factors were compared to fractionation factors expected based on a CGM type model. For the column experiment, the trends of four chlorine isotopologues were tracked and chlorine isotopologue fractionation was compared to chlorine isotope fractionation on an experimental and theoretical level.

3.2 Experimental methods

To derive high precision equilibrium isotope fractionation factors for NAPL-vapor equilibration and air-water partitioning, a multistep equilibration approach was used that cumulates isotope shifts and excludes kinetic effects such as diffusive transport. For comparison, NAPL vaporization was also investigated using a kinetic approach denoted as continuous vaporization. Finally, the interaction between NAPL-vapor partitioning and diffusion of isotopologues was investigated in a column study, referred to as diffusion-controlled vaporization experiment.

3.2.1 Stepwise vaporization

An experimental device was designed to quantify carbon and chlorine isotope fractionation of TCE during NAPL-vapor equilibration (Figure 1). The experimental setup consisted of two 5 ml gas-tight syringes fixed together with a stainless steel connector. A single micro-drop of pure solvents (25μl), which remained intact throughout the experiment, was placed in one of the syringes and TCE volatilizes partly in a 5 ml volume. After an equilibration period of 15 minutes, the gas phase was transferred to the second syringe for analyses. The advantage of this system is that the effect of vaporization is measured without any influence of diffusion unlike previous experiments (Huang & al., 1999; Poulson & Drever, 1999; Kuder & al., 2009). During sampling only advection occurs which does not induce any isotope fractionation. Measurements of $\delta^{13}C$ and $\delta^{37}Cl$ values were carried out after each equilibration step. By repeating the vaporization phase 13 times, a higher isotope shift could be obtained and hence the fractionation factor was determined with a higher precision. The experiment was repeated three times.

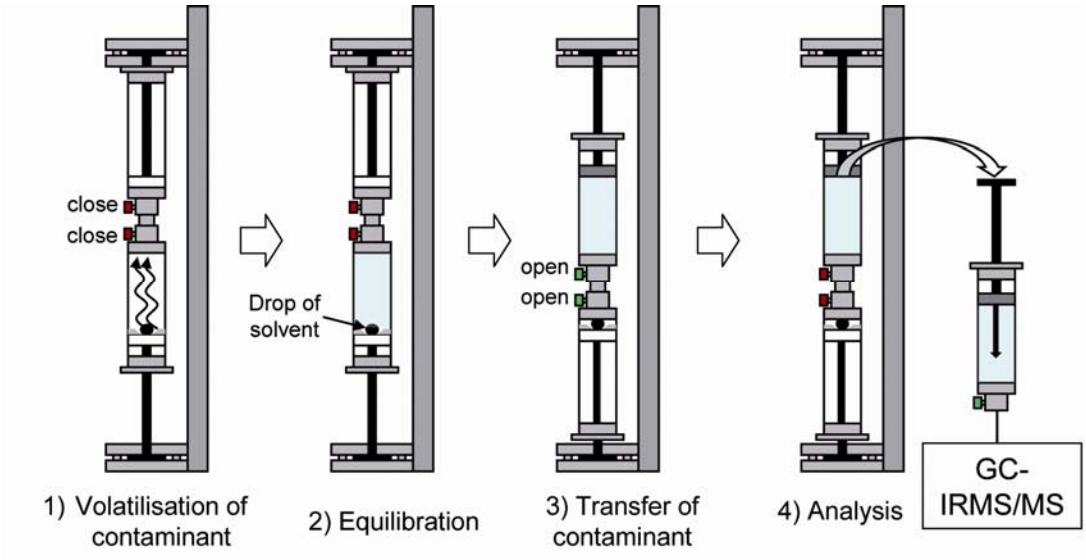

Figure 1: Setup and procedure for stepwise vaporization experiments.

As the Rayleigh equation is strictly only valid for continuous processes, a mathematical approach was developed to extract isotope enrichment factors from a stepwise equilibration process. Derivations of these equations can be found in Appendices b. As there is no significant difference in the isotope enrichment factors obtained by the two approaches, data are presented and evaluated according to the more common Rayleigh approach. The good agreement between the two approaches is due to the elevated number of equilibration steps (13) used in the experiments. The results were thus plotted and evaluated using the following equations:

$$\ln[(\delta + 1000)/(\delta_i + 1000)] = (\alpha - 1) \ln f \qquad \textit{(equation 1)}$$

$$\varepsilon = (\alpha - 1) \cdot 1000 \qquad \textit{(equation 2)}$$

where δ is the isotopic composition of TCE for a particular value of f, δ_i is the initial isotopic composition of TCE, f is the fraction of liquid TCE remaining, α is the isotope fractionation factor, and ε is the isotope enrichment factor. The uncertainty was characterized using the standard uncertainty of the slope obtained by linear regression using the least square method.

3.2.2 Continuous vaporization

For comparison, continuous vaporization experiments were performed at 25°C similarly to previous studies (Huang & al., 1999; Poulson & Drever, 1999). A volume of 6 ml of TCE was introduced into serum vials of 6 (experiment 1), 12 (experiment 2) and 20ml (experiment 3) with the same diameter but different heights and simply allowed to evaporate in a fume hood. Various vial heights were studied in order to take into account various diffusion lengths. Each experiment with a given vial height was carried out once. NAPL (non-aqueous phase liquid) samples of 1 µl were periodically taken with a 10 µl syringe. The vials were weighted before and after sampling in order to determine the amount that had vaporized and to quantify the amount of NAPL removed during sampling. The 1 µl NAPL samples were then dissolved in 40 ml vials filled with water before analysis of $\delta^{13}C$ and $\delta^{37}Cl$. The results were plotted according to equation 1 and 2.

3.2.3 Air-water partitioning

For quantification of isotope fractionation during air-water partitioning, a 50 ml gas-tight syringe was partially filled with 25 ml of an aqueous solution of TCE of 2 mg/l with 25 ml of gas phase remaining. The samples were placed on a rotary shaker at 200 rpm in horizontal position to promote the equilibration of TCE between the aqueous and gas phase. A period

of 20 minutes was found to be sufficient to reach equilibrium. Experiments with an increasing number of equilibration steps (n=1 to 9) were carried out and after the last step of each experiment the aqueous phase was transferred into 20 ml vials before analysis of $\delta^{13}C$ and $\delta^{37}Cl$. A higher number of equilibration steps leads to a lower fraction f of remaining compound in the system. Each experiment was repeated two times. The results were plotted according to equation 1 and 2.

3.2.4 Diffusion-controlled vaporization in column

The main aim of the column experiment was to investigate how the carbon and chlorine isotope and isotopologue ratios of a TCE NAPL source shifts over time when vaporization is diffusion-controlled and to relate the observed isotope and isotopologue fractionation to fundamental fractionation factors for vaporization and diffusion. The experiments relied on laboratory columns (diameter of 5 cm, length of 70 cm) filled with dry quartz sand (grain size of 0.7-1.2 mm) and open to the atmosphere (Figure 2). Due to the use of quartz sand that doesn't contain organic matter or clays, sorption of TCE can be excluded. The columns were placed on an analytical balance in a fume hood to be able to link the loss of TCE by diffusion out of the column to the isotope evolution.

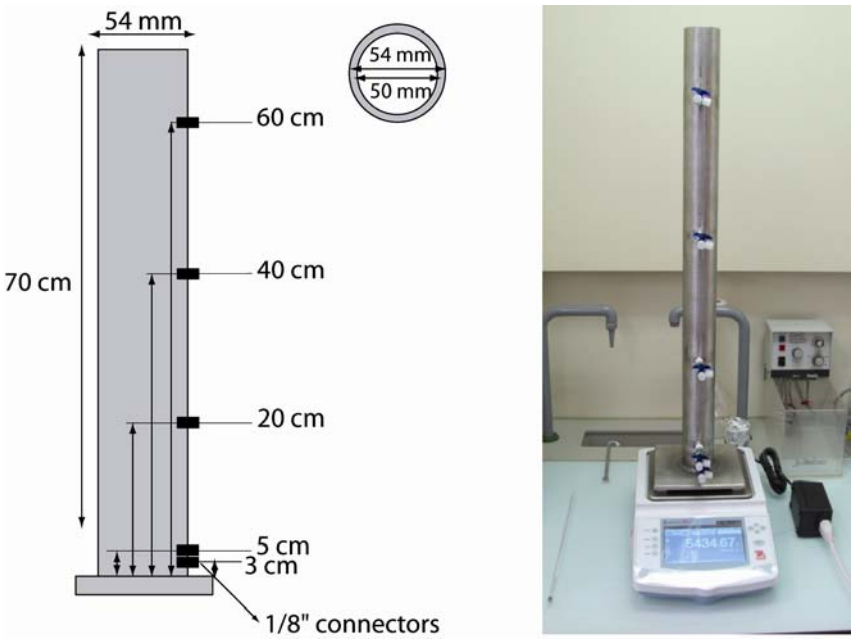

Figure 2: Setup for column experiments.

Two column experiments were carried out with a different NAPL volume. In experiment 1, it was evaluated how long it takes to establish uniform carbon and chlorine stable isotope profiles throughout the column and whether these profiles remain uniform as the NAPL

vaporization proceeds. In this experiment, 1 ml of TCE was injected 2 cm from the bottom of the column and gaseous samples were taken at 2, 20, 40 and 60 cm above the source injection point for $\delta^{13}C$, $\delta^{37}Cl$ and relative concentration analysis. In experiment 2, only the isotope evolution of the source was followed but over a larger range of TCE removal which was possible due to the emplacement of a larger source (4.5 ml of TCE). Since it is not possible to retrieve NAPL from the column, the gas phase close to the source was sampled for $\delta^{13}C$ and $\delta^{37}Cl$ analysis.

For the evaluation of the isotope data, a mathematical model for isotopologue fractionation during diffusion-controlled vaporization was developed (see chapter 2.3). Based on the local equilibrium assumption (LEA) for vaporization in porous media, isotopologue fractionation is expected to result from a combination of fractionation during NAPL-vapor equilibration and diffusion. Furthermore, it is assumed that vaporization is sufficiently slow that no concentration gradients of isotopologues form in the liquid phase. The validity of these assumptions can be verified by comparing calculated to expected isotopologue fractionation factors. As outlined in more details in the chapter 2.3, under these assumptions, effective fractionation factors for pairs of isotopologues can be expressed by the product of the equilibrium and diffusion fractionation factors:

$$\alpha_{Eff}^{ITL} = \alpha_{Eqm}^{ITL} \cdot \alpha_{Diff}^{ITL} \qquad \textit{(equation 3)}$$

whereby, the isotopologue fractionation factor for diffusion corresponds to:

$$\alpha_{Diff}^{ITL} = \frac{D_h}{D_l} = \sqrt{\frac{(MW_h + MW_{air}) \cdot MW_l}{(MW_l + MW_{air}) \cdot MW_h}} \qquad \textit{(equation 4)}$$

where D_h and D_l are the diffusion coefficient for heavy and light isotopologues respectively, MW_l is the molecular weight of the light molecule, MW_h the molecular weight of the heavy molecule and MW_{air} the molecular weight of air (28.8 in this case). For carbon, a value of 0.99932 is obtained and for the isotopologue pair with zero and one heavy chlorine isotopes a value of 0.99826 is found.

Inversely, if evaporation is rapid, isotopologue fractionation will occur in the liquid phase, too. The occurrence of isotopologue fractionation in the liquid phase can be evaluated by the advective-diffusive isotopic model developed by He & Smith (1999) adapted to the situation where a NAPL vaporizes through a porous media to a gas phase in which the concentration of the vaporizing compound is close to zero (h=0 in He and Smith model). During slow evaporation, the diffusion of isopologues in the boundary layer is sufficiently fast to prevent

differences in isotopologue ratios between the surface and the bulk liquid. In contrast, during faster vaporization, light isotopologues become depleted in the surface layer, which leads to a reduction of the effective fractionation factor for vaporization. The speed to vaporization relative to the thickness of the boundary layer can be characterized using a dimensionless number N according to (He & Smith, 1999):

$$N = \frac{u \cdot L_1}{D_L} \qquad \textit{(equation 5)}$$

Where μ is the vaporization rate from an open surface (m/s), L_1 the thickness of the liquid boundary layer (m) and D_L the diffusion coefficient of the compound in the liquid phase (m^2/s). The effective fractionation factor is given by (He & Smith, 1999):

$$\alpha_{Eff} = \frac{\alpha_{Eqm} \cdot \alpha_{Diff}}{\exp(-N) - \alpha_{Eqm} \cdot \alpha_{Diff} \cdot (\exp(-N) - 1)} \qquad \textit{(equation 6)}$$

For N → - ∞ (very slow vaporization), α_{Eff} approaches $\alpha_{Eqm} \cdot \alpha_{Diff}$ corresponding to equation 3 while for the case N → +∞ (very fast vaporization), α_{Eff} approaches 1, i.e. no fractionation occurs during vaporization. In Figure 3, it is illustrated how α_{Eff} varies as a function of N. As N increases, the effective chlorine isotope enrichment factor decreases towards 0, while the value for carbon changes very little as it is already close to zero for a small N.

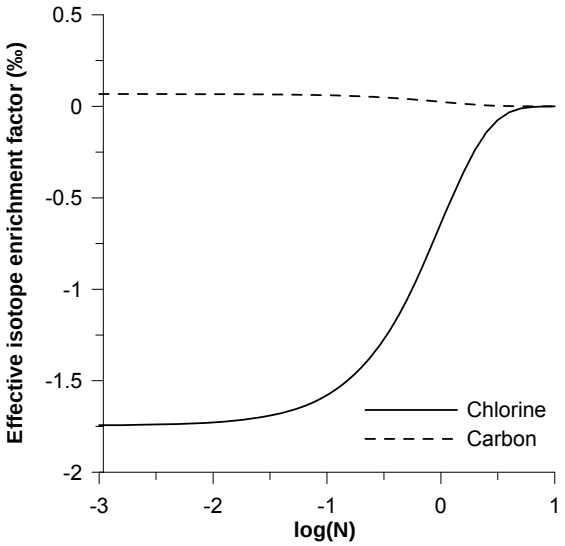

Figure 3. Evolution of the effective isotope enrichment factor as a function of dimensionless parameter N.

3.2.5 Sample storage and analysis

For each experiment, all samples were collected and analyzed in a single run to maximize the precision of the analysis. Gaseous compounds from the vaporization and diffusion experiments were dissolved in water until analysis for several reasons. Aqueous samples were found to be more stable for storage until an experiment was completed, samples can easily be diluted to obtain constant peak sizes and hence to maximize the precision and accuracy of the analysis, and an identical analytical method can be used for all samples. Gas samples were introduced into 120 ml bottles filled with 70 ml of water and capped with Valco Mininert valve. The injected gas volume was adjusted such that similar aqueous and gas phase concentrations were obtained for all samples after equilibration, with the exception of the initial samples from the column experiment, which had lower concentrations. However, tests covering the whole concentration range of these samples showed that carbon isotope ratios varied by less than < ±0.2‰. The samples were placed on rotary shaker at 200 rpm and equilibrated during 24 hours at 25°C. The water was then transferred in 40 and 20ml vials before analysis. Isotope enrichment factors were calculated using linear regression based on equation 1. As isotope ratios are plotted relative to the initial isotope ratio determined by the same method, the small isotope fractionation during air-water partitioning cancels.

Carbon isotope ratios of trichloroethylene were analyzed by a TRACE^{TM} gas chromatograph (GC) coupled to an isotope-ratio mass spectrometer (IRMS) via a combustion III interface (Thermo Finnigan, Germany). The samples were preconcentrated with a purge-and-trap concentrator (Tekmar Velocity XPT, USA) connected to a cryogenic trap (ATAS GL, The Netherlands) installed inside the GC oven. A 25 ml sample was purged for 10 minutes at a rate of 40 ml/min and retained in a trap filled with Vocarb 3000. The trap was then heated to 250°C. The desorbed compounds were trapped again at -80°C on the GC column with a cryotrap before releasing them to the GC by heating to 180°C at a flow rate of 1.7 ml/min. The chromatographic separation was performed using a DB-VRX column (60 m, 0.25 mm, 1.4 μm, Agilent) with a constant helium flow of 1.7 ml/min. Each sample was analysed twice.

Compound-specific chlorine isotope analysis was performed using a new method based on gas chromatography/quadrupole mass spectrometry (GC/qMS) developed by Sakaguchi-Söder et al. (2007) and modified by Aeppli et al. (2010). In this study, the method developed by Aeppli et al. (2010), which relies on molecular ions of two isotopologues, was extended to consider the four chlorine isotopologues of trichloroethylene (mass 130, 132, 134 and 136)

which were quantified for the same injection by cycling through the different masses. The raw isotopic ratios were then calculated using an equation proposed by Jin et al. (2011):

$$R_{TCE} = \frac{I_{132} + 2 \cdot I_{134} + 3 \cdot I_{136}}{3 \cdot I_{130} + 2 \cdot I_{132} + I_{134}} \qquad \textit{(equation 7)}$$

where I is the corresponding molecular ion abundance at different m/z values.

A calibration was then performed with two external standards (with values of 3.05‰ and -2.70‰) to obtain delta values on the SMOC scale. A recent interlaboratory comparison showed that two standards are required to obtain accurate chlorine isotopic ratio on the SMOC scale using a GC/qMS (Bernstein & al., 2011). Five replicates of each standard were analyzed at the beginning and the end of each analytical sequence. An Agilent 7890A GC coupled to an Agilent 5975C quadrupole mass selective detector (Santa Clara, CA, USA) was used for the measurements. Headspace injections were performed using a CombiPal Autosampler (CTC Analytics, Zwingen, Switzerland). The chromatographic separation was performed using a DB-5 column (30 m, 0.25 mm, 0.25 μm, Agilent) with a constant helium flow of 1.2 ml/min. Each sample was analysed five times. The concentrations were determined based on the combined peak area of all four chlorine isotopologues (mass 130, 132, 134 and 136) using a calibration curve based on external standards. The concentrations were normalized relative to the initial concentration for each experiment.

All isotope ratios were reported relative to a standard using the delta notation $\delta=(R/R_{std}-1)*1000$ [‰], where R and R_{std} are the isotope ratio of the sample and the standard (VPDB for carbon, SMOC for chlorine), respectively.

3.3 Results

3.3.1 Stepwise vaporization, continuous vaporization and air-water partitioning

For continuous vaporization (Figure 4A) and stepwise vaporization (Figure 4B), significant carbon and chlorine isotope fractionation occurs. The isotope evolution follows a Rayleigh trend and isotope enrichment factors were calculated using equations 1 and 2 (Table 1). The isotope enrichment factors agree well for replicate experiments (Table 1) and hence only average values will be discussed. Although various vial heights were used for the continuous vaporization experiment in order to consider different diffusion lengths, no significant changes can be observed (Table 1). Carbon and chlorine isotopes show opposite isotope fractionation trends although they are present in the same bond within the molecule. For both experiments, carbon becomes depleted in the heavy isotope (inverse isotope effect), while chlorine becomes enriched in the heavy isotope (normal isotope effect). However, the magnitude of isotope fractionation is different for the two experiments. For continuous vaporization, chlorine isotope fractionation is stronger (ε_{Cl} = -1.35±0.03‰ instead of -0.39±0.03‰) and carbon isotope fractionation weaker (ε_{C} = +0.28±0.03‰ instead of +0.75±0.04‰) compared to the stepwise vaporization experiment. For air-water partitioning, no significant chlorine isotope fractionation occurs, while an inverse carbon isotope effect (ε_{C} = +0.38±0.04‰) is observed similarly as in the vaporization experiments (Figure 4C).

Table 1: Carbon and chlorine isotope enrichment factors (e) for TCE vaporization and air-water partitioning. The uncertainty was characterized using the standard uncertainty of the slope of the regression line.

		Expt.1	Expt. 2	Expt. 3	Mean values
Continuous vaporization	ε_{C}	+0.33‰ (±0.03‰)	+0.25‰ (±0.03‰)	+0.26‰ (±0.03‰)	+0.28‰ (±0.03‰)
	ε_{Cl}	-1.35‰ (±0.03‰)	-1.42‰ (±0.04‰)	-1.27‰ (±0.03‰)	-1.35‰ (±0.03‰)
Stepwise vaporization	ε_{C}	+0.75‰ (±0.04‰)	+0.78‰ (±0.04‰)	+0.71‰ (±0.04‰)	+0.75‰ (±0.04‰)
	ε_{Cl}	-0.39‰ (±0.02‰)	-0.43‰ (±0.03‰)	-0.36‰ (±0.04‰)	-0.39‰ (±0.03‰)
Air-water partitioning	ε_{C}	+0.38‰ (±0.04‰)	+0.37‰ (±0.03‰)		+0.38‰ (±0.04‰)
	ε_{Cl}	-0.07‰ (±0.05‰)	-0.05‰ (±0.04‰)		-0.06‰ (±0.05‰)
Diffusion-controlled vaporization	ε_{C}	+0.07‰ (±0.04‰)	+0.13‰ (±0.05‰)		+0.10‰ (±0.05‰)
	ε_{Cl}	-1.38‰ (±0.08‰)	-1.39‰ (±0.03‰)		-1.39‰ (±0.06‰)

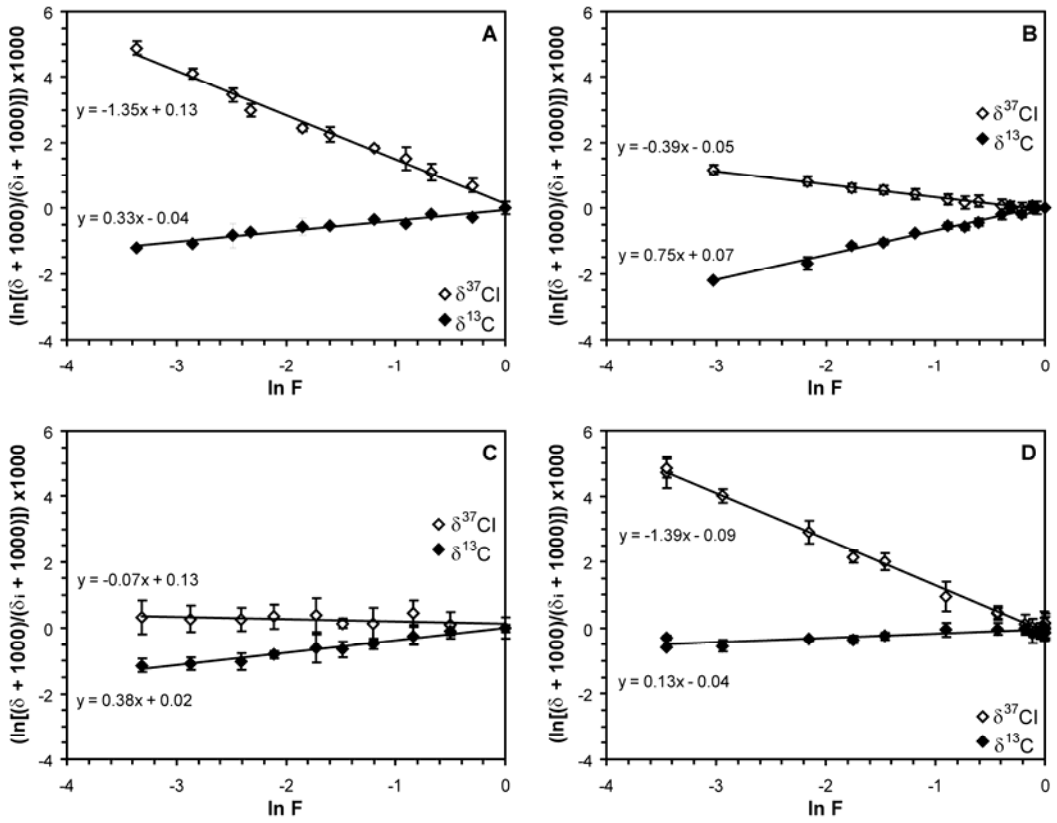

Figure 4: Rayleigh plots for continuous vaporization (A), stepwise vaporization (B), air-water partitioning (C) and diffusion-controlled vaporization in a sand-filled column (D). Error bars represent standard deviations. Plots for replicate experiments are shown in Appendices (Figure A1).

3.3.2 Diffusion-controlled vaporization in column

In experiment 1, non-linear concentration profiles are observed shortly after emplacing the TCE source which approach linear profiles within about 10 hours (Figure 5C). The mass remaining in the column, which was determined with a balance, linearly decreases over time (Figure 5D) which is consistent with the constant concentration gradients observed between 10 and 102h across the column.

The magnitude of isotope fractionation is much larger for chlorine (Figure 5B) compared to carbon (Figure 5A). For both elements, a depletion of heavy isotopes with increasing distance from the source is observed during the initial hours of the experiments, which is however more pronounced for chlorine. Once linear concentration profiles are established (10h), constant isotope profiles are observed from the source to the top of the column, corresponding to a steady state situation. Between 10 and 102h, no significant variations of

carbon isotope ratios are observed, while chlorine becomes increasingly depleted in ^{37}Cl with a total shift of +3.8‰. Since the residual amount of TCE in the column and the isotope ratio are known with a high precision, the chlorine isotope trend in the sampling port at the source can be further evaluated using a Rayleigh plot. In Figure 4D, the results from experiment 2 are plotted because vaporization took place over a larger range of TCE removal due to the higher initial mass. The obtained isotope enrichment factors where the same for both experiments (Table 1). Unlike in the continuous and stepwise vaporization experiments, no significant carbon isotope fractionation occurs, while normal chlorine isotope fractionation is observed (-1.39±0.06‰) that is substantially stronger than for stepwise vaporization but in the same range as for continuous vaporization.

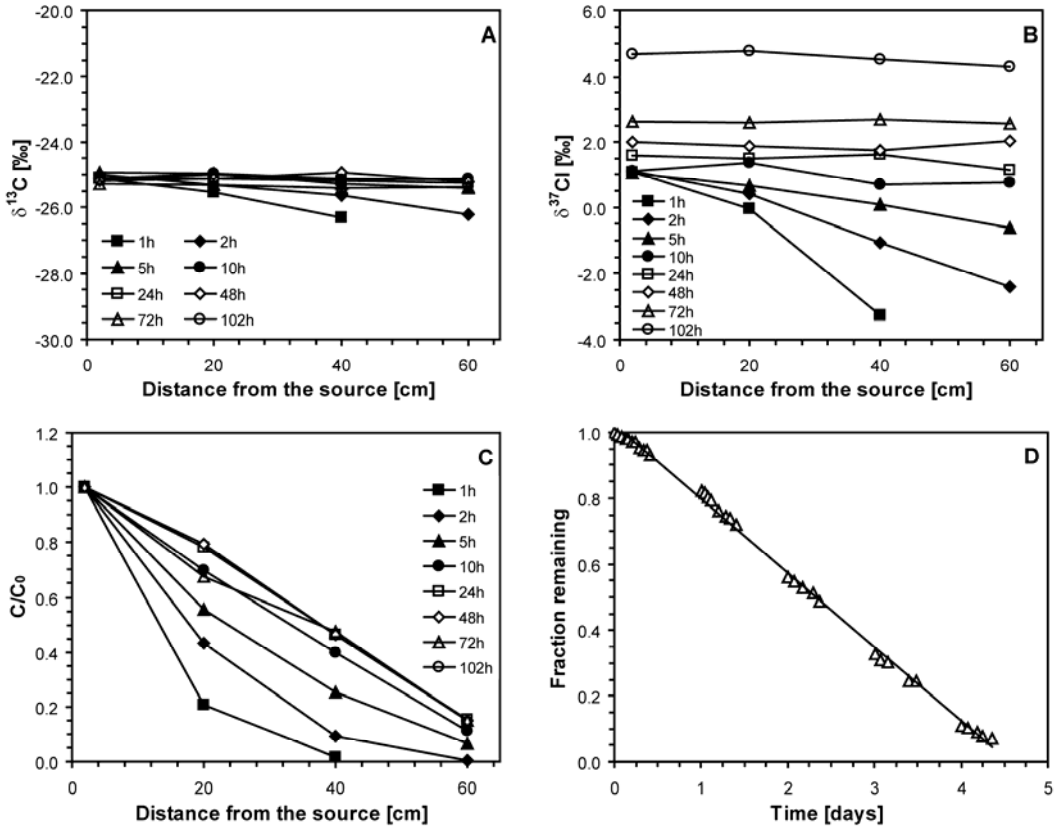

Figure 5: (A) $\delta^{13}C$ and (B) $\delta^{37}Cl$ values at selected times and distance from the source during the column experiment 1 (mean standard deviation for $\delta^{13}C$ measurements: ±0.13‰ and for $\delta^{37}Cl$ values: ±0.34‰), (C) relative concentrations measured in the column at selected times and (D) remaining fraction of NAPL.

3.4 Discussion

3.4.1 Stepwise vaporization, continuous vaporization and air-water partitioning

The different isotope enrichment factors for continuous and stepwise vaporization demonstrate that the experimental design strongly influences the obtained values. For continuous vaporization our results (ε_C = +0.28‰ and ε_{Cl} = -1.35‰) are close to values obtained in previous studies with a similar open vial experimental design that reported isotope enrichment factors of +0.35±0.02‰, +0.24‰±0.06‰ (Poulson & Drever, 1999) and +0.31±0.04‰ for carbon (Huang & al., 1999) and -1.64‰±0.13‰ and -1.81‰±0.22‰ for chlorine (Huang & al., 1999; Poulson & Drever, 1999).

The shift of carbon and chlorine isotope enrichment factors in the direction of a normal isotope effect in the continuous compared to the stepwise experiment indicates that continuous vaporization is influenced by diffusion. Indeed, the change of the isotope enrichment factor between the two experiments is approximately twice as high for chlorine (0.96±0.04‰) compared to carbon (0.37±0.05‰). Such a trend is expected for a diffusion contribution given that chlorine isotopes are two mass units apart and carbon isotope only one. The difference in isotope fractionation is probably related to the experimental design. In the continuous vaporization experiment, a stagnant air layer is present in the headspace of the vial above the organic phase, through which molecules have to diffuse before reaching the advective flow zone in the fume hood. In contrast, the device for stepwise evaporation was built to avoid any influence of diffusion during experimentation. Samples are taken after a NAPL-vapor equilibrium is reached and the sampling relies on advective transport only. Since advection is not associated with isotope fractionation, the values obtained from the stepwise experiments can be considered to represent isotope enrichment factors for NAPL-vapor equilibration in isolation. This is a major advantage compared to continuous vaporization experiments from which isotope fractionation factors for NAPL-vapor equilibration can only be derived indirectly after subtracting the contribution of diffusion effects. For NAPL-vapor equilibration, opposite isotope fractionation trends are observed for carbon and chlorine. A similar pattern was observed previously for carbon tetrachloride (Baertschi & al., 1953) and chloroform (Jansco & al., 1983). Isotope fractionation during vaporization reflects interactions between molecules in the condensed phase. The direction of isotope fractionation is the result of an interplay between the effect of the restricted rotation and translation in the condensed phase (external mode) and the shift of internal vibrational frequencies upon condensation (internal mode). The former always leads to a normal isotope effect because the molecular motion becomes hindered, while the latter is usually associated with an inverse isotope effect because frequencies of internal vibration

are lower due to the interaction between molecules in the condensed phase (Jansco & al., 1974; Van Hook, 2006). The observed trends for TCE indicate that in the case of carbon changes in the internal mode dominate while for chlorine changes in the external mode control isotope fractionation.

During the air-water partitioning experiments, carbon and chlorine isotope fractionation is smaller than for NAPL-vapor equilibration. This is likely due to the weaker interactions between water molecules and TCE compared to interactions in the NAPL and hence a smaller perturbation of internal and external modes of motion upon dissolution compared to condensation. A similar trend was previously observed for dissolution and condensation of methane at low temperature (Bacsik & al., 2002).

3.4.2 Diffusion-controlled vaporization in column

In the column study, vapor concentrations at the source were close to saturation as indicated by the excellent agreement between observed and calculated TCE removal. Hence, it can be assumed that isotope fractionation associated with the NAPL-vapor transfer step corresponds to the enrichment factors for NAPL-vapor equilibration reported above. No significant effective carbon isotope fractionation was observed for TCE. This is in contrast to similar studies with petroleum hydrocarbons, which yielded carbon isotope enrichment factors of -2.14±0.22‰ for pentane (Bouchard & al., 2008) and -1.0±0.1‰ for MTBE (Kuder & al., 2009). The absence of carbon isotope fractionation for TCE has two reasons: (i) the inverse isotope fractionation related to NAPL-vapor equilibration is larger for TCE compared to pentane or MTBE and (ii) the diffusion isotope fractionation is smaller due to the larger molecule mass of TCE compared to pentane and MTBE. As a result, the inverse isotope fractionation during NAPL-vapor equilibration and normal isotope fractionation during diffusion cancel for TCE but not for pentane or MTBE. In contrast, for chlorine, isotope fractionation is normal for both NAPL-vapor equilibration and diffusion and hence they cumulate. Furthermore, diffusion isotope fractionation is twice as large for chlorine compared to carbon due to the mass difference of two between the two stable isotopes. As a result, large chlorine isotope fractionation is observed during diffusion-controlled vaporization of TCE despite of the relatively large molecular weight. Chlorine isotope fractionation of TCE is in the same range as carbon isotope fractionation for much lighter molecules such as pentane and MTBE.

If vaporization is sufficiently slow to prevent the formation of isotopologue concentration gradients in the liquid phase, the observed isotope enrichment factor should correspond to the value obtained from equation 3. Strictly, this equation is only valid on an isotopologue basis as fractionation during vaporization and diffusion takes place among isotopologues and not directly isotopes. However, as justified in the chapter 2.3, for both processes, chlorine isotope and isotopologue fractionation is proportional in good approximation as previously also shown for reactive processes (Elsner & Hunkeler, 2008). As a result, isotope and isotopologue fractionation factors for pairs of isotopologues differing in one heavy isotope are identical and equation 3 applies to both isotopes and isotopologues pairs. Combining the diffusion and vaporization isotope effects for the column experiment according to equation 3, effective isotope enrichment factors of 0.07‰ for carbon and -1.76‰ for chlorine are obtained. For chlorine isotopes, the calculated value is slightly smaller than the observed value, while for carbon a good agreement is obtained. In a previous study, Kuder et al. (2009) also observed a smaller effective isotope enrichment factors than expected for carbon and hydrogen in MTBE. The observed deviations from the expected value in our study suggests formation of isotopologue concentration gradients in the liquid phase, which leads to a reduction of the effective isotope fractionation for chlorine but not for carbon since for carbon the value is expected to be close to zero even for slow evaporation (see chapter 3.2.4 and equation 6 for more information). The possible liquid phase effect might be due to the relatively rapid evaporation in the laboratory study and might not occur under field conditions where steady state concentration gradients are flatter due to longer diffusion distances and hence vaporization rates slower.

Since the GC-qMS method makes it possible to track chlorine isotopologue ratios directly, the expectation that isotope fractionation and isotopologue fractionation is proportional and hence isotope fractionation follows a Rayleigh trend even when several isotopologues with multiple heavy isotopes are present (see chapter 2.3 for derivation) can be experimentally verified. As expected, in the column study, the shifts of the isotopologue pairs 132/130 and 134/132 are proportional to the shift in the isotope ratios (Figure 6). The observed slopes of 3.01 (132/130) and 0.98 (134/132), respectively agree very well with the expected slopes of 3.0 and 1.0 obtained when assuming a statistical distribution of heavy isotopes among the isotopologues (Figure 6). These findings justify that also for systems with significant isotope fractionation due to vaporization and diffusion, isotope ratios can reliably be determined by measuring only some of the isotopologues using either qMS or isotope-ratios mass spectrometry (IRMS) methods and isotope fractionation factors can be derived from these data.

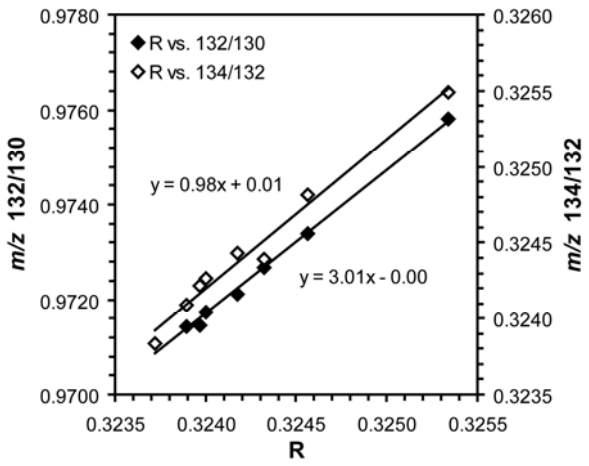

Figure 6: Comparison between isotopic ratio (R) and isotopologues ratios 132/130 and 134/132 at the source of the contamination of the column experiment.

3.5 Conclusions

The study demonstrates that during diffusion-controlled vaporization of chlorinated hydrocarbons in porous media contrasting trends of carbon and chlorine isotope fractionation can be observed. These trends will likely not be affected by sorption as sorption does not influence the isotope ratio profiles any longer once a steady state is reached. Indeed in a recent field study, uniform carbon and chlorine isotope ratios of TCE were observed across a sandy unsaturated zone of 18m thickness while concentrations varied by several orders of magnitude (Hunkeler & al., 2011). During diffusion-controlled vaporization, the combined effect of vaporization and diffusion lead to a constant carbon isotope ratio while the chlorine isotope ratio becomes enriched. An older source might thus have a distinct heavy chlorine isotope ratio. This enrichment trend could help to differentiate subsurface source of different age even if they have a similar starting isotope signature. The dual isotope approach (or 2D-CSIA) may also be useful to differentiate between different processes contributing to the removal of chlorinated hydrocarbons from the vadose zone as previously suggested for MTBE

Finally, the study also highlights the need for isotope fractionation factors for physico-chemical processes determined under well-constrained conditions as a basis for the evaluation of field isotope data and for modelling of isotope trends.

3.6 References

- **Aeppli**, C.; Holmstrand, H.; Andersson, P.; Gustafsson, O. Direct compound-specific stable chlorine isotope analysis of organic compounds with quadrupole gc/ms using standard isotope bracketing. *Anal. Chem.* **2010**, 82 (1), 420-426.
- **Broholm**, M.M.; Christophersen, M.; Maier, U.; Stenby, E.H.; Hohener, P.; Kjeldsen, P. Compositional evolution of the emplaced fuel source in the vadose zone field experiment at airbase Vaerlose, Denmark. *Environ. Sci. Technol.* **2005**, 39 (21), 8251-8263.
- **Bacsik**, Z.; Lopes, J. N. C.; Gomes, M. F. C.; Jancso, G.; Mink, J.; Padua, A. A. H. Solubility isotope effects in aqueous solutions of methane. *J. Chem. Phys.* **2002**, 116 (24), 10816-10824.
- **Baertschi**, P.; Kuhn, W.; Kuhn, H. Fractionation of isotopes by distillation of some organic substances. *Nature* **1953**, 171 (4362), 1018-1020.
- **Bernstein**, A.; Shouakar-Stash, O.; Ebert, K.; Laskov, C.; Hunkeler, D.; Jeannottat, S.; Sakaguchi-Söder, K.; Laaks, J.; Jochmann, M. A.; Cretnik, S.; Jager, J.; Haderlein, S. B.; Schmidt, T. C.; Aravena, R.; Elsner, M. Compound-specific chlorine isotope analysis: A comparison of gas chromatography/isotope ratio mass spectrometry and gas chromatography/quadrupole mass spectrometry methods in an interlaboratory study. *Anal. Chem.* **2011**, 83 (20), 7624-7634.
- **Bouchard**, D.; Hunkeler, D.; Gaganis, P.; Aravena, R.; Hohener, P.; Broholm, M. M.; Kjeldsen, P. Carbon isotope fractionation during diffusion and biodegradation of petroleum hydrocarbons in the unsaturated zone: Field experiment at Vaerlose airbase, Denmark, and modeling. *Environ. Sci. Technol.* **2008**, 42 (21), 596-601.
- **Bouchard**, D.; Hohener, P.; Hunkeler, D. Carbon isotope fractionation during volatilization of petroleum hydrocarbons and diffusion across a porous medium: A column experiment. *Environ. Sci. Technol.* **2008**, 42 (21), 7801-780.
- **Cappa**, C. D.; Smith, J. D.; Drisdell, W. S.; Saykally, R. J.; Cohen, R. C., Interpreting the H/D isotope fractionation of liquid water during evaporation without condensation. *J. Phys. Chem. C* **2007**, 111, (19), 7011-7020.
- **Conant**, B.H.; Gillham, R.W.; Mendoza, C.A. Vapor transport of trichloroethylene in the unsaturated zone: Field and numerical modeling investigations. *Water Resour. Res.* **1996**, 32 (1), 9-22.
- **Craig**, H.; Gordon, L. I., Deuterium and oxygen 18 variations in the ocean and the marine atmosphere. In Stable isotopes in oceanographic studies and paleotemperatures, Tongiorgi, E., Ed. Laboratorio di geologia nucleare: Pisa, Italy, 1965; pp 9-130.
- **Elsner**, M.; Hunkeler, D. Evaluating chlorine isotope effects from isotope ratios and mass spectra of polychlorinated molecules. *Anal. Chem.* **2008**, 80 (12), 4731-4740.
- **Harrington**, R. R.; Poulson, S. R.; Drever, J. I.; Colberg, P. J. S.; Kelly, E. F. Carbon isotope systematics of monoaromatic hydrocarbons: Vaporization and adsorption experiments. *Org. Geochem.* **1999**, 30 (8A), 765-775.
- **He**, H.; Smith, R. B., An advective-diffusive isotopic evaporation-condensation model. *J. of Geophys. Res.-Atmos.* **1999**, 104 (D15), 18619-18630.
- **Horita**, J.; Rozanski, K.; Cohen, S., Isotope effects in the evaporation of water: a status report of the Craig-Gordon model. *Isot. Environ. Healt. S.* **2008**, 44 (1), 23-49.
- **Huang**, L.; Sturchio, N. C.; Abrajano, T.; Heraty, L. J.; Holt, B. D. Carbon and chlorine isotope fractionation of chlorinated aliphatic hydrocarbons by evaporation. *Organic Geochemistry* **1999**, 30 (8A), 777-785.
- **Hunkeler**, D.; Aravena, R.; Shouakar-Stash, O.; Weisbrod, N.; Nasser, A.; Netzer, L.; Ronen, D. Carbon and chlorine isotope ratios of chlorinated ethenes migrating through a thick unsaturated zone of a sandy aquifer. *Environ. Sci. Technol.* **2011**, 45 (19), 8247-8253.
- **Jancso**, G.; Van Hook, W. A. Condensed phase isotope-effects (especially vapor-pressure isotope-effects). *Chem. Rev.* **1974**, 74 (6), 689-750.

- **Jancso**, G.; Jakli, G.; Fetzer, C. Vapor-pressure isotope effects of chloroform*. Z. Naturfors. Sect. A-J. Phys. Sci.* **1983**, 38 (2), 184-190.
- **Jin**, B. A.; Laskov, C.; Rolle, M.; Haderlein, S. B. Chlorine isotope analysis of organic contaminants using GC-qMS: Method optimization and comparison of different evaluation schemes. *Environ. Sci. Technol.* **2011**, 45 (12), 5279-5286.
- **Kuder**, T.; Philp, P.; Allen, J. Effects of volatilization on carbon and hydrogen isotope ratios of MTBE. *Environ. Sci. Technol.* **2009**, 43 (6), 1763-1768.
- **Poulson**, S. R.; Drever, J. I. Stable isotope (C, Cl, and H) fractionation during vaporization of trichloroethylene. *Environ. Sci. Technol.* **1999**, 33 (20), 3689-3694.
- **Sakaguchi-Soder**, K.; Jager, J.; Grund, H.; Matthaus, F.; Schuth, C. Monitoring and evaluation of dechlorination processes using compound-specific chlorine isotope analysis. *Rapid Commun. Mass Spectrom.* **2007**, 21 (18), 3077-3084.
- **Shin**, W. J.; Lee, K. S. Carbon isotope fractionation of benzene and toluene by progressive evaporation. *Rapid Commun. Mass Spectrom.* **2010**, 24 (11), 1636-1640.
- **Van Hook**, A.W. Condensed matter isotope effects. In Isotope Effects in Chemistry and Biology; Kohen, A.; Limbach, H.-H, Eds.; CRC Press - Taylor & Francis Group, LLC: Boca Raton 2006; pp 1096.

Chapter 4

Chlorine and carbon isotope fractionation during transport of tetrachloroethylene from the saturated to the unsaturated zone of porous media

Abstract

The isotopic evolution of tetrachloroethylene (PCE) during its transport from a groundwater plume through the unsaturated zone to the soil surface was studied based on laboratory studies and numerical modeling. During air-water partitioning, carbon and chlorine isotope ratios evolve in opposite directions, with a normal isotope effect for chlorine (ε = -0.20‰) and an inverse effect for carbon (ε = +0.46‰). During the migration of PCE from groundwater to the unsaturated zone in a 2D laboratory system, small shifts of carbon and chlorine isotope ratios are observed between the saturated and the unsaturated zone. Numerical modeling shows that these shifts are associated with isotope fractionation of air-water partitioning, as well as to the preferential loss of light isotopologues from the unsaturated zone due to diffusion. Constant carbon and chlorine isotopic profiles are then observed through the unsaturated zone (above the capillary fringe) at steady state. However, depending on the thickness of the unsaturated zone and the lithology, depletion in heavy isotopes may occur with distance during the transient migration of contaminants through the unsaturated zone. Additionally, variations of 1.5‰ were observed in the unsaturated zone for chlorine isotopes during water table fluctuations. However, if a steady state is reached, it seems possible to link a groundwater plume to gas phase contamination and/or to differentiate sources of contamination.

Submitted to Environmental Science and Technology:

- Jeannottat, S.; Hunkeler, D. Can soil gas VOCs be related to groundwater plumes based on their isotope signature? Environ. Sci. Technol.

4.1 Introduction and aim of the study

There is an increasing interest to apply CSIA in unsaturated zone studies to relate vapor phase contamination in the unsaturated zone to NAPL source or groundwater plumes and to demonstrate reactive processes in the unsaturated zone. However, previous laboratory studies have suggested that, in the unsaturated zone, isotope ratios may also be influenced by transport and partitioning processes. Isotope fractionation was observed for diffusion of VOCs across a porous media, vaporization from a NAPL phase, and air-water partitioning (Poulson & Drever, 2003; Wang & Huang, 2003; Bouchard & al, 2008; Kuder & al, 2009). In chapter 3, the vaporization and diffusion from a NAPL source located in the unsaturated zone was studied. As chlorinated solvents can also diffuse through the unsaturated zone from a contaminant plume located in groundwater, this scenario needs to be studied. A previous field and numerical study for a site where NAPL is present in a thick unsaturated zone suggested that constant isotope ratios from groundwater to the soil surface are only expected once a steady state is reached (Hunkeler & al., 2011). However, potential variations of isotope ratio during the transfer of contaminants from a groundwater contaminant plume to the unsaturated zone have not yet been studied experimentally.

The main aim of this study is to investigate isotope fractionation during the migration of tetrachloroethylene (PCE) from groundwater across the capillary fringe and through the unsaturated zone towards the atmosphere using laboratory studies and numerical modeling. Carbon and chlorine isotopes are investigated together as in practical applications a dual isotope approach is more promising to relate isotope variations to different sources and processes. Isotope fractionation during air−water partitioning was first evaluated in isolation using a multistep equilibration approach that excluded a contribution of diffusion to isotope fractionation. The effect of the transport of PCE from groundwater across the capillary fringe and through the unsaturated zone on the isotope ratios was then evaluated using a 2D laboratory system. In a first experiment, steady state flow conditions were established and the transient migration of PCE was investigated. In the second experiment, groundwater flow was also transient. As the PCE is stable under oxic conditions which are typically encountered in sandy unsaturated zones (Bradley, 2000), it was possible to evaluate the effect of transport and partitioning processes in isolation, without any degradation. In order to generalizing the results of the laboratory experimental study and to study various scenarios, numerical modeling was also carried out. The numerical modeling makes it possible to gain additional insight into the physical processes influencing isotope fractionation. Based on the experimental and numerical study, it was finally possible to draw conclusions about the use of CSIA to fingerprint VOC contamination under variably saturated conditions.

4.2 Materials and methods

4.2.1 Air-water partitioning

As a basis for the interpretation of the 2D laboratory experiments, it needs to be known how air-water partitioning influences isotope fractionation in isolation. The effect of air-water partitioning was investigated using a similar approach as the one developed in chapter 3.2.3. The air-water partitioning experiments were carried out with a 50 ml gas-tight syringe partially filled with 30 ml of an aqueous solution of PCE at 5 mg/L with 20 ml of gas phase remaining. After an equilibration time of 20 minutes on a rotary shaker at 200 rpm in a horizontal position the aqueous phase was transferred into a 20ml vial before analysis. Experiments with an increasing number of equilibration steps (n=1 to 7) were carried out and sampling was performed after the last step of each experiment. The whole experimental procedure was repeated twice. As the study of TCE in chapter 3 has shown that isotope fractionation in such a multistep equilibration process follows in good approximation a Rayleigh distillation trend, the results of the experiments were plotted and evaluated using the following equations:

$$ln[(\delta + 1000)/(\delta_i + 1000)] = (\alpha - 1)\, ln\, f \qquad \text{(equation 1)}$$

$$\varepsilon = (\alpha - 1) \cdot 1000 \qquad \text{(equation 2)}$$

where δ is the isotopic composition of PCE for a particular value of *f*, δ_i is the initial isotopic composition of PCE, *f* is the fraction of liquid PCE remaining, α is the isotope fractionation factor, and ε is the isotope enrichment factor.

4.2.2 Transport of PCE through the capillary fringe and the unsaturated zone

The transfer of PCE from groundwater across the capillary fringe and the unsaturated zone was investigated in a 2D laboratory system. This 2D system was 0.07 m wide, 0.3 m long and 0.8 m high and was built mainly in stainless steel with a glass panel on one side to be able to observe variations of the water table. Sampling ports were installed in the centre of the system at various heights along the model. Quartz sand (grain size of 0.7−1.2 mm) was packed inside the system. A gear pump was used to establish a pulse free, horizontal water flow in the bottom of the model system. The experimental setup is illustrated in Figure 1. At the beginning of the experiment, the 2D system was completely filled with water from the bottom with the gear pump. Based on the volume of water added (6.2 l) and the total volume of the system (15.1 l), the porosity is estimated to be of 0.41. Water was then removed from the system (5.1 l), and the setup was filled and empty again in order to establish a typical drainage water saturation profile. Two different experiments were carried out. The first experiment was carried out under steady state flow conditions with a constant water table and a well-established capillary fringe. The water table was set to 0.12 m with a horizontal

water flow velocity of approximately 25 cm/day for two weeks in order to create stable hydraulic conditions. An aqueous solution with PCE at saturation (200 mg/l at 25°C) prepared in a 5 l glass bottle was then circulated continuously through the 2D system in a closed loop with the outlet of the 2D system connected to the glass bottle. The glass bottle contained excess PCE NAPL and was stirred with a magnetic stirrer to ensure a constant PCE concentration. The upper part of the 2D system was tightly closed and purged with clean humidified synthetic air at 15 ml/min to remove the gaseous PCE from the system and to maintain the humidity profile. Samples for concentrations and isotope ratios analyses were taken at different heights (0, 10, 20, 30, 40, 50 and 60 cm) in the centre of the system after 1, 1.5, 2, 3, 4, 10 and 20 days. Steady state flow conditions were maintained for 20 days at the end of the first experiment and before the beginning of the second study. The second study investigated the concentration and isotope evolution during water level fluctuations. Two gear pumps were used to increase or decrease the water table in the system; one at the inlet of the 2D system and one in the outlet. The outflow was set to the same flow rate as for the first experiment. To raise the water level the inflow rate was increased, and to drop the water level the inflow was reduced. The water table was first raised during 1.5 day from 0.12 to 0.25 m and stabilized for 3 days. The water level was then lowered back to 0.12 m in a period of 1.5 day and stabilized for 3 more days before a final increase of water table from 0.12 to 0.25 m.

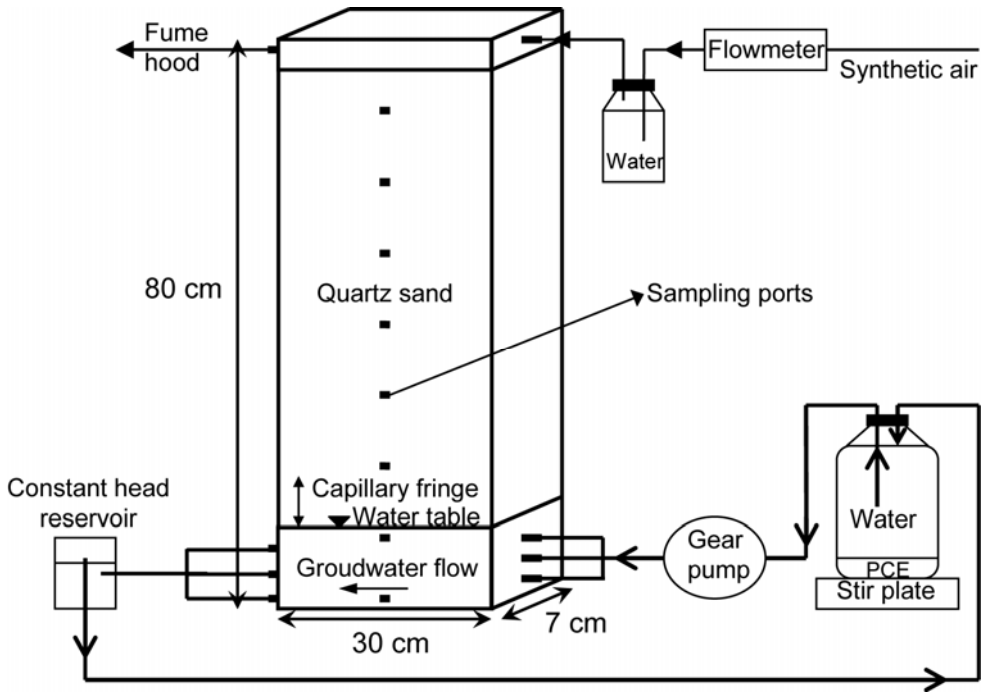

Figure 1: Setup used for the aquifer model experiments.

4.2.3 Sample storage and analysis

Gaseous samples were dissolved into water as described in chapter 3. In fact, aqueous samples were found to be more stable for storage until an experiment was completed in order to analyse all the samples in a single run. Moreover, samples can easily be diluted to obtain identical peak areas from a run to the other and hence to maximize the precision and accuracy of the analysis. Gas samples were introduced into 120 ml bottles filled with 70 ml of water and closed with gas-tight Vici Mininert valves. The samples were placed on rotary shaker at 200 rpm and equilibrated during 1 day at 25 °C. The water was then transferred in 40 and 20 ml vials before analysis. Liquid samples in the saturated zone were taken with 1 ml syringes and diluted in 40 ml vials filled with water. $\delta^{13}C$, $\delta^{37}Cl$ and concentrations analyses were performed. As gaseous PCE is equilibrated with water and about 45% of the compound is dissolved in water, the variations during air-water partitioning must be taken into account to obtain true isotopic ratios in the gas phase. As 45% of the compound is dissolved in water, measured isotope ratios were shifted +0.33‰ for carbon and -0.16‰ for chlorine isotopes, according to air-water partitioning experiments results. Compound-specific carbon isotope analysis of the PCE were analyzed with a TRACE^{TM} gas chromatograph (GC) coupled to a DeltaPlus XP isotope ratio mass spectrometer (IRMS) via a combustion III interface (Thermo Finnigan, Germany) and equipped with a purge-and-trap concentrator (Tekmar Velocity XPT, USA). Each sample was analyzed twice. Compound-specific chlorine isotope analysis was performed using a standard quadrupole MS (Agilent 7890A, Agilent 5975C) following the method developed by Sakaguchi-Söder & al. (2007) and modified by Aeppli et al. (2010). In this study, the method proposed by Aeppli et al. (2010), where two molecular ions are measured, was extended to include four chlorine isotopologues (chemically identical molecule with a different isotopic composition) of the PCE (mass 164, 166, 168, and 170). The raw isotopic ratios were calculated using an equation developed by Jin et al. (2011):

$$R_{PCE} = \frac{I_{166} + 2 \cdot I_{168} + 3 \cdot I_{170}}{3 \cdot I_{164} + 2 \cdot I_{166} + I_{168}} \qquad \text{(equation 3)}$$

where I is the corresponding molecular ion abundance at different m/z values. A calibration was performed with two external standards to obtain delta values on the SMOC scale. Five replicates of each standard were analyzed at the beginning and the end of each analytical sequence. In order to maximize the precision of the analysis all samples were diluted to the same concentration (with the exception of the samples of the uppermost sampling point) and each sample was analyzed five times.

4.2.4 Numerical modeling

The migration of the PCE from the groundwater plume through the capillary fringe and unsaturated zone was simulated using the finite-element code COMSOL Multiphysics. The main goal of the modeling was to gain additional insight into factors that influence the isotope ratios during migration of compounds from saturated to the unsaturated zone. Water flow and distribution under variably saturated conditions were simulated based on Richard's equation. Soil water retention curves were characterized with the Van Genuchten equation (Van Genuchten, 1980). The transport of the PCE was assumed to be driven by advection, dispersion, and diffusion in the saturated zone and in the capillary fringe. In the unsaturated zone, only diffusion was assumed to occur. No flow boundary conditions were defined at the top and the bottom of the system, as well as along both sides of the unsaturated part. In the saturated zone, a constant flow boundary was defined at the inflow side (0.25 m/day) and a constant head boundary (0.12 m) at the outflow side. In the vertical, the mesh was finer close to the capillary fringe and become coarser with distance from the capillary fringe. In the horizontal, the mesh size was constant. All the parameters except transverse vertical dispersivity were determined independently in order to evaluate whether the isotope trends may be reproduced. The Henry coefficient, the isotope fractionation factor between light and heavy isotopes during air-water partitioning and the porosity were determined experimentally. The values of Van Genuchten parameters, residual water content, saturated hydraulic conductivity and diffusion coefficients in the air and water were defined according to the literature. All the parameters are described more in detail below and are summarized in Table 1.

Water saturation is considered to be the most important parameter that influence the vapor diffusion in soils (Millington & Quirk, 1961; Moldrup & al., 2000) and shows significant variations in vertical profiles. The Van Genuchten equations are selected to characterize the soil water retention curves and the soil moisture distribution is determined by the equation (Van Genuchten 1980):

$$\theta = \theta_r + (\theta_s - \theta_r)\,[1+ (\alpha\, H_p)^{1/(1-n)}]^{n} \qquad \textit{(equation 4)}$$

where θ_r is the residual water content, θ_s the saturated water content, H_p the water pressure and α and n are unitless Van Genuchten (VG) parameters. Fluid flows are mainly influenced by the hydraulic conductivity which may decrease when saturation decreases. In the present model, the hydraulic conductivity is defined by the Van Genuchten equations as:

$$K(\theta) = K_s \cdot \sqrt{S_e}\,[1-(1-S_e^{\,1/n})^{n}]^2, \qquad S_e=(\theta - \theta_r)/(\theta_s - \theta_r) \qquad \textit{(equation 5)}$$

As the values of the Van Genuchten parameters of the sand packed in the aquifer model during this experiment are not know, values for sand compiled by Carsel & Parrish (1988) based on grain size distribution (mean values) were used. These authors give values of 14.5 m^{-1} for α and 2.68 for n. The porosity was estimated experimentally, with a value of 0.41, and the residual water content for sand was set at 0.045 according to Carsel & Parrish (1988). The saturated hydraulic conductivity (K_s) was set to $8.25 \cdot 10^{-5}$ m/s according to the same authors.

The mass transport of the PCE was simulated using the advection dispersion equation for variably saturated porous media, assuming equilibrium partitioning between the aqueous and gas phase. A concentration of zero was specified at the top boundary of the model, according to low concentrations in the atmosphere and an inflow of 200 mg/L of PCE was applied in the first 0.12 m of the left boundary. As clean quartz sand was used for the experiment, sorption can be neglected. The governing equation is thus given by:

$$(\theta_w + \theta_a \cdot K_h) \cdot (\delta C_w / \delta t) = \nabla [(\theta_w \cdot D_w + D_e) \cdot C_w] - q \cdot \nabla C_w \qquad \textit{(equation 6)}$$

where C_w is the aqueous phase concentration, θ_w the water volume fraction, θ_a the gas volume fraction, K_h the Henry coefficient, D_w the dispersion tensor, D_e the effective diffusion coefficient and q the specific-discharge vector. The experimental enrichment factor and the Henry coefficient of 0.65 determined during the air-water partitioning by measuring PCE concentrations in gas and water phase at several equilibration steps (data not shown) were applied for the numerical modeling, too. The effective diffusion coefficient is given by:

$$D_e = \theta_w \cdot \tau_L \cdot D_L + \theta_a \cdot \tau_a \cdot D_a \cdot K_h \qquad \textit{(equation 7)}$$

where D_L is the aqueous phase diffusion coefficient, D_a the gas phase diffusion coefficient, τ_L the aqueous phase tortuosity and τ_a the gas phase tortuosity. The tortuosity was quantified using the Millington and Quirk model (Millington & Quirk, 1961):

$$\tau_L = \theta_w^{7/3} \cdot (\theta_w + \theta_a)^{-2}, \quad \tau_G = \theta_a^{7/3} \cdot (\theta_w + \theta_a)^{-2} \qquad \textit{(equation 8)}$$

The diffusion coefficient in the air determined experimentally by Lugg (1968) (value of 0.0797 cm^2/sec) were used for the modeling. The diffusion coefficient in water was calculated using an empirical equation of Worch (1993):

$$D_w^0 = \frac{3{,}595e^{-7} \cdot T}{\mu \cdot M_{PCE}^{0.53}} \qquad \textit{(equation 9)}$$

where T is the temperature (in °K), M_{PCE} the molecular weight of the PCE and μ the dynamic viscosity of the water in centipoise, and has a value of $8.0193 \cdot 10^{-6}$ cm^2/sec.

The diffusion coefficient is dependent on the mass of the molecule, as light isotopologues diffuse faster than heavy ones. The fractionation factor between light and heavy isotope must be taken into account. As shown in chapters 2 and 3, in a diffusion controlled system, isotopes and pairs of isotopologues differing in one heavy isotope fractionate the same way. Isotope fractionation factors can thus be used to quantify the behavior of isotopologues and isotope ratios can reliably be determined by modeling only some of the isotopologues. The mass of the major PCE isotopologues were therefore taken into account for the modeling (165.83 and 166.83 for carbon and 165.83 and 167.83 for chlorine). The total concentration at the inflow boundary was also partitioned between light and heavy isotopes molecules in order to obtain an isotope ratio of -24.9‰ for carbon and 0.2‰ for chlorine isotopes. The various masses were simulated individually. The isotopic ratios was calculated using the relationship $\delta = (C_H/C_L/R_{std}-1)*1000$ [‰], where C_L and C_H are the concentrations of the light and heavy molecules, respectively and R_{std} is the isotope ratio of the standard (VPDB for carbon, SMOC for chlorine). The fractionation factor for diffusion was given by (Cerling et al., (1991):

$$\alpha_{Diff} = \frac{D_h}{D_l} = \sqrt{\frac{(MW_h + MW_m) \cdot MW_l}{(MW_l + MW_m) \cdot MW_h}} \qquad \textit{(equation 10)}$$

where D_h and D_l are the diffusion coefficient for heavy and light isotopologues, respectively; MW_l and MW_h are the molecular weight of the light and heavy molecule, respectively and MW_m the mass of molecules in the media through which diffusion takes place. While this equation is well established for gas phase diffusion, it is not the case for diffusion of organic compounds in water that might show a smaller dependence on molecular weight (LaBolle & al., 2008). This relationship was therefore used for the modeling and can be considered to represent an upper limit for isotope fractionation by aqueous diffusion (Hunkeler & al., 2011).

Transverse dispersion is a key process for the mass transfer of contaminants across the capillary fringe, too. According to previous laboratory experiments, transverse vertical dispersivity in sands is most of the time quite small (< 1mm), and values between 0.226 mm and 3.3 cm were observed for the TCE in some studies (Klenk & Grathwohl, 2002). Transverse dispersivity was varied between 0.2 and 5 mm in the present study. As no significant variations of isotope ratios were observed in this range of values, a value of 1 mm was chosen for the modeling in this study. Mass dependency were not taken into account for the calculation of vertical dispersivity as proposed by Van Breukelen & Rolle (2012) because this dependency is small for the chosen groundwater flow velocity and the porous medium grain size set in the present experimental setup.

Equilibrium is assumed between concentrations in the gas and water phase and only aqueous phase concentrations are reported. In order to compare more easily results between the saturated and the unsaturated zone, as well in the capillary fringe, experimental results measured in the gas phase were thus transformed in aqueous values, taking into account Henry coefficient (0.65) and isotope fractionation factors during air-water partitioning experiments. The concentrations measured in the gas phase were thus multiplied by 0.65 and, isotopic values measured in the gas phase during the 2D experiment were shifted of -0.46‰ and +0.2‰ for carbon and chlorine isotopes, respectively.

Additionally, various scenarios were evaluated in order to understand which parameters may influence isotope fractionation in the subsurface. The influence of the lithology and unsaturated zone thickness on isotope fractionation was especially evaluated. The parameters of the different lithologies are summarized in the Table 2.

Table 1: Parameters used during the numerical modeling study (sand):

Parameters	Values	Units
Inflow PCE concentrations	200	[ppm]
Flow velocity	0.25	[m/j]
Water table	0.12	[m]
Porosity	0.41	[-]
Van Genuchten parameter α	14.5	m^{-1}
Van Genuchten parameter n	2.68	[-]
Residual water content	0.045	[-]
Saturated hydraulic conductivity	8.25E-05	[m/s]
Diffusion coeffient in the air	0.0797	[cm^2/sec]
Diffusion coeffient in water	8.02E-06	[cm^2/sec]
Henry coefficient (Kgw)	0.65	[-]
Transverse vertical dispersivity	1	[mm]

Table 2: Lithology and corresponding values of porosity, residual water content, hydraulic conductivity and Van Genuchten parameters used for the modelling of various lithology (Carsel & Parrish, 1988):

Lithology	Porosity	Residual water content	Hydraulic conductivity	Van Genuchten parameters	
				α	n
	[-]	[-]	[m/sec]	[1/m]	[-]
Sand	0.41	0.045	8.25E-05	14.5	2.68
Sandy loam	0.41	0.065	1.23E-05	7.5	1.89
Sandy clay loam	0.39	0.1	3.64E-06	5.9	1.48
Sandy clay	0.38	0.1	3.33E-07	2.7	1.23

4.3 Results and discussion

4.3.1 Air-water partitioning

Significant chlorine and carbon isotope fractionation occurs during air-water partitioning (Figure 2). The isotope evolution during air-water partitioning of chlorinated compound follows a Rayleigh trends and isotope enrichment factors are calculated with equations 1 and 2. As duplicate experiments show similar results, the average values will be discussed here. Chlorine and carbon isotopes show opposite fractionation trends, with a normal isotope effect for chlorine isotopes (enrichment in heavy isotopes) and an inverse isotope effect for carbon isotopes (depletion in heavy isotopes) (Figure 2). The chlorine isotope enrichment factor for air-water partitioning has a value of ε_{Cl}=-0.20±0.04‰, while the enrichment factor for the carbon has a value of ε_{C}=+0.46±0.04‰ (Figure 2). These results agree with the isotopic fractionation trends observed in chapter 3 for the TCE, which showed the same opposite trends for carbon and chlorine isotope fractionation. The enrichment factors are higher for PCE than for TCE during the air-water partitioning (ε_{Cl}=-0.20±0.04‰ vs. -0.06±0.05‰ and ε_{C}=+0.46±0.03‰ vs. +0.38±0.04, respectively). Bacsik & al. (2002) and Costa-Gomez & Grolier (2001) have also measured opposite enrichments factors for carbon and hydrogen isotopes of methane during air-water partitioning, with a normal isotope effect for hydrogen and an inverse isotope effect for carbon isotopes. Jansco & Van Hook (1974 & 2002) has shown that hindered translations and rotations (external mode) will always lead to a normal isotope effect. In contrast, the frequencies of the internal vibrations (internal mode) will in most cases shift toward lower frequencies (red shift) upon dissolution of molecules, leading to an inverse isotope effect. The observed trends for PCE indicate that changes in the internal modes control isotope fractionation for carbon, whereas for chlorine changes in the external modes dominate.

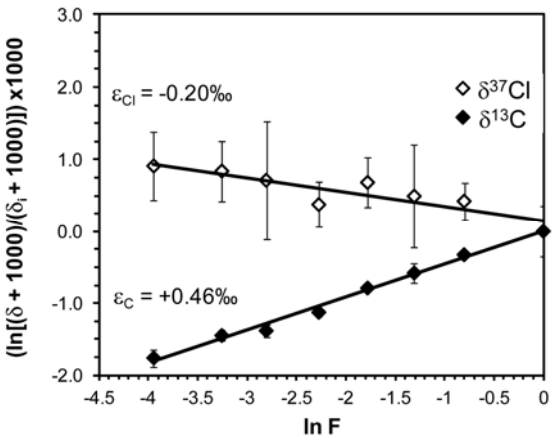

Figure 2: Rayleigh plots for air-water partitioning. Each point is a mean value of duplicates and error bars represent standard deviations.

4.3.2 Transport of PCE through the capillary fringe and the unsaturated zone: laboratory experiments and numerical modeling

During the first 4 days of the experiment, concentrations in the gas phase steadily increase. After 4 days, concentrations become nearly constant indicating that a steady state was reached (Figure 3a). The small increase of concentrations from 4 to 20 days observed in figure 3a is due to a concentration increase in the top of the column, where PCE vapors did not seem to be evacuated efficiently enough to keep concentrations close to 0. The aqueous phase concentrations at the top of the water table reach 180 mg/l at steady state (data not shown). In the lowest gas phase sampling point, the gas phase concentration is thus 30 times smaller than in the aqueous phase (Figure 3a). This large decrease of concentrations is consistent with similar experiments carried out with TCE by McCarthy & Johnson (1993), where very low concentrations were found in the unsaturated zone compared to groundwater. As the diffusion coefficient in water is very small compares to the gas phase and as the vertical transverse dispersivity is small, transport of PCE in the unsaturated zone is very rapid in comparison to the capillary fringe. The rapid upward diffusion leads to low gas phase concentrations and to a strong concentration gradient in the capillary fringe.

Isotope profiles generally do not vary with distance from the water table at a given time. However, the chlorine isotopic ratios globally tend to shift to more positive values over time. Carbon and chlorine isotopic ratios thus show only small variations in the unsaturated zone, even at transient state (Figure 3b&c). This contrasts with previous results for diffusion from a NAPL source where a strong depletion of heavy isotopes with distance from a TCE source was observed during the transient expansion of a vapor plume at a similar length scale (chapter 3). When substances diffuse out of the water, it takes more time to reach a steady state due to the mass transfer resistance of capillary fringe which was absent in case of the NAPL source. Hence the isotope profiles have time to constantly readjust, which is not the case during rapid NAPL vaporization. This conclusion is consistent with the shape of the concentration profiles which are nearly linear even at early times suggesting pseudo steady state conditions. After 480h, a difference of about 0.8‰ was observed between and aqueous and gaseous values across the capillary fringe for both carbon and chlorine isotopes, which represents a statistically significant variation ($p<0.05$ according to student t test). At steady state, a difference of 0.45‰ was measured between the $\delta^{13}C$ values of the PCE in the saturated zone (-24.8‰) and the mean $\delta^{13}C$ value in the gas phase of the unsaturated zone (-24.35‰), which represents a statistically significant variation ($p<0.05$). For chlorine isotope, a mean difference of 0.50‰ was observed between the values at the top of the saturated (0.35‰) and the unsaturated zone (mean value at steady state of

0.85‰), which is not statistically significant (p=0.20). If the difference of isotope ratios observed between the saturated zone and the gas phase of the unsaturated zone was only related to air-water partitioning, a shift of +0.46‰ and -0.2‰ would be expected for carbon and chlorine, respectively (blue vertical dotted lines in Figure 3b&c). While this shift corresponds to measured experimental values for carbon, this is not the case for chlorine isotopes, where an additional offset seems to influence isotope ratios during the migration of contaminants by diffusion through the capillary fringe. In order to evaluate the influence of each physical process (air-water partitioning and diffusion) and their combination on the isotope ratios in the capillary fringe, numerical modeling of the 2D system experiment was performed.

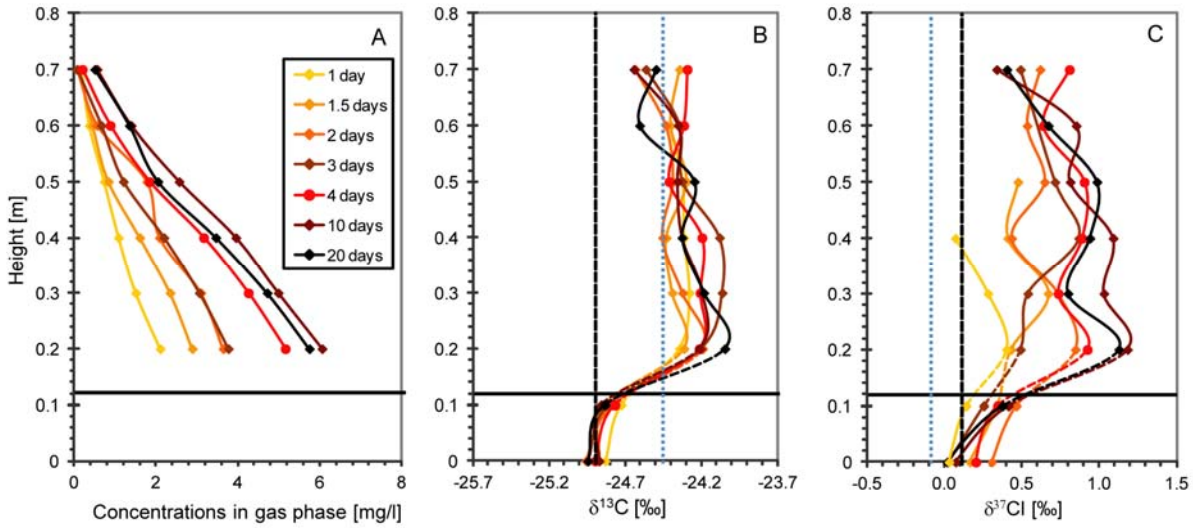

Figure 3: (A) Concentration of PCE in the unsaturated zone (gas phase), (B) $\delta^{13}C$ and (C) $\delta^{37}Cl$ values in the saturated (in water at 0 and 0.1m) and unsaturated zone (in the gas phase from 0.2 to 0.7m) in the middle of the 2D system (mean standard deviation for $\delta^{13}C$ values: ±0.11‰ and for $\delta^{37}Cl$ values: ±0.43‰). The horizontal line indicates the location of the water table and the horizontal lines the isotope ratio of the dissolved PCE in aqueous (dashed black) and gas phase (dotted blue).

The numerical modeling made it possible to evaluate the effect of different physical processes on isotope fractionation during transport of PCE between the saturated and unsaturated zone, as well as to generalize the findings of the laboratory study by considering different scenarios. In order to compare more directly isotope ratios from the saturated and the unsaturated zone, only aqueous phase concentrations are reported in Figure 4. The same trends are obtained for experimental values and the numerical modeling for both concentrations and isotopic values. The conceptual and mathematical model developed to

describe isotope fractionation is thus coherent with observed values. Concentration profiles are linear in the unsaturated zone above the capillary fringe and increase over time until a steady state is reached (Figure 4a). A sharp concentrations gradient is observed in the capillary fringe.

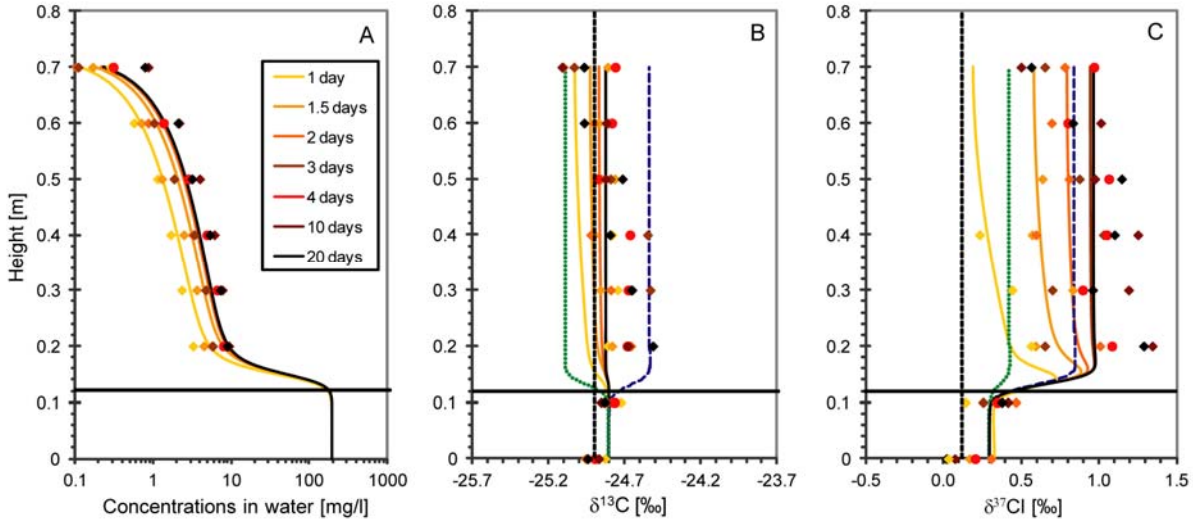

Figure 4: (A) Concentration, (B) $\delta^{13}C$ and (C) $\delta^{37}Cl$ values of the PCE measured (points) and modelled (lines) in the middle of the 2D system. All the values are presented as equivalent in the water phase. Blue dashed curves represent isotopic values at steady state with only diffusion isotope effect. Green dotted curves represent isotopic values at steady state with air-water partitioning isotope effect only. The horizontal line indicates the location of the water table and the vertical dashed line the isotope ratio of the dissolved PCE at the source.

The isotope profiles observed with numerical modeling are consistent with experimental results for both carbon and chlorine isotopes. As observed in the laboratory experiment, the depletion of heavy isotopes with distance during the transient migration of the PCE due to diffusion remains below the detection limit of the method. Additionally, constant isotopic values are observed at steady state through the unsaturated zone above the capillary fringe. In the case of chlorine isotopes, a small offset of aqueous phase isotopic values is observed across the capillary fringe (0.7‰) (Figure 4c). In contrast, no significant change across the capillary fringe was observed for carbon (<0.1‰). The absence of isotope fractionation for carbon in the capillary fringe, but not for chlorine, was explored further using the numerical modeling. In Figure 4b&c, the dashed blue curves represent the isotopic values at steady state with the influence of diffusion only (normal isotope effect with ε = -0.44‰ for carbon and ε = -0.88‰ for chlorine). The dotted green curves represent the isotopic values at

steady state with the influence of air-water partitioning only (inverse isotope effect with ε = +0.46‰ for carbon and ε = -0.2‰ for chlorine). For carbon isotopes, the normal isotope effect of diffusion in the capillary fringe is partly cancelled by isotope effect of air-water partitioning (black curve of Figure 4b). In contrary, in the case of chlorine isotopes, the normal isotope effect of diffusion and the normal isotope effect for air-water partitioning partly cumulate, leading to a larger enrichment in heavy isotopes in the capillary fringe (black curve of Figure 4c). As the offset observed for chlorine in the aqueous phase of the capillary fringe seems mainly influenced by the fractionation caused by the diffusion (Figure 4c), it is expected to be higher for lighter molecules (diffusion enrichment factor of -1.5‰ for the cis-DCE; calculated with equation 10).

As it is possible to reproduce the 2D system experiment, various scenarios were studied in order to evaluate the effect of lithology and unsaturated zone thickness on the isotope evolution. Chlorine isotopes were modeled, as they show larger variations than carbon. Four different lithologies (from sand to sandy clay) were varied in the capillary fringe and the unsaturated zone, but not in the saturated zone where the same sand as before is used, in order to maintain the same flow condition and a flow of 25 cm/day. The same 0.8 meter 2D system was assumed. Values of porosity, residual water content, hydraulic conductivity and Van Genuchten parameters were chosen according to values given by Carsel & Parrish (1988). These values can be found in Table 2. δ^{37}Cl values observed 0.5 m above the water table at transient and steady state are discussed below (Figure 5). With the presence of finer sediments, PCE in the unsaturated zone is initially depleted in ^{37}Cl compared to groundwater. The depletion is the higher the finer the sediments are. However, at steady state, the offset across the capillary fringe becomes smaller for fine grained sediments compared to sand (Figure 5). This offset is smaller because the diffusion across lower permeability sediments partly restricts the flux toward the atmosphere. Finally, the height of the setup was increased to 3 meters while maintaining all other factors. For a 3 meters thick unsaturated zone, δ^{37}Cl values need more time to stabilise and the depletion of heavy isotope with distance is larger than with the 0.8m high 2D system at transient state (magnitude of > 6‰ instead of 0.7‰ while height is increased 3 times)) (Figure 6). However, the same values as for the 0.8m high 2D system are reached at steady state. The extension of the unsaturated zone, as well as the lithology, thus influences significantly the transient isotope fractionation in the unsaturated zone and the time needed to reach a steady state. Moreover, the lithology influences the steady state offset of isotopic ratios in the capillary fringe, which however always remains small.

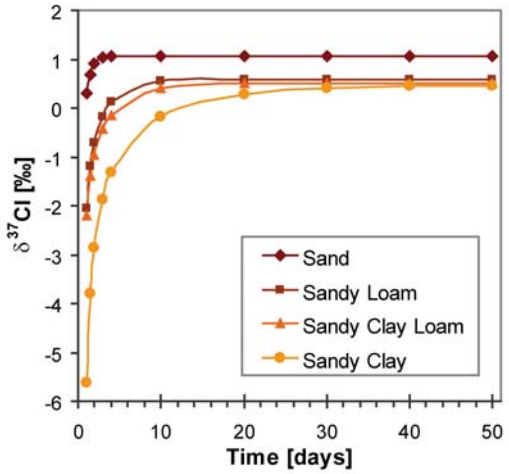

Figure 5: Influence of lithology on $\delta^{37}Cl$ values. Results plotted correspond to $\delta^{37}Cl$ values modelled 0.5 m above the water table in the 0.8 meter 2D system.

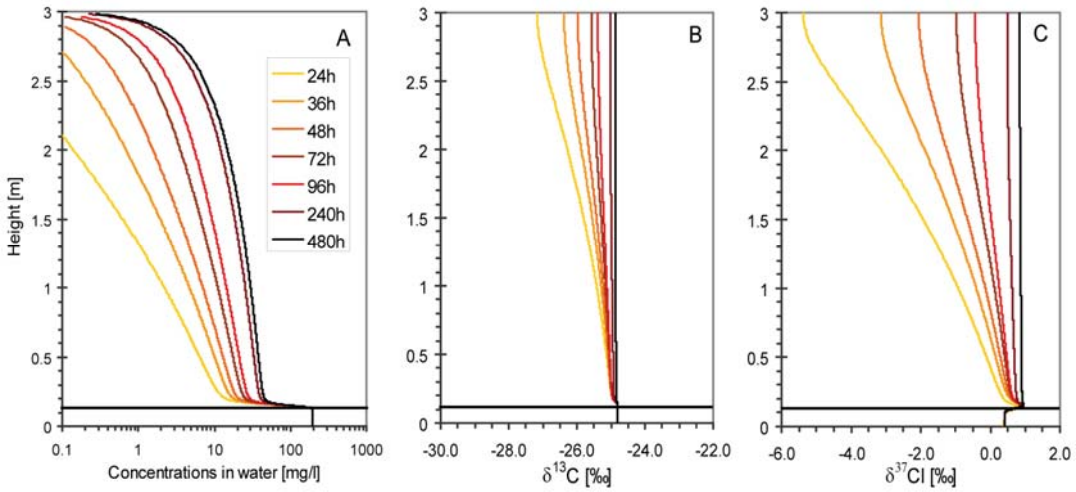

Figure 6: (A) Concentration, (B) $\delta^{13}C$ and (C) $\delta^{37}Cl$ values of the PCE modelled in 3 meters high aquifer model. All the values are presented as equivalent in the water phase. The horizontal line indicates the location of the water table.

While it is possible to reach constant isotopic profiles at steady state throughout the unsaturated zone above the capillary fringe, how will isotopic ratios change in the presence of more dynamic environmental conditions? To address this question the water table was changed several times in a period of 15 days. The water level was increased from 0.12 m to 0.25 m at 9 cm/day, stabilized during 3 days, lowered at the same velocity and to the initial water table, stabilized during 3 days and finally risen back to a level of 0.25 m (Figure 7a).

When the water level increases, the concentrations in the unsaturated zone decrease (Figure 7b). Conversely, during water table drop, concentrations increase considerably in the unsaturated zone. The concentrations decrease again when water table is raised for the second time. The same trends were observed by McCarthy & Johnson (1993).

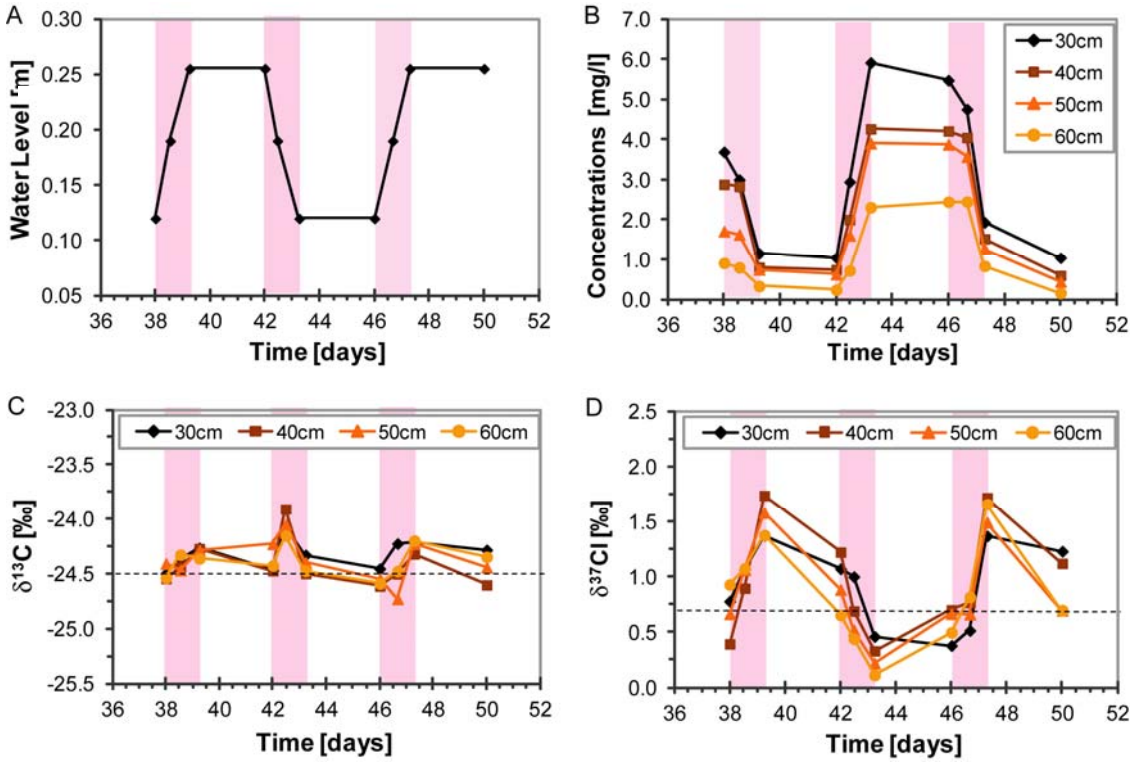

Figure 7: Results of water level fluctuations experiments. Variations of (A) the water level, (B) concentrations, (C) $\delta^{13}C$ and (D) $\delta^{37}Cl$ values in the gas phase over time (mean standard deviation for $\delta^{13}C$ values: ±0.10‰ and for $\delta^{37}Cl$ values: ±0.45‰) at various heights. The horizontal lines represent isotopic values at steady state.

Carbon isotopes do not show significant variations during water table fluctuations. In contrary, $\delta^{37}Cl$ values fluctuate around the steady state values (Figure 7c&d, dashed line). When water level increases, PCE becomes more enriched in ^{37}Cl, and when water level drops, it becomes more depleted. The isotope ratios of PCE in the unsaturated zone depends on two factors: (i) the rate of loss of molecules via diffusion through the unsaturated zone, which preferentially removes light molecules and (ii) the rate of transfer of molecules from the aqueous to the gaseous phase which is less isotope sensitive (as air-water partitioning is small) or which might deliver preferentially light isotopes due to isotope fractionation associated with aqueous phase diffusion. During the water table fluctuation, the balance between the two factors is disturbed. When the water level drops, the contact area

between water and gas phase increases, leading to a temporary increase of concentrations in the gas phase. As the delivery of lighter molecules thus increases, at least temporarily, isotope fractionation drops and δ^{37}Cl values in the unsaturated zone become closer to source values. When the water level rises, less molecules are transferred from the water to the gas phase as indicated by the lower concentrations. As light isotopes diffuse out of the system faster, a depletion of light isotopes occurs in the capillary fringe. Chlorine isotopes show thus a significant range of variation of 1.5‰ during the 13 cm water table fluctuations. However, because transport in the gas phase is rapid, the δ^{37}Cl values tend to go to the steady state values after 3 days if the water level is stabilized. Conversely, carbon isotopes do not show significant variations during water table fluctuations as isotopic effects of air-water partitioning and diffusion cancel each other.

4.4 Conclusions

At steady state, a small enrichment in heavy isotope is expected between the saturated zone and the gas phase of the unsaturated zone for carbon and chlorine isotopes during the release of PCE from a groundwater plume towards the atmosphere. Numerical modeling highlights that this shift are associated with isotope fractionation of air-water partitioning, as well as to the preferential loss of light isotopologues from the unsaturated zone due to diffusion. It decreases as the unsaturated zone becomes less permeable. Constant isotopic profiles can be observed for the PCE in the unsaturated zone above the capillary fringe at steady state. However, if the unsaturated zone is thick and/or layer of fine sediments are present, a depletion in heavy isotopes is expected along concentration gradients during the transient migration of PCE through the unsaturated zone. This depletion is the higher the finer the sediments are. Moreover, chlorine isotope variations occur in the unsaturated zone during water table fluctuations. Hence potential isotope variations due to non-steady state conditions should be considered when applying CSIA methods at field sites, especially if the unsaturated zone is thick, if layers of fine sediments are present in the site and/or if large and rapid water table variations occur. However, at steady state, stable isotope analysis can be used to link a soil gas contamination of chlorinated solvents to a plume located in groundwater as offsets are expected to be small. The present study also shows that, additionally to laboratory experiments, numerical modeling is an effective tool to gain additional insight into factors that influence the isotope ratios during migration of compounds from saturated to the unsaturated zone.

4.5 References

- **Aeppli**, C.; Holmstrand, H.; Andersson, P.; Gustafsson, O. Direct compound-specific stable chlorine isotope analysis of organic compounds with quadrupole GC/MS using standard isotope bracketing. *Anal. Chem.* **2010**, 82 (1), 420-426.
- **Bacsik**, Z.; Lopes, J. N. C.; Gomes, M. F. C.; Jancso, G.; Mink, J.; Padua, A. A. H. Solubility isotope effects in aqueous solutions of methane. *J. Chem. Phys.* **2002**, 116 (24), 10816-10824.
- **Bouchard**, D.; Hunkeler, D.; Gaganis, P.; Aravena, R.; Hohener, P.; Broholm, M. M.; Kjeldsen, P. Carbon isotope fractionation during diffusion and biodegradation of petroleum hydrocarbons in the unsaturated zone: Field experiment at Vaerlose airbase, Denmark, and modeling. *Environ. Sci. Technol.* **2008**, 42 (2), 596-601.
- **Bouchard**, D.; Hohener, P.; Hunkeler, D. Carbon isotope fractionation during volatilization of petroleum hydrocarbons and diffusion across a porous medium: A column experiment. *Environ. Sci. Technol.* **2008**, 42 (21), 7801-780.
- **Bradley**, P. M. Microbial degradation of chloroethenes in groundwater systems. *Hydrogeol. J.* **2000**, 8 (1), 104-111.
- **Carsel**, R. F.; Parrish, R. S. Developing joint probability-distributions of soil-water retention characteristics. *Water Resour. Res.* **1988**, 24 (5), 755-769.
- **Cerling**, T. E.; Solomon, D. K.; Quade, J.; Bowman, J. R. On the isotopic composition of carbon in soil carbon-dioxide. *Geochim. Cosmochim. Acta* **1991**, 55 (11), 3403-3405.
- **Costa Gomes**, M. F. ; Grolier, J. P. Determination of Henry's law constants for aqueous solutions of tetradeuteriomethane between 285 and 325 K and calculation of the H/D isotope effect. *Phys. Chem. Chem. Phys.* **2001**, 3 (6), 1047-1052.
- **Hunkeler**, D.; Aravena, R.; Shouakar-Stash, O.; Weisbrod, N.; Nasser, A.; Netzer, L.; Ronen, D. Carbon and chlorine isotope ratios of chlorinated ethenes migrating through a thick unsaturated zone of a sandy aquifer. *Environ. Sci. Technol.* **2011**, 45 (19), 8247-8253.
- **Jin**, B. A.; Laskov, C.; Rolle, M.; Haderlein, S. B. Chlorine isotope analysis of organic contaminants using GC-qMS: Method optimization and comparison of different evaluation schemes. *Environ. Sci. Technol.* **2011**, 45 (12), 5279-5286.
- **Jancso**, G.; Van Hook, W. A. Condensed phase isotope-effects (especially vapor-pressure isotope-effects). *Chem. Rev.* **1974**, 74 (6), 689-750.
- **Jancso**, G. Interpretation of isotope effects on the solubility of gases. *Nukleonika* **2002**, 47, S53-S57.
- **Klenk**, I. D.; Grathwohl, P. Transverse vertical dispersion in groundwater and the capillary fringe. *J. Contam. Hydrol.* **2002**, 58 (1-2), 111-128.
- **Kuder**, T.; Philp, P.; Allen, J. Effects of volatilization on carbon and hydrogen isotope ratios of MTBE. *Environ. Sci. Technol.* **2009**, 43 (6), 1763-1768.
- **LaBolle**, E. M.; Fogg, G. E.; Eweis, J. B.; Gravner, J.; Leaist, D. G. Isotopic fractionation by diffusion in groundwater. *Water Resour. Res.* **2008**, 44 (7), 15.
- **Lugg**, G. A. Diffusion coefficients of some organic and other vapors in air. *Anal. Chem.* **1968**, 40 (7), 1072-&.
- **McCarthy**, K. A.; Johnson, R. L. Transport of volatile organic-compounds across the capillary-fringe. *Water Resour. Res.* **1993**, 29 (6), 1675-1683.
- **Millington**, R.; Quirk, J. P. Permeability of porous solids. *Transactions of the Faraday Society* **1961**, 57 (8), 1200-&.
- **Moldrup**, P.; Olesen, T.; Gamst, J.; Schjonning, P.; Yamaguchi, T.; Rolston, D. E. Predicting the gas diffusion coefficient in repacked soil: Water-induced linear reduction model. *Soil Sci. Soc. Am. J.* **2000**, 64 (5), 1588-1594.
- **Poulson**, S. R.; Drever, J. I. Stable isotope (C, Cl, and H) fractionation during vaporization of trichloroethylene. *Environ. Sci. Technol.* **1999**, 33 (20), 3689-3694.

- **Sakaguchi-Soder**, K.; Jager, J.; Grund, H.; Matthaus, F.; Schuth, C. Monitoring and evaluation of dechlorination processes using compound-specific chlorine isotope analysis. *Rapid Commun. Mass Spectrom.* **2007**, 21 (18), 3077-3084.
- **Van Breukelen**, B. M.; Rolle, M. Transverse hydrodynamic dispersion effects on isotope signals in groundwater chlorinated solvents' plumes. *Environ. Sci. Technol.* **2012**, 46 (14), 7700-7708.
- **Van Genuchten**, M. T. A closed-form equation for predicting the hydraulic conductivity of unsaturated soils. *Soil Sci. Soc. Am. J.* **1980**, 44 (5), 892-898.
- **Wang**, Y.; Huang, Y. S. Hydrogen isotopic fractionation of petroleum hydrocarbons during vaporization: Implications for assessing artificial and natural remediation of petroleum contamination. *Appl. Geochem.* **2003**, 18 (10), 1641-1651.
- **Worch**, E. Eine neue Gleichung zur Berechnung von Diffusionskoeffizienten gelöster Stoffe. Vom Wasser 1993, 81, 289-297.

Chapter 5

Carbon isotope fractionation during biodegradation and diffusive transport of vinyl chloride

Abstract

The isotope fractionation related to biodegradation in variable saturated conditions was studied with microcosm experiments and numerical modeling, using vinyl chloride (VC) as a model compound. During the biodegradation of VC in microcosm experiments, an enrichment factor of -7.2‰ was observed for carbon. Additionally, isotope fractionation related to biodegradation during the migration of VC from groundwater through unsaturated zone towards the atmosphere was investigated by modeling of a 2D system. In unsaturated conditions where diffusion is the major transport process, the effective isotope fractionation for biodegradation is smaller than in saturated conditions where advection is the main transport process. An effective isotope enrichment factor of -2.1‰ was determined for VC in such conditions. Numerical modeling has highlighted that isotope effect related to biodegradation may be identified in a diffusion-controlled system if the degradation rate is high enough to overcome the isotope effect due to diffusion. The signal of biodegradation is amplified if layers of fine sediments are present and/or if the unsaturated zone is thick. Conversely, if degradation rate is low and/or transfer time through the unsaturated zone is too rapid, almost constant isotopic profile are observed through the unsaturated zone and biodegradation effect is no longer observable. It is also highlighted that a significant part of the biodegradation takes place in the first centimeter of the unsaturated zone (near the saturated zone), where effective diffusivity is lower.

5.1 Introduction and aim of the study

In the chapter 4, the effect of transfer across the capillary fringe and diffusion through the unsaturated zone on isotope ratios was investigated with laboratory experiments and numerical modeling. As tetachloroethene (PCE) is stable under oxic conditions which are typically encountered in sandy unsaturated zones (Bradley, 2000), PCE was used as a model compound. In the present chapter, the effect of biodegradation on isotope ratios of VOCs in the unsaturated zone is explored using numerical modeling. The behaviour of vinyl chloride (VC) was simulated as this compound degrades under oxic conditions. VC tends to accumulate at chlorinated ethene sites if conditions are not sufficiently reducing or if microorganisms capable of complete reduction of tetrachloroethene (PCE) and trichloroethene (TCE) to ethene (ETH) are absent or inactive (Harkness & al., 1999; Fennell & al., 2001; Chartrand & al., 2005). Degradation of VC may however occur under both anoxic and oxic conditions. Under anoxic conditions, VC can be reductively dechlorinated to ethene (Bradley & al., 1996 & 1998), while under oxic conditions VC can be oxidized to CO_2 and CH_4 (Bradley & Chapelle, 2000). Coleman & al. (2002) has shown that oxidation of VC in various contaminated sites was correlated with the presence of Mycobacterium JS60 and Nocardioides JS614. As oxic conditions are more common in the unsaturated zone, the present chapter focuses on aerobic degradation of VC.

Significant carbon isotope fractionation was previously reported for aerobic oxidation of VC, with enrichments factors (ε) between -3.2 and -8.2‰ (Chu & al., 2004; Chartrand & al., 2005; Abe & al., 2009). In the case of reductive dechlorination of VC, enrichments factors were bigger, with values between -22.4 to -31.1‰ (Bloom & al., 2000; Hunkeler & al., 2002; Abe & al., 2009). In the unsaturated zone, isotope fractionation may also occur due to phase partitioning and diffusive transport, in addition to biodegradation. Little is known about the combined effect of phase partitioning, diffusion and biodegradation on the isotope ratio of organic compounds in porous media under variably saturated conditions. Bouchard & al. (2008) have investigated the effect of volatilization, diffusion, and biodegradation on the isotope evolution of a mix of petroleum hydrocarbons. They have shown that, as the preferential removal of ^{12}C-molecules due to biodegradation is partly counterbalanced by the larger mass flux of ^{12}C-molecules brought along by diffusion from the source, the effective enrichment factor for biodegradation was reduced compared to the enrichment factor for biodegradation only. If Bouchard & al (2008) has studied the coupling of biodegradation and diffusion through the unsaturated zone on isotope fractionation from a NAPL source, this relation was not studied before for the migration of contaminants from a plume.

The main goal is thus to assess the magnitude of isotope fractionation of VC in a system where biodegradation and diffusion are the dominant processes and compare it to isotope fractionation when biodegradation occurs in isolation. Numerical modeling was carried out in order to investigate isotope fractionation during the migration of VC from a groundwater plume through unsaturated zone towards the atmosphere in combination with biodegradation. Parameters for the model were determined during the experiment and modeling of chapter 4 and the same setup was used. The main objective of the numerical modeling part was to evaluate if isotope fractionation due to biodegradation occurs in a diffusion-controlled system, as diffusive transport in gas phase is rapid and as diffusion partly counterbalance the isotope fractionation due to biodegradation. Microcosm experiments were first carried out with sediments from a field site in France where biodegradation of VC were documented in order to evaluate isotope fractionation due to biodegradation in isolation. The obtained enrichment factor was then used during numerical modeling.

5.2 Material and methods

5.2.1 Microcosm experiments

Microcosms were conducted in 160 ml sterile glass bottles capped with butyl-rubber (Viton) stoppers (Wheaton). The bottles were filled with 50 g of homogenized soil material and the soil moisture content was set to 20% w/w. Soil material was collected at a field site in France contaminated with PCE and TCE, and where VC is found in significant concentrations (with concentration typically around 400 to 700 μg/l in the unsaturated zone). Microcosms were amended with VC (Sigma Aldrich 99.5 % purity) at a concentration of 5-10 mg/l. Two different gas phase compositions (N_2/O_2 80%/20% or N_2 100%) and two temperatures (15°C and 25°C) of incubation were studied. Control microcosms (one per gas phase composition and temperature) were autoclaved before the experiment. Three replicates were prepared for each gas phase composition and temperature. Sampling was carried out with gas-tight syringes of 1 ml. In order to follow concentrations variations, GC-FID measurements were carried out 2 times per week with direct injections using a loop. Gas samples for carbon isotope analysis were diluted in water as described in chapter 3.2.5., in order to perform analyses in a single run and to maximize the precision.

Carbon isotope ratios of VC were analyzed with a TRACE^{TM} gas chromatograph (GC) coupled to a DeltaPlus XP isotope ratio mass spectrometer (IRMS) via a combustion III interface (Thermo Finnigan, Germany). The samples were preconcentrated with a purge-and-trap concentrator (Tekmar Velocity XPT, USA). A 25 ml sample was purged for 10 min at a rate of 40 ml/min and retained in a trap filled with Vocarb 3000. The trap was then heated to 250°C. The desorbed compounds were trapped again at −120 °C with cryogenic trap (ATAS GL, The Netherlands) installed inside the GC oven before releasing them to the GC by heating to 180°C. The chromatographic separation was performed using a DB-QSPlot column (30 m, 0.32 mm, 0.32 µm, Restek) with a constant helium flow of 1.7 ml/min. Each sample was analyzed twice. In addition to $\delta^{13}C$ values, concentrations of VC were determined based on the peak area of major CO_2 mass ion (m/z 44) for every sample. Previous studies (Bloom & al., 2000; Chartrand & al., 2005; Abe & al., 2009) have shown that isotope fractionation associated with biodegradation follows a Rayleigh distillation trend. The results were thus plotted and evaluated using the following equations:

$$\ln[\delta + 1000)/(\delta_i + 1000)] = (\alpha - 1) \ln f \quad \text{and} \quad \varepsilon = (\alpha - 1) \cdot 1000 \qquad \textit{(equation 1)}$$

where δ is the isotopic composition of VC for a particular value of *f*, δ_i is the initial isotopic composition of VC, *f* is the fraction of VC remaining, α is the fractionation factor, and ε is the isotope enrichment factor.

5.2.2 Numerical modeling

The migration of the VC from the groundwater plume through the unsaturated zone to the atmosphere was simulated using the finite-element code COMSOL Multiphysics. The model setup was based on the 2D system studied in chapter 4 (method in section 4.2.2), with the same boundary conditions and governing equations. The concentration trends of two isotopologues with masses 62.5 and 63.5 were simulated and based on the isotopologue concentrations, isotope ratios were calculated. The same parameters were used (see Table 1 of chapter 4), except for diffusion coefficients, Henry coefficient and fractionation factors. In addition, a reaction term, corresponding to first order kinetics, was added in the advection dispersion equation to simulate the decrease of contaminant due to biodegradation. For the Henry coefficient, a value of 0.99 was chosen according to Sander (1999). A gas phase diffusion coefficient of 0.1104 cm^2/sec was obtained using the FSG (Fuller-Schettler-Giggings) method (Lyman & al., 1990):

$$D_a = \frac{1e^{-3} \cdot T^{1.75} \cdot \sqrt{M_{VC}}}{P \cdot (V_{air}^{1/3} + V_{VC}^{1/3})^2} \qquad \textit{(equation 2)}$$

where T is the temperature (in °K), M_{VC} the molecular weight of the VC, P the pressure (in atm) and V_{air} and V_g the molar volume of air and gaseous VC, respectively. Diffusion coefficient in the liquid was set to $1.3451 \cdot e^{-5}$ cm^2/sec according to Worch (1993):

$$D_w^0 = \frac{3{,}595e^{-7} \cdot T}{\mu \cdot M_{VC}^{0.53}} \qquad \textit{(equation 3)}$$

where μ is the dynamic viscosity of the water in centipoise, and has a value of $8.0193 \cdot 10^{-6}$ cm^2/sec. The carbon isotope enrichment factor for air-water partitioning was set to -0.20‰ according to the value reported in Hunkeler & al. (1999).

An isotope enrichment factor (ε) of 2.49‰ was calculated for diffusion in the air and an enrichment factor of 1.77‰ was calculated for diffusion in the water according to the following equation (Craig, 1953):

$$\alpha_{Diff} = \frac{D_h}{D_l} = \sqrt{\frac{(MW_h + MW_m) \cdot MW_l}{(MW_l + MW_m) \cdot MW_h}} \quad \textit{and} \quad \varepsilon_{Diff} = (\alpha_{Diff} - 1) \cdot 1000 \qquad \textit{(equation 4)}$$

where, D_h and D_l are the diffusion coefficient for heavy and light isotopologues respectively, MW_l and MW_h is the molecular weight of the light and heavy molecule, respectively and MW_m the mass of molecules in the media through which diffusion takes place.

Various scenarios were studied in order to evaluate under which conditions biodegradation can be identified with CSIA under variably saturated conditions. The influence of the lithology and unsaturated zone thickness on isotope fractionation was especially evaluated, as finer sediments slow down diffusive transport and a thicker unsaturated zone will increase the time available for biodegradation. Two different lithologies (sand and sandy loam) were used in the unsaturated zone for the same 0.8 meter high 2D system as in chapter 4. Lithologies were defined homogeneously in the unsaturated zone. Parameters of these two litholgies can be found in Table 2 of chapter 4. In both scenarios, sand was considered in the saturated zone in order to not disturb water flow. Additionally, a similar setup than the 0.8 meter 2D system was studied, but the height of the setup was increased to 3 meters. The same length was used for the domain and, in order to perform the modeling in the same conditions, the simulation was also made in 2D. Aerobic degradation of VC at a rate of 0.48 d^{-1} was first used. This degradation rate was measured by Thiem & al. (2008) with an enriched culture at room temperature (25°C) and represents a fast degradation rate. In order to determine the contribution of the capillary fringe to isotope fractionation during biodegradation of VC, the same degradation rate of 0.48 d^{-1} was used, but without degradation in the first 5 cm of the unsaturated zone. As temperatures in the field are most of the time lower and microorganisms are also less active than in the laboratory, a 10 times lower degradation rate was also evaluated (0.048 d^{-1}), which is close to the degradation rates observed in the microcosm experiments. For all the scenarios, the fractionation factor determined in microcosm experiments is used.

5.3 Results and discussion

5.3.1 Microcosm experiments

After the injection of VC in microcosms with aerobic conditions, concentrations decrease progressively, with a half life of about 40 days at 25°C and 100 days at 15°C, which correspond to degradation rates of 0.017 and 0.007 d^{-1}, respectively (Figure 1). However, the concentrations tend to decrease more rapidly after 25% of degradation. This change may reflect an acclimation period necessary to reactivate the microorganisms. For microcosms at 25°C, the degradation rate even becomes almost twice as large after 25% of degradation.

All the results of 3 replicates (with aerobic conditions) are plotted in Figure 2. Isotopic ratios are progressively shifted from -28‰ for the initial source to -10‰ after about 90% of VC degraded at 25°C and -12.5‰ at 15°C. An isotope enrichment factor of -7.2‰ was obtained at 25°C and -7.0‰ at 15°C (Figure 2) which is in the same range as in previous studies. Abe

& al. (2009) has compiled values of isotope enrichment factors for aerobic biodegradation of VC and has reported values between -3.2 and -8.2‰. Control microcosms have not shown any significant variations in $\delta^{13}C$ during experimental period (data not shown).

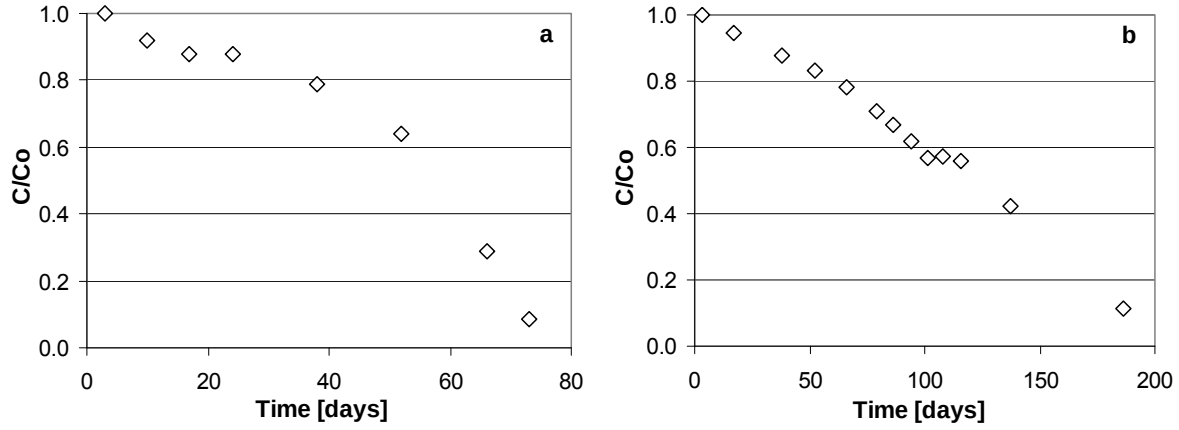

Figure 1: Decrease of concentration in function of time for microcosms at (a) 25°C and (b) 15°C (mean values of 3 replicates for each time) in aerobic conditions

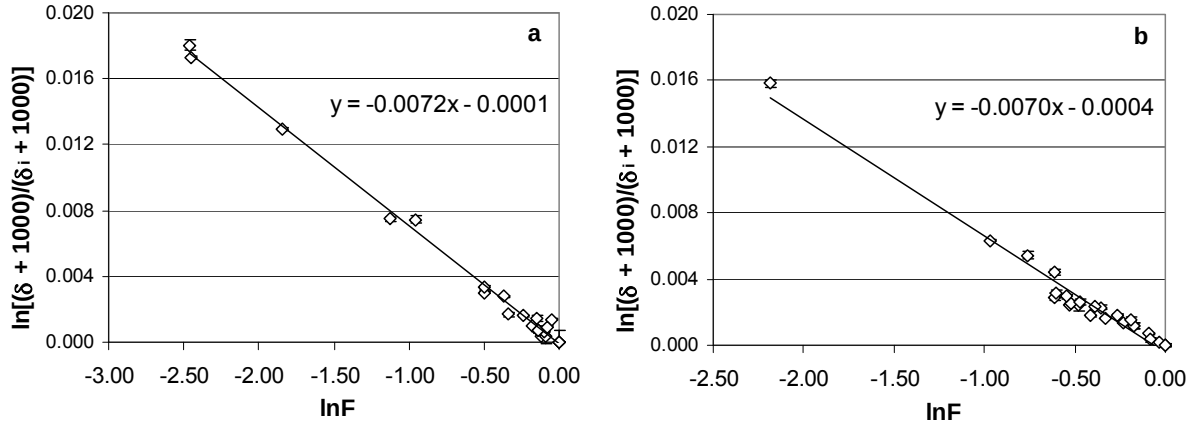

Figure 2: Rayleigh plots for degradation of VC (carbon isotopes): a) microcosms at 25°C and b) at 15°C in aerobic conditions. All the values of 3 replicates are plotted. Error bars represent standard deviation.

5.3.2 Numerical modeling

In Figure 3, all the data represent profiles at steady state. Water level was set at 0.12 m. For all the scenarios, a large drop of concentrations is observed between the saturated and the unsaturated zone (Figure 3a,c,e). In absence of biodegradation, it was observed in chapter 4 that the concentrations decrease linearly with distance across the unsaturated zone located above the capillary fringe. However, when degradation occurs in the unsaturated zone, this decrease become non linear. As expected, concentrations become lower when

biodegradation occurs (Figure 3a,c,e). This variation is nevertheless quite small for a degradation rate of 0.048 d^{-1}.

Significant changes are observed between isotope profiles where degradation occurs and profiles with no degradation. At steady state, isotope profiles are constant in the unsaturated zone above the capillary fringe in absence of biodegradation for the two lithologies and unsaturated zone thicknesses (Figure 3 b, d, f). In contrast, when degradation occurs, the isotopic profiles vary with distance from the water table. In the case of a 0.8 meter high 2D system filled with sand (Figure 3b), a shift of about 3.5‰ is observed at the top of the unsaturated zone between the scenarios without and with degradation (rate of 0.48 d^{-1}). If no degradation occurs in the first 5 cm of the unsaturated zone (of 70 cm high), this shift is reduced to 1.5‰. Finally, if the degradation rate is 10 time lower (0.048‰), which is more close to field conditions, the difference between scenarios with and without biodegradation is reduced to 0.35‰.

The same trends are observed in the case of the 2D system filled with sandy loam (Figure 3c&d). However, larger shift are observed between isotope profiles with and without biodegradation than for a sandy system. A shift of 5.5‰ is observed if degradation occurs in the entire unsaturated zone at 0.48 d^{-1} and a shift 3‰ is observed if the first 5 cm are not influenced by degradation. Such results were expected as diffusion is slowed down in finer sediments and microorganisms have more time to degrade contaminants than in sands. For a degradation rate of 0.048 d^{-1}, this shift is less pronounced (0.8‰). In the case of a 3 meters thick unsaturated zone, even larger isotopic shifts are observed (Figure 3e&f). At the top of the unsaturated zone, the shift between profiles with and without biodegradation are of 11‰, 9‰, 2‰ for degradation rates of 0.48 d^{-1}, 0.48 d^{-1} (except for the first 5 cm of the unsaturated zone) and 0.048d^{-1}, respectively. A significant isotope fractionation is observed for unsaturated conditions when the degradation rate is high (0.48 d^{-1}). Effective isotope fractionation related to biodegradation is small when the degradation rate is (0.048d^{-1}), if the thickness of the unsaturated zone is small or if only sands are present.

Numerical modeling suggests that, in the unsaturated zone, a major part of the biodegradation seems to occur in the capillary fringe. In fact, significant changes in isotopic ratios are observed if biodegradation is active in the first 5 cm of the unsaturated zone at a rate of 0.48 d^{-1}. For example, in the case of the 0.8 meter 2D system filled with sand, these 5 cm represent only 7% of the unsaturated zone height. But, at the top the unsaturated zone the isotope shift is more than twice as high if biodegradation is assumed to occur in the capillary fringe, compared to the scenario where no degradation occurs in the first 5 cm of

the unsaturated zone (3.5‰ vs 1.5‰, Figure 3b). The larger effect of the capillary fringe compared to the rest of the unsaturated zone can probably be explained with the longer residence time of contaminants in this zone due to a lower effective diffusivity.

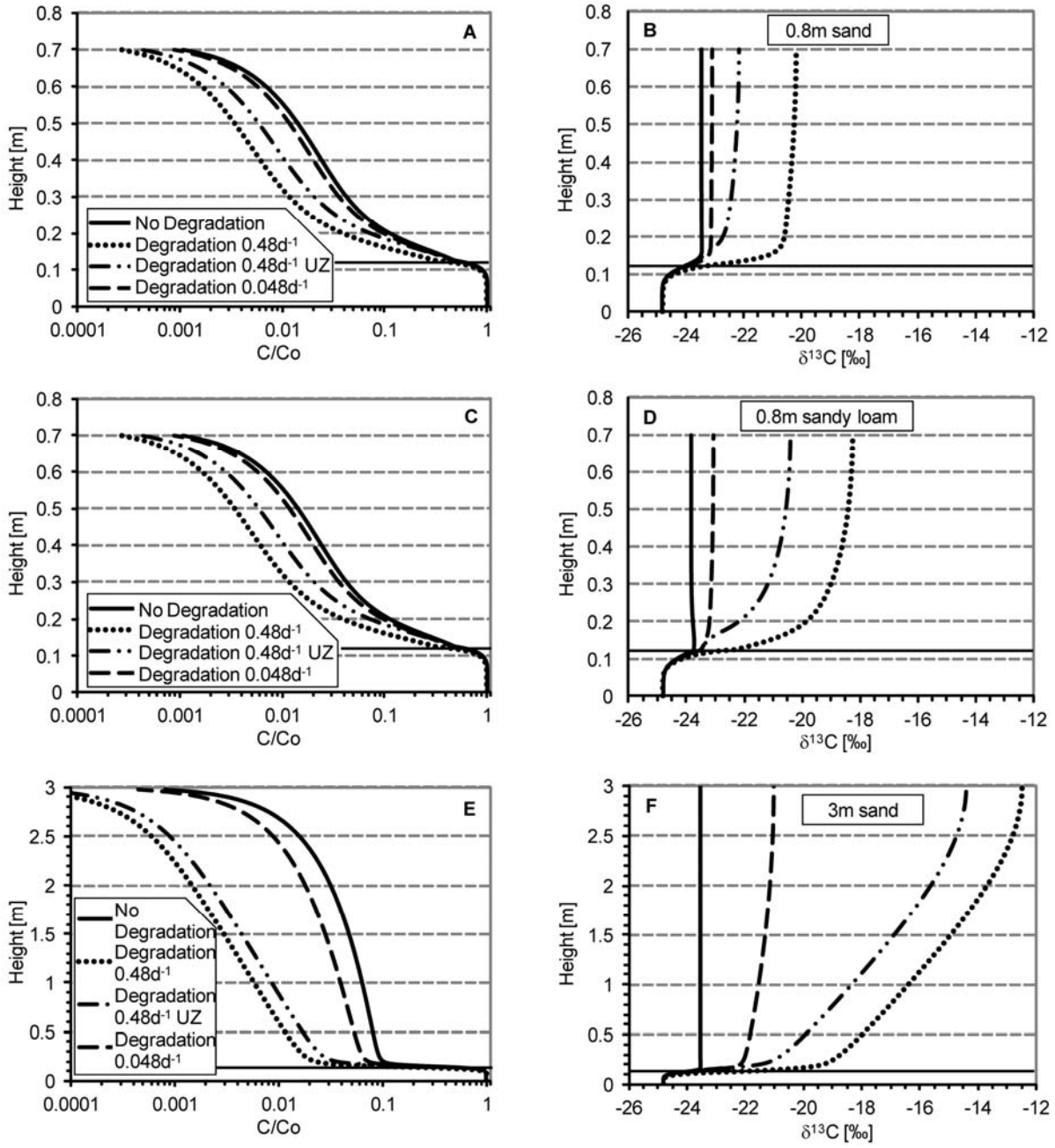

Figure 3: Concentrations and carbon isotopic ratio evolution in 2D systems with different degradation rates in numerical modeling (Degradation 0.48d^{-1} UZ = without degradation in the first 5 centimeters of the unsaturated zone): for a 0.8 meter high 2D system filled with sand (a&b), and filled with sand (in the saturated zone) and sandy loam (in the unsaturated zone) (c&d) and for a 3 meters high 2D system filled with sand (e&f). The horizontal black lines indicate the location of the water table.

Numerical modeling also shows that biodegradation may be identified in a diffusion-controlled system using CSIA if the degradation rate is high enough and/or if the residence time is sufficiently long. Hence biodegradation at a lower degradation rate can be detected if layers of fine sediments are present in the unsaturated zone and/or if unsaturated zone is thick. Nevertheless, even with almost 3 meters of sand, an enrichment of less than 1% is observed with a degradation rate of only 0.048 d^{-1}. Sufficiently high degradation rates are thus required to detect biodegradation using CSIA. However, in the field, temperatures are lower than in the laboratory and microorganisms are less active than in microcosm experiments.

Additionally, as the preferential removal of ^{12}C-molecules due to biodegradation is partly counterbalanced by the larger mass flux of ^{12}C-molecules brought along by diffusion from the source, the effective isotope fractionation due to biodegradation is partly cancelled compared to the isotope fractionation for biodegradation only. However, as already shown by Bouchard & al. (2008), it is not possible to use the classical Rayleigh approach in a diffusion-controlled system to evaluate the effect of biodegradation, as the concentrations decrease in the system even in absence of biodegradation. In order to estimate an effective isotope enrichment fact in such a system, $\delta^{13}C$ values can be related to mass-flux instead of concentrations (Bouchard & al., 2008). In the case of the 3 meters thick unsaturated zone scenario, an effective enrichment factor of -2.1‰ is then found (Figure 4) which is much smaller that the enrichment factor determined for biodegradation in microcosm experiments (-7.2‰). For the 0.8m high 2D system, the effective enrichment factors vary between 1.9 and 2.1‰ (data not shown).

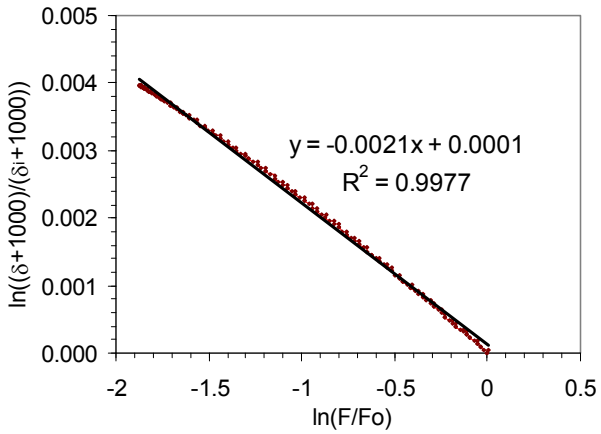

Figure 4: Rayleigh plot for biodegradation in a diffusive system as function of mass-flux. The slope corresponds to the effective isotope enrichment factor of diffusion and biodegradation.

It can be shown that the effective enrichment factor for biodegradation in a system where diffusion is the major transport process follows in good approximation the following analytical equation (Hunkeler, D.; in preparation):

$$\varepsilon_{eff} = \frac{1}{2} \cdot (\varepsilon_{Deg} + \varepsilon_{Diff}) \qquad \textit{(equation 5)}$$

where ε_{Deg} and ε_{Diff} are the enrichment factor of biodegradation (-7.2‰) and diffusion (+2.5), respectively. Using this equation, an effective enrichment factor of -2.35‰ is obtained which is close to the -2.1‰ found with numerical modeling. Moreover, according to equation 5, even if transport doesn't cause any fractionation, the effective isotope fractionation factor in a diffusion-controlled system is smaller than the isotope fractionation factor associated with biodegradation in isolation.

5.4 Conclusions

Microcosm experiments have shown that biodegradation of VC occurs in unsaturated conditions using material from a contaminated site. An enrichment factor of -7.2‰ was obtained. However, during the assessment of biodegradation in unsaturated zone, the isotope fractionation related to diffusion and volatilization must also be taken into account. As the enrichment of ^{13}C due to biodegradation is partly counterbalanced by preferential diffusion of ^{12}C-molecules through the unsaturated zone, the effective isotope fractionation factor for biodegradation in diffusion-controlled system is smaller than in saturated conditions where advection is the main transport process. Numerical modeling has highlighted that biodegradation may be identified in a diffusion-controlled system using CSIA if degradation rate is high enough. The signal of biodegradation is magnified if layers of fine sediments are present and/or if unsaturated zone is thick, which is most of the time the case in the field. Moreover, a significant part of the biodegradation seems to take place in the first centimeters of the unsaturated zone (capillary fringe) because of the longer residence time of contaminants in this zone due to a lower effective diffusivity. In contrast, if microorganisms are less active and biodegradation rate is low, the effective isotope fractionation related to biodegradation is small and almost constant isotope profiles are observed with distance across the unsaturated zone. Since constant isotopic values are expected across the unsaturated zone at steady state in absence of biodegradation (or if biodegradation rate is low), a shift of isotopic values across the unsaturated zone will indicate the presence of a significant biodegradation. All these results wait to be confirmed experimentally.

5.5 References

- **Abe**, Y.; Aravena, R.; Zopfi, J.; Shouakar-Stash, O.; Cox, E.; Roberts, J.D.; Hunkeler, D. Carbon and chlorine isotope fractionation during aerobic oxidation and reductive dechlorination of vinyl chloride and cis-1,2-dichloroethene. *Environ. Sci. Technol.* **2009**, 43 (1), 101-107.
- **Bloom**, Y.; Aravena, R.; Hunkeler, D.; Edwards, E.; Frape, S.K. Carbon isotope fractionation during microbial dechlorination of trichloroethene, cis-1,2-dichloroethene, and vinyl chloride: Implications for assessment of natural attenuation. *Environ. Sci. Technol.* **2000**, 34 (13), 2768-2772.
- **Bouchard**, D.; Hohener, P.; Hunkeler, D. Carbon isotope fractionation during volatilization of petroleum hydrocarbons and diffusion across a porous medium: A column experiment. *Environ. Sci. Technol.* **2008**, 42 (21), 7801-7806.
- **Bradley**, P.M.; Chapelle, F.H. Anaerobic mineralization of vinyl chloride in Fe(iii)-reducing, aquifer sediments. *Environ. Sci. Technol.* **1996**, 30 (6), 2084-2086.
- **Bradley**, P.M.; Chapelle, F.H.; Wilson, J.T. Field and laboratory evidence for intrinsic biodegradation of vinyl chloride contamination in a Fe(iii)-reducing aquifer. *J. Contam. Hydrol.* **1998**, 31 (1-2), 111-127.
- **Bradley**, P.M. Microbial degradation of chloroethenes in groundwater systems. *Hydrogeol. J.* **2000**, 8 (1), 104-111.
- **Bradley**, P.M.; Chapelle, F.H. Acetogenic microbial degradation of vinyl chloride. *Environ. Sci. Technol.* **2000**, 34 (13), 2761-2763.
- **Chartrand**, M.M.G.; Waller, A.; Mattes, T.E.; Elsner, M.; Lacrampe-Couloume, G.; Gossett, J. M.; Edwards, E.A.; Sherwood Lollar, B. Carbon isotopic fractionation during aerobic vinyl chloride degradation. *Environ. Sci. Technol.* **2005**, 39 (4), 1064-1070.
- **Chu**, K.H.; Mahendra, S.; Song, D.L.; Conrad, M.E.; Alvarez-Cohen, L. Stable carbon isotope fractionation during aerobic biodegradation of chlorinated ethenes. *Environ. Sci. Technol.* **2004**, 38 (11), 3126-3130.
- **Clark**, I.D.; Fritz, P. Environmental Isotopes in Hydrogeology; Lewis Publishers: Boca Raton, FL, **1997**.
- **Coleman**, N.V.; Mattes, T.E.; Gossett, J.M.; Spain, J.C. Phylogenetic and kinetic diversity of aerobic vinyl chloride-assimilating bacteria from contaminated sites. *Appl. Environ. Microbiol.* **2002**, 68 (12), 6162-6171.
- **Craig**, H. The geochemistry of the stable carbon isotopes. *Geochim. Cosmochim. Acta* **1953**, 3 (2-3), 53-92.
- **Fennell**, D.E.; Carroll, A.B.; Gossett, J.M.; Zinder, S.H. Assessment of indigenous reductive dechlorinating potential at a tce-contaminated site using microcosms, polymerase chain reaction analysis, and site data. *Environ. Sci. Technol.* **2001,** 35 (9), 1830-1839.
- **Harkness**, M.R.; Bracco, A.A.; Brennan, M.J.; Deweerd, K.A.; Spivack, J.L. Use of bioaugmentation to stimulate complete reductive dechlorination of trichloroethene in Dover soil columns. *Environ. Sci. Technol.* **1999**, 33 (7), 1100-1109.
- **Hunkeler**, D.; Aravena, R.; Butler, B.J. Monitoring microbial dechlorination of tetrachloroethene (PCE) in groundwater using compound-specific stable carbon isotope ratios: Microcosm and field studies. *Environ. Sci. Technol.* **1999**, 33 (16), 2733-2738.
- **Hunkeler**, D.; Aravena, R.; Cox, E. Carbon isotopes as a tool to evaluate the origin and fate of vinyl chloride: Laboratory experiments and modeling of isotope evolution. *Environ. Sci. Technol.* **2002**, 36 (15), 3378-3384.
- **Lyman**, W.L ; Reehl, W.F. ; Rosenblatt, D.H. Handbook of chemical property estimation methods : environmental behavior of organic compounds. Mc Graw – Hill, New York. **1990**.
- **Tiehm**, A.; Schmidt, K.R.; Pfeifer, B.; Heidinger, M.; Ertl, S. Growth kinetics and stable carbon isotope fractionation during aerobic degradation of cis-1,2-dichloroethene and vinyl chloride. *Water Res.* **2008**, 42 (10-11), 2431-2438.
- **Worch**, E. Eine neue Gleichung zur Berechnung von Diffusionskoeffizienten gelöster Stoffe. *Vom Wasser* **1993**, 81, 289-297.

Chapter 6

Summary, conclusion and outlook

The main aim of this study was to investigate whether compound specific isotope analysis (CSIA) can be used to differentiate different sources of contamination and/or to assess biodegradation of chlorinated ethenes in unsaturated zone contamination studies. For both applications, it had to be taken into account that isotope ratios in the unsaturated zone can vary due to vaporization, air-water partitioning and diffusion in addition to biodegradation. For the interpretation of field data, the effect of these physical processes on isotope ratios thus needed to be known. Various laboratory experiments and numerical modeling were carried out to evaluate the contribution of different processes to isotope fractionation in isolation, as well as during their combination. Carbon and chlorine isotopes were investigated together as in practical applications a dual isotope approach is more promising to relate isotope variations to different processes.

As a basis for the experimental work, it was necessary to first develop analytical methods and methods for data interpretation of chlorine isotopes. The accuracy, precision and amount dependency of chlorine isotope ratio analyses performed with gas chromatography quadrupole mass-spectrometry (GC-qMS) were evaluated for two Agilent and Thermo instruments. The Agilent CG-qMS was shown to be more adapted for chlorine isotopes measurements. The study has shown that it was necessary to use at least two standards to calibrate raw instrument data against SMOC scale (Standard Mean Ocean Chlorine). Moreover, this calibration must be repeated at least in the beginning and in the end of each measurement sequence to provide accurate results. Additionally, the standards and the samples must have the same concentrations to avoid amount dependency. A precision of $1\sigma \approx 0.2\text{-}0.5\%$ (n=10) was reached for TCE measurements with the Agilent GC-qMS. 5-10 replicates have to be analyzed for each sample and standard. Moreover, standards must be analyzed regularly along an analytical sequence. This technique is thus time consuming.

Isotope fractionation observed during the vanishing of a NAPL source of TCE located in the unsaturated zone was then evaluated. It was first demonstrated that opposite isotope fractionation trends of carbon and chlorine isotope fractionation can be observed during vaporization, although they are present in the same bond within the molecule. Inverse and

normal isotope effects were observed for carbon (ε_C=+0.75±0.04‰) and chlorine isotopes (ε_{Cl}=-0.39±0.03‰), respectively. During diffusion-controlled vaporization, the combined effect of vaporization and diffusion led to a constant carbon isotope ratio at the NAPL source, while heavy chlorine isotopes became enriched (ε_{Cl}=-1.39±0.06‰). An older source might thus have a distinct heavy chlorine isotope ratio. This enrichment trend could help to differentiate subsurface sources of different age even if they have a similar starting isotope signature. It was also demonstrated theoretically and experimentally that chlorine isotope and isotopologue fractionation is proportional in good approximation during vaporization, diffusion and combination of them (diffusion-controlled vaporization), although several isotopologues with multiple heavy isotopes are present. It seems thus possible to derive isotope ratios from isotopologue ratios even if not all isotopologues are measured and to quantify fractionation factors from either isotopologue or isotope ratios.

Additionally, isotope fractionation during the migration of chlorinated ethenes from a groundwater plume to the soil surface through the unsaturated zone was evaluated. In this case, isotope fractionation was affected by air-water partitioning and diffusion. Carbon and chlorine isotopes showed opposite isotope fractionation trends during air-water partitioning, but to a lower extend than for vaporization (ε_C=+0.46±0.04‰ and ε_{Cl}=-0.20±0.04). During the migration of PCE from groundwater to the unsaturated zone in a 2D system, small shifts of carbon and chlorine isotope ratios were observed between the saturated zone and the gas phase of the unsaturated zone. Numerical modeling has highlighted that these shifts are related to isotope fractionation associated with air-water partitioning and a preferential loss of isotopologues from the unsaturated zone by gas phase diffusion. Constant carbon and chlorine isotopic profiles were observed through the unsaturated zone (above the capillary fringe) at steady state. However, depending on the thickness of the unsaturated zone and the lithology, depletion in heavy isotopes might occur with distance during the transient migration of contaminant through the unsaturated zone. Chlorine isotope variations occurred in the unsaturated zone during water table fluctuations. If water levels stabilize again for a sufficiently long period, isotopic ratios will return to their initial values.

Finally, the interaction of diffusion and biodegradation was investigated, using vinyl chloride as a model compound. Isotope fractionation during biodegradation was first evaluated in isolation with microcosm experiments and an enrichment factor of -7.2‰ was observed. Numerical modeling has highlighted that biodegradation may be identified in a diffusion-controlled system using CSIA if degradation rate is fast enough or the residence time in the unsaturated zone sufficiently long. The isotope shift due to biodegradation was amplified if layers of fine sediments were present and/or if unsaturated zone is thick. However, as

isotope fractionation due to biodegradation is partly counterbalanced by faster diffusion of ^{12}C-molecules in the gas phase, the effective isotope fractionation factor for biodegradation in diffusion-controlled system is expected to be smaller than in saturated conditions where advection is the main transport process. Numerical modeling also suggested that a significant part of the biodegradation takes place in the first centimeters of the unsaturated zone, because of the longer residence time of contaminants in this zone due to a lower effective diffusivity. Since constant isotopic values are expected across the unsaturated zone at steady state in absence of biodegradation (or if biodegradation rate is low), an enrichment of heavy isotopes across the unsaturated zone indicates the presence of significant biodegradation.

In summary, this PhD thesis confirms that significant isotope fractionation can be observed during physical processes affecting VOCs in the unsaturated zone even for molecules with a relatively large mass such as TCE (mass 135) and PCE (mass 162). Larger isotope effects might be expected for chlorine that for carbon given that chlorine isotopes are two masses apart while carbon isotopes have only a mass difference of one. While this is indeed the case for diffusion, this is not the case for other physical processes for which carbon isotope effect was larger than the chlorine isotope effect. In case of the diffusion, isotope fractionation is controlled by the overall molecules weight, while for vaporization and air water partitioning the relative differences in atomic weight are relevant, as the isotope effects originate from differences in vibrational frequencies. Under field conditions, the observed isotope trends are usually a net effect of the combination of several processes. This thesis has demonstrated that when different processes occur simultaneously, isotope effects can reinforce or partly cancel each other. In the case of diffusion-controlled vaporization from a NAPL source located in the unsaturated zone, diffusion will always be associated with a normal isotope effect, while vaporization can be normal or inverse. For PCE and TCE, inverse isotope effects are observed for carbon and normal effects for chlorine. Similar trends will likely also occur for other chlorinated hydrocarbons. Hence, a fairly strong isotope effect for diffusion-controlled vaporization can generally be expected for chlorine, dominated by the fairly large diffusion effect due to the mass difference of two. Indeed, chlorine isotope fractionation associated with diffusion-controlled vaporization was the largest effect for physical processes observed experimentally in this study. During the transfer of compounds though the capillary fringe from a groundwater plume to the unsaturated zone, air-water partitioning (normal and inverse isotope effect for chlorine and carbon, respectively) and the preferential lost of light isotopologues from the unsaturated zone due to diffusion cancel for carbon isotopes, but reinforce each other for chlorine. In the case of biodegradation in the unsaturated zone, both processes that control the net isotope fractionation are usually

associated with a normal isotope effect. Hence it can be generally expected that isotope effects partially can each other. Preferential removal of light molecules due to biodegradation is partly counterbalanced by the larger mass flux of light molecules brought along by diffusion from the source. For chlorine isotopes, the net isotope effect might often be fairly small, as chlorine isotope effect associated with biodegradation tend to be relatively small (due to the rather small relative mass difference between isotopes), while diffusion effect is fairly large (due to the mass difference of two among isotopes). Finally, the extent of the observed isotope shifts strongly depends whether a system is under steady state or in a transient state conditions. Thereby, two different situations can be distinguished, in case of diffusion of compounds through the unsaturated zone away from a NAPL source or groundwater plume. For a NAPL source, significant variations of isotope ratios are observed during the transient migration of contaminants by diffusion through the unsaturated zone, with a depletion of heavy isotopes with increasing distance from the source. However, this depletion in heavy isotope vanishes when a steady state is reached and constant isotope profiles occur. In the case of a groundwater source, isotope profiles generally do not vary with distance from the water table at a given time and carbon and chlorine isotopic ratios show only small variations in the unsaturated zone, even at transient state. When substances diffuse out of the water, it takes more time to reach a steady state due to the mass transfer resistance of capillary fringe. Hence the isotope profiles have time to constantly readjust, which is not the case during rapid NAPL vaporization. However, if the unsaturated zone is thick and/or layer of fine sediments are present, a depletion in heavy isotopes is expected along concentration gradients during the transient migration of chlorinated ethenes accross the unsaturated zone. If biodegradation occurs, isotope profiles will vary with distance even at steady state as long as the net isotope fractionation factor is sufficiently high.

This study has several implications for the application of CSIA methods to characterize sources of contamination and/or to assess biodegradation of chlorinated ethenes in unsaturated zone contamination studies. CSIA might be of great interest to distinguish between separate releases of NAPL entrapped in the unsaturated zone, to link contaminants found in groundwater plumes to those present in the unsaturated zone or building, as well as to distinguish compounds from groundwater and a NAPL source. Based on this study, it can be expected that the isotope signature of the vapor around an unsaturated zone NAPL source does not vary with distance as long as steady state conditions are reached. However, a small offset equivalent to the vaporization enrichment factor is expected between the vapor contamination and the NAPL source. This offset will nevertheless not affect the source identification methods as it will be the same for each NAPL source.

Moreover, as diffusion controlled-vaporization leads to an enrichment of heavy chlorine isotope at the NAPL source, an older source will have a distinct heavy chlorine isotope ratio. This enrichment trend could help to differentiate subsurface source of different age even if they have a similar starting isotope signature. Under field conditions, these effects will likely be lower than in the laboratory due to the heterogeneous distribution of NAPL. For groundwater source, a small isotopic shift between the groundwater and the gas phase (in the unsaturated zone) must also be taken into account depending on subsurface lithology. This shift is expected to be small for heavy molecules and if fine sediments are present in the capillary fringe. However, as this shift is mainly influenced by diffusion, it will be larger for lighter molecules, especially for chlorine isotopes. Since constant isotopic values are expected across the unsaturated zone at steady state in absence of biodegradation, an enrichment of heavy isotopes indicates the presence of significant biodegradation. It seems thus possible to assess biodegradation in unsaturated zone studies. However, the effective isotope fractionation factor for biodegradation in diffusion-controlled system is smaller than in saturated conditions where advection is the main transport process. This smaller isotope fractionation factor must be taken into account when the kinetic of the biodegradation is evaluated using CSIA under variably saturated conditions.

A number of areas have also been identified that require further research in the area of CSIA applications under variably saturated conditions:

- Laboratory experiments should be carried out to investigate the coupling of biodegradation and diffusion of VC in unsaturated conditions in order to confirm conclusions drawn from numerical modeling.
- The various isotope trends observed in the unsaturated zone during the laboratory experiments must also be investigated in the field using a dual isotope approach in order to link vapour contaminations with their source, differentiate sources of contamination and/or to assess biodegradation. It can be first investigated if constant isotopic ratios are also observed in the field under steady state conditions. Various scenarios can be also of special interest:
  - a field study where various sources of contamination were already identified in order to evaluate if they can be differentiated in the unsaturated zone with CSIA;
  - a dynamic aquifer with strong water level changes, for example close to a pumping well, to evaluate if isotopic variations are observed in these conditions at field scale;
  - a field site where biodegradation of VC take place in the unsaturated zone in order to evaluate if isotope fractionation occur;
  - to observe isotopic ratio before and after a major rain event, in order to evaluate if isotopic profiles vary in these conditions.

But some technical issues need to be solved before any field investigation regarding sampling and chlorine isotope analyses (see next two points below).

- In order to carry out investigations in soil air, methods for the sampling of chlorinated solvents at low concentrations and compatible with carbon and chlorine measurements must be developed. Sampling tubes filled with sorbent are of great interest for this purpose. Especially the potential interference with other volatile compounds in soil air which might affect isotope analysis at low concentration needs to be further investigated. An alternative technique would be to purge soil air into solvents (as methane for example) to trap VOCs.

- Until now, chlorine isotope ratios measurements with GC-qMS were mainly performed for individual compounds. In order to apply this method at contaminated sites, the method has been tested using mixtures of contaminants. The most straightforward approach would be to jump between masses in SIM (selected ion monitoring) mode between each compound. However, preliminary tests have shown that the mass spectrometer need time to stabilise again while changing masses in SIM mode from a compound to the other. Additionally, in order to perform analyses of chlorine isotope at lower concentrations, the reliability of other extraction method than headspace, as ITEX, SPME or Purge&Trap systems, must be evaluated. However, these extraction methods require more analytical time than headspace and, as 5 to 10 analyses are required for each standard and sample, it will restrict the number of samples that can be analysed. A system to inject peaks of standards directly in the MS during the analyses of the samples can for example be developed to avoid standard analyses in individual run and to save time.

- δ^{37}Cl measurements with GC-qMS require two standards for calibration. As isotope ratios of chlorinated solvents of various manufacturers are often close and fractionation related to processes as biodegradation is often large, it is necessary to produce new calibration standards. The enrichment factor observed during diffusion-controlled vaporization may for example be used to produce standards. Pure compound can be enriched in heavy isotopes by vaporization and diffusion through porous material. To obtain material with different signatures, diffusion-controlled vaporization can be coupled with condensation.

- Finally, in order to complete the knowledge of isotope fractionation effect affecting chlorinated ethenes in the environment, isotope fractionation during additional physical processes such as dissolution and/or diffusion of contaminants in water should be investigated using various experimental systems.

Appendices

a.

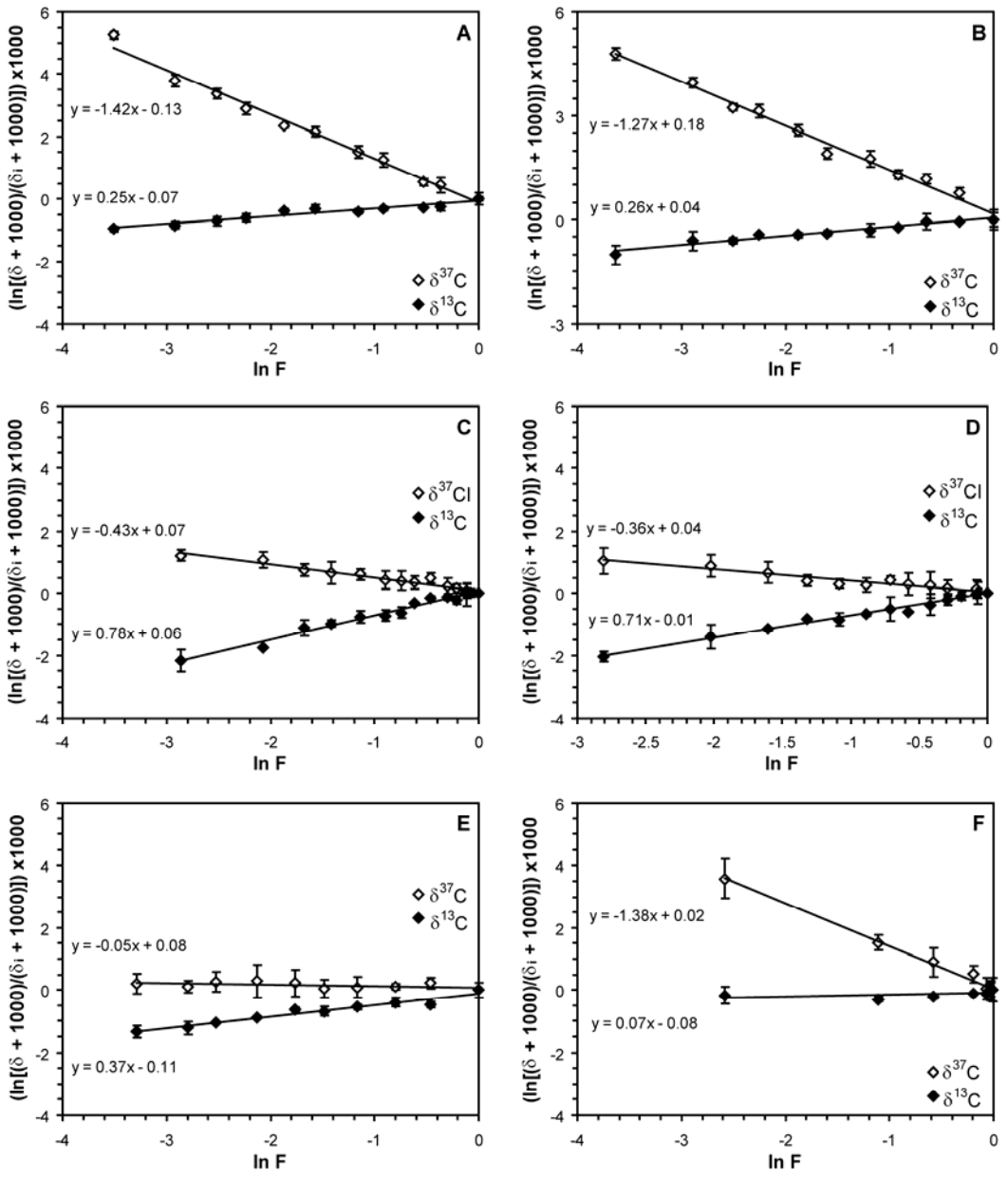

Figure A1: Rayleigh plots for replicate experiments of continuous vaporization (A & B), stepwise vaporization (C & D), air-water partitioning (E) and diffusion-controlled vaporization in a sand-filled column (F). Error bars represent standard deviation.

b. Quantification of isotope fractionation during stepwise experiments

As the Rayleigh relationship can strictly only be applied to continuous processes, equations that describe the isotope evolution during a stepwise partitioning process were derived. The equations were used to quantify the enrichment factor and to evaluate if the data from the stepwise experiments can be approximated by the Rayleigh equation. For each equilibration step, the isotope ratios in the two phases are related by the following isotope balance equation:

$$\delta^{13}C_L^{n+1} = \delta^{13}C_L^n \cdot f_L + \delta^{13}C_g^n \cdot (1 - f_L) \qquad \textit{(equation A1)}$$

with

$$\varepsilon = \delta^{13}C_g^n - \delta^{13}C_L^n \qquad \textit{(equation A2)}$$

with

$\delta^{13}C_L^{n+1}$	isotope ratio in the liquid phase (water or NAPL) before equilibration
$\delta^{13}C_L^n$	isotope ratio in the liquid phase (water or NAPL) after equilibration
$\delta^{13}C_g^n$	isotope ratio in the gas phase after equilibration
f_L	fraction of compound in the liquid phase
ε	isotope enrichment factor for equilibrium partitioning

Inserting a rearranged form of equation A2 in equation A1 to substitute $\delta^{13}C_g^n$ and rearrangement leads to:

$$\Delta\delta^{13}C_L = \delta^{13}C_L^{n+1} - \delta^{13}C_L^n = \varepsilon \cdot (1 - f_L) \qquad \textit{(equation A3)}$$

In case of air-water partitioning, f_L is constant. Hence the shift in $\delta^{13}C$ is equal in each step and the shift after n steps is given by:

$$\Delta\delta^{13}C_L^n = n \cdot \Delta\delta^{13}C_L = n \cdot \varepsilon \cdot (1 - f_L) \qquad \textit{(equation A4)}$$

Whereby f_L can be related to the measured concentration by:

$$f_L = \left(\frac{C_n}{C_0}\right)^{1/n} \qquad \textit{(equation A5)}$$

where C_n is the concentration in aqueous phase after n equilibration steps and C_0 the initial concentration in aqueous phase.

In case of NAPL-vapor equilibration, f_L for step n is given by:

$$f_L = \frac{V_g \cdot p / RT}{M_n} \qquad \textit{(equation A6)}$$

With M_n the mass of compound in the NAPL before the n^{th} equilibration step.

Since f_L diminishes with each step, the shift in $\delta^{13}C$ increases (i.e. is not constant as in case of air-water partitioning). The shift after n steps is given by:

$$\Delta\delta^{13}C_L^n = \varepsilon \cdot \frac{p \cdot V}{R \cdot T} \cdot \sum_{n=1}^{n} \frac{1}{M_n} \qquad \textit{(equation A7)}$$

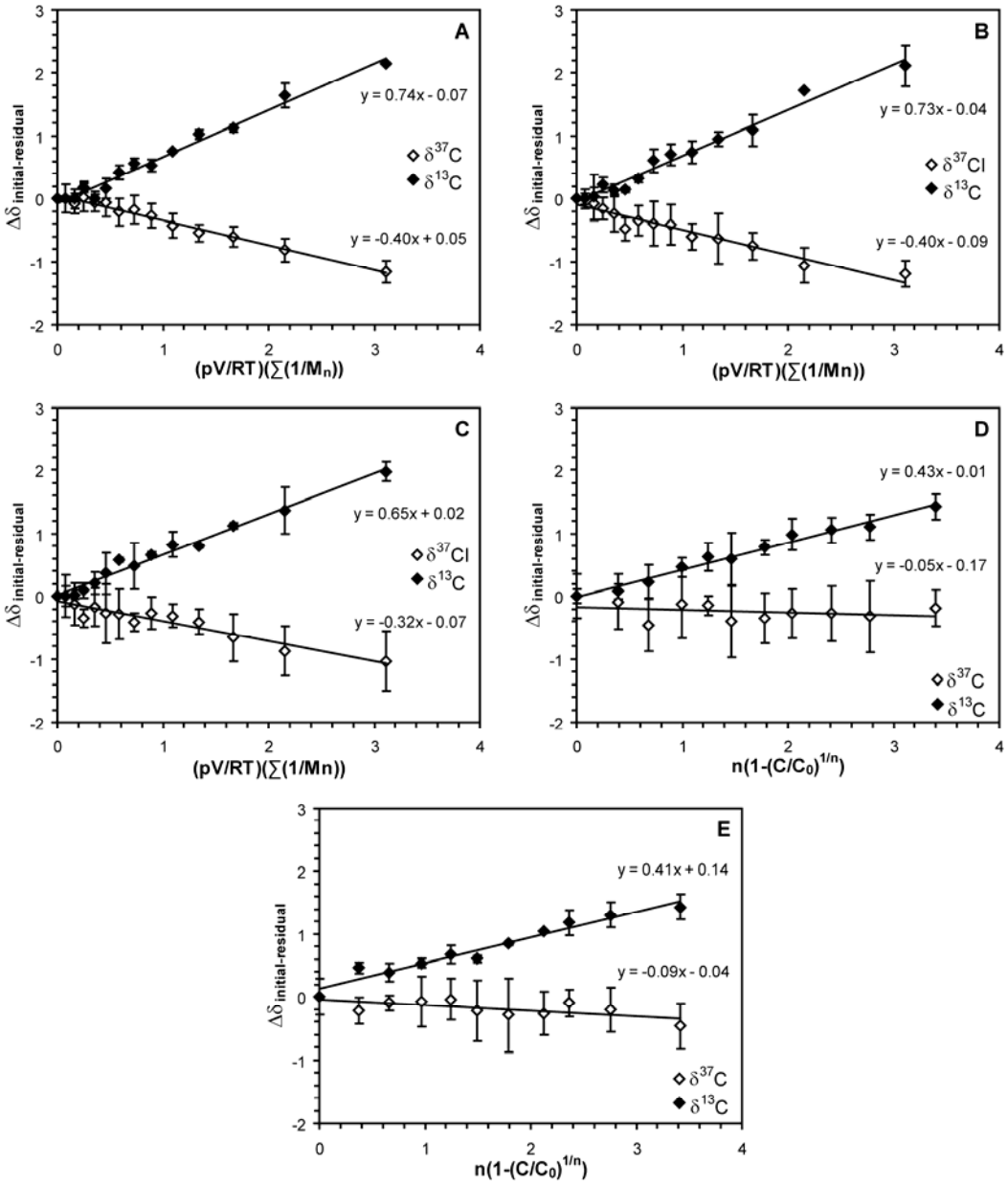

Figure A2: Stepwise fractionation plots for the vaporization and air-water partitioning experiments: (A, B and C) stepwise vaporization, (D and E) air-water partitioning. Error bars represent standard deviation.

Table A1 : Enrichment factor (ε) values of carbon and chlorine for the stepwise vaporization and air-water partitioning experiments using the stepwise calculation approach. The uncertainty was calculated using the standard error of the slope for all measurements.

		Expt.1	Expt. 2	Expt. 3	Mean values
Stepwise vaporization	ε_C	+0.74‰ (±0.02‰)	+0.73‰ (±0.03‰)	+0.65‰ (±0.03‰)	+0.71‰ (±0.03‰)
	ε_{Cl}	-0.40‰ (±0.02‰)	-0.40‰ (±0.02‰)	-0.32‰ (±0.03‰)	-0.37‰ (±0.02‰)
Air-water partitioning	ε_C	+0.43‰ (±0.05‰)	+0.41‰ (±0.03‰)		+0.42‰ (±0.04‰)
	ε_{Cl}	-0.05‰ (±0.05‰)	-0.09‰ (±0.04‰)		-0.07‰ (±0.05‰)

Table A2 : Comparison between the carbon and chlorine enrichment factors (ε) of the classical Rayleigh and stepwise approach for the stepwise vaporization and air-water partitioning experiments. The uncertainty was calculated using the standard error of the slope for all measurements.

		Rayleigh data evaluation	Stepwise data evaluation
Stepwise vaporization	ε_C	+0.75‰ (±0.04‰)	+0.71‰ (±0.03‰)
	ε_{Cl}	-0.39‰ (±0.03‰)	-0.37‰ (±0.02‰)
Air-water partitioning	ε_C	+0.38‰ (±0.04‰)	+0.42‰ (±0.04‰)
	ε_{Cl}	-0.06‰ (±0.05‰)	-0.07‰ (±0.05‰)

For stepwise vaporization (Figure A2A, B&C) and air-water partitioning experiments (Figure A2D&E) the isotopic values plotted vs. the fraction of compound in the liquid phase follow a linear trend. The enrichment factors were calculated using equations A4, A5 and A7 (Table A1). There is no significant difference in the isotope enrichment factors between the two approaches (Table A2). The good agreement between the two approaches is due to the elevated number of equilibration steps used in the experiments. Therefore, data were plotted according to the classical Rayleigh approach in the manuscript.

c) Stepwise vaporization and diffusion-controlled vaporization of PCE

c.1) Materials and methods

The experimental setup chosen to study stepwise and diffusion-controlled vaporization used a similar approach that the one previously developed for the TCE in chapter 3.2. Each experiment was repeated twice. The stepwise vaporization experimental setup consists of two 5ml syringes connected together. A drop of 7.5 μl of PCE is place in the lower syringe. At each step, a certain amount of PCE is vaporized partly in this first syringe and is then transfer into the second syringe after an equilibration time of 15 minutes before $\delta^{13}C$ and $\delta^{37}Cl$ analysis. As this vaporization phase is repeated 14 times, a higher isotope shift could be obtained and hence the fractionation factor was determined with a higher precision. This experimental setup is designed to exclude a contribution of diffusion to isotope fractionation and to observe the fractionation caused by the vaporization in isolation. Isotope fractionation during diffusion controlled-vaporization of the PCE is investigated using a laboratory column (diameter of 5 cm, length of 70 cm) filled with dry quartz sand (grain size of 0.7−1.2 mm) open to the atmosphere. An emplaced NAPL source of 3 ml is located in the bottom of the column, from where PCE can volatilize. The columns were placed on an analytical balance in order to link the loss of PCE by diffusion-controlled vaporization to the $\delta^{13}C$ and $\delta^{37}Cl$ evolution. As it is not possible to retrieve NAPL from the column, the gas phase just above the source was sampled.

Gaseous samples were handled in the same way as described in chapter 3.2. Gas samples were introduced into 120 mL bottles filled with 70 mL of water and closed with gas-tight Valco Mininert valves. The samples were placed on rotary shaker at 200 rpm and equilibrated during 1 day at 25 °C. The water was then transferred in 40 and 20 ml vials before analysis of $\delta^{13}C$, $\delta^{37}Cl$ and concentrations with GC-IRMS and GC-qMS.

c.2) Results and discussion

Significant chlorine and carbon isotope fractionation occurs during stepwise vaporization, diffusion-controlled vaporization. As vaporization of chlorinated compound follows a Rayleigh trends and in order to compare these isotopic evolutions, Rayleigh and isotope enrichment factors are calculated using Rayleigh equations (Poulson & Drever, 2003). As duplicate experiments show similar results, the average values will be discussed here (Figure A3). For the two experiments, carbon and chlorine isotopes show opposite fractionation trends, with an inverse isotope effect for carbon isotopes (depletion in heavy isotopes) and a normal isotope effect for chlorine isotopes (enrichment in heavy isotopes). However, the magnitude of fractionation changes from an experiment to the other.

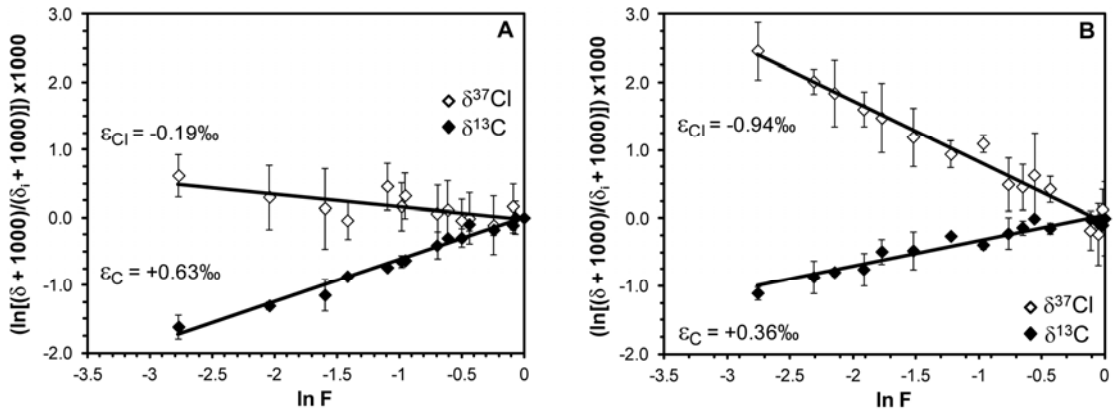

Figure A3: Rayleigh plots for stepwise vaporization (A) and diffusion-controlled vaporization (B). Each point is a mean value of duplicates & error bars represent standard deviations.

Chlorine isotope enrichment factor is much smaller for air-NAPL equilibration that for diffusion controlled vaporization (ε_{Cl}=-0.19±0.07‰ instead of -0.94±0.08‰ respectively), while the opposite is observed for carbon isotope enrichment factors (ε_{C}=+0.63±0.04‰ instead of +0.36±0.03‰ respectively) (Figure A3).

These results agree with the isotopic fractionation trends observed for the TCE during the same experiments (chapter 3). The same opposite trends were observed for carbon and chlorine isotope fractionation, and the same variations were observed between stepwise vaporization and diffusion-controlled vaporization as well. The enrichment factors are lower for the PCE than for TCE during stepwise vaporization (ε_{Cl}=-0.19±0.07‰ vs. -0.39±0.03‰ and ε_{C}=+0.64±0.04‰ vs. +0.75±0.04‰ respectively). During diffusion-controlled vaporization, the carbon isotope enrichment factor for the PCE is higher than for the TCE (ε_{C}=+0.34±0.03‰ vs. +0.10±0.05‰ respectively), and the opposite is found for chlorine isotopes (ε_{Cl}=-0.94±0.08‰ vs. -1.39±0.06‰ respectively).

d. References

- Craig, H. The geochemistry of stable carbon isotopes. *Geochim. Cosmochim. Acta* **1953**, 3, 53–92.
- Crank, J. The Mathematics of Diffusion, 2nd ed.; Clarendon Press, Oxford, 1975.
- Fuller, E.N.; Schettler, P.D.; Giddings, J.C. A new method for prediction of binary gas-phase diffusion coefficients. *Ind. Eng. Chem* **1966**, 58, 19-27.
- Li, C.; Voudrias, E. A. Migration and sorption of jet fuel aliphatic vapors in unsaturated soil. *Wat. Res.* **1994**, 28, 2447-2456.
- Lugg, G. A. Diffusion coefficients of some organic and other vapors in air. *Anal. Chem.* **1968**, 40, 1072–1077.
- Wang, G.; Reckhorn, S.B.F.; Grathwohl, P. Volatile Organic Compounds Volatilization from Multicomponent Organic Liquids and Diffusion in Unsaturated Porous Media. *Vadose Zone Journal* **2003**, 2, 692–701.